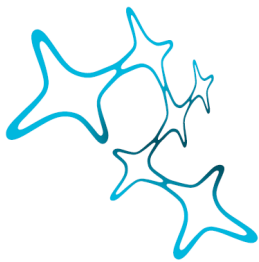

Information Integration and Neural Plasticity in Sensory Processing Investigated at the Levels of Single Neurons, Networks, and Perception

Sebastian Thomas Philipp



Graduate School of
Systemic Neurosciences
LMU Munich



München 2013

**Information Integration and
Neural Plasticity in Sensory
Processing Investigated at the
Levels of Single Neurons,
Networks, and Perception**

Dissertation
an der Graduate School of Systemic Neurosciences
der Ludwig-Maximilians-Universität
München

vorgelegt von
Sebastian Thomas Philipp
geboren am 13.10.1982 in Eschwege

München 2013, den 17. Juni

Erstgutachter: PD Dr. Thomas Wachtler
Zweitgutachter: Prof. Dr. Andreas Herz
Mündliche Prüfung abgelegt am 18. Oktober 2013

"agitate; annotate; arbitrate; artistry; back and forth; brevity; ca d'etai; candidate; can't you see; can't you stay; cape cod you say; card estate; cardio tape; car district; catch a tape; cavitate; cha cha che; cogitate; compute; conjugate; conscious state; counter tape; count to ten; count to three; count yer tape; cut the steak; entity; fantasy; God to take; God you say; got a date; got your pay; got your tape; gratitude; gravity; guard the tit; gurgitate; had to take; kinds of tape; majesty; marmalade."

Perceived words reported by a subject who was exposed to a looped recording of the word "cogitate". First switch from the perception of "cogitate" to another meaningful word after one to two minutes. Alternates switched every 10 to 30 presentations [von Foerster (1988); Naeser and Lilly (1971)].

Contents

| | | |
|----------|--|-----------|
| 1 | Summary | 5 |
| 2 | Main Introduction | 7 |
| 2.1 | Main Questions | 8 |
| 2.2 | Outline | 9 |
| 2.3 | Sensory Organs and Neurons | 10 |
| 2.3.1 | Sensory Organs | 10 |
| 2.3.2 | Neurons, Synapses & Action Potentials | 11 |
| 2.4 | Neural Representations | 13 |
| 2.4.1 | Receptive Fields | 13 |
| 2.4.2 | Topographic Maps | 14 |
| 2.5 | Contextual or Multimodal Integration | 15 |
| 2.6 | Learning and Early Perceptual Development | 16 |
| 2.6.1 | The Brain as a Self-Organizing System | 16 |
| 2.6.2 | Sensory Experience and Development | 16 |
| 2.6.3 | Synaptic Plasticity | 17 |
| 2.6.4 | Spike-Timing-Dependent Plasticity | 18 |
| 2.6.5 | Self-Organization of Topographic Maps | 18 |
| 2.6.6 | Temporal Invariance Learning | 19 |
| 2.6.7 | Invariance Learning in Self-Organizing Networks | 20 |
| 2.6.8 | Self-Organization of Contextual Interactions | 21 |
| 2.7 | Neural Plasticity in Adults | 21 |
| 2.7.1 | Adult Sensory Representations Adapt to Significant Changes in the Environment | 22 |
| 2.7.2 | Perceptual Learning | 22 |
| 2.8 | Attention | 23 |
| 2.8.1 | Input Attention and Controlled Attention | 24 |
| 2.8.2 | Neural Correlates of Attention | 25 |
| 2.8.3 | Attention and Perceptual Learning | 25 |
| 3 | Multiplication in Neurons via Permissive Gating | 27 |
| 3.1 | Abstract | 27 |

| | | |
|----------|--|-----------|
| 3.2 | Introduction | 27 |
| 3.2.1 | Permissive Gating | 30 |
| 3.2.2 | Permissive Gating and Multiplicative Interactions | 31 |
| 3.2.3 | Scope of this study | 32 |
| 3.3 | Methods | 32 |
| 3.4 | Results | 36 |
| 3.4.1 | Generation of Single Spikes - Complete Model Neuron | 36 |
| 3.4.2 | Influence of the Gating Mechanism on Output Firing Rates - Simplified Model Neuron | 37 |
| 3.4.3 | Gating Mechanism in the Complete Model Neuron | 44 |
| 3.4.4 | Effects of Input Synchrony | 47 |
| 3.5 | Discussion | 49 |
| 3.5.1 | Comparison to a Detailed Biophysical Model | 49 |
| 3.5.2 | Multiplicative Interactions with Small Gating Weights | 49 |
| 3.5.3 | Exact and Nearly Multiplicative Interactions | 50 |
| 3.5.4 | Robustness of Models that Explain Multiplicative Interactions via a Network Approach | 51 |
| 3.6 | Outlook to Chapter 3 | 52 |
| 4 | Unsupervised Learning of Gaze-Invariance | 53 |
| 4.1 | Abstract | 53 |
| 4.2 | Introduction | 53 |
| 4.2.1 | Coordinate Transformations and Basis Function Networks | 55 |
| 4.2.2 | Development of Gaze-Invariant Representations | 57 |
| 4.3 | Methods | 58 |
| 4.3.1 | Network Architecture | 58 |
| 4.3.2 | Neuron Model & Synapse Types | 60 |
| 4.3.3 | Learning Rule | 62 |
| 4.3.4 | Stimuli, Training & Testing Procedure | 63 |
| 4.4 | Results | 65 |
| 4.4.1 | Receptive Fields and Topographic Maps in Map Formation Layer Neurons | 65 |

| | | |
|----------|---|-----------|
| 4.4.2 | Receptive Fields and Coding Properties of Output Layer Neurons | 67 |
| 4.4.3 | Reduction of the Dimension of the Map Formation Layer | 73 |
| 4.4.4 | Stable Head-Centered Representations and Choice of Model Neurons | 74 |
| 4.5 | Discussion | 76 |
| 4.5.1 | Gain Fields and Structure of Topographic Maps | 77 |
| 4.5.2 | Coordinate Transformations and Eye Velocity Gain Fields | 78 |
| 4.5.3 | A General Mechanism for Information Integration? . . | 79 |
| 4.6 | Outlook to Chapter 4 | 80 |
| 5 | Improvement of Tactile Perception by Meditation | 81 |
| 5.1 | Abstract | 81 |
| 5.2 | Introduction | 81 |
| 5.2.1 | Neural Plasticity Without External Stimulation | 82 |
| 5.3 | Methods | 83 |
| 5.3.1 | Measures of Tactile Abilities | 83 |
| 5.3.2 | 2-Point Discrimination Thresholds | 84 |
| 5.3.3 | Localization Performance | 85 |
| 5.3.4 | Subjects, Measurement Protocol & Meditative Inter- vention | 86 |
| 5.3.5 | Data Acquisition, Software, and Investigator | 88 |
| 5.4 | Results | 88 |
| 5.4.1 | 2pd Thresholds | 89 |
| 5.4.2 | Localization Performance | 92 |
| 5.5 | Discussion | 93 |
| 5.5.1 | Learning Mechanisms that Could Underlie the Observed Effects | 95 |
| 5.5.2 | Joint Changes in Perceptual Measures and Immobilization | 96 |
| 5.5.3 | Possible Experimenter Effects | 96 |
| 5.5.4 | Relation to Other Studies | 97 |
| 5.5.5 | Conclusion | 99 |

| | | |
|----------|---|------------|
| 6 | Main Discussion | 100 |
| 6.1 | Multiplicative Interactions in Single Neurons | 100 |
| 6.2 | Unsupervised Learning of Gaze-Invariance | 101 |
| 6.3 | Improvement of Tactile Perception by Meditation | 103 |
| 6.4 | Neural Plasticity and Mental States | 105 |
| 6.5 | Activity-Dependent Plasticity, the Inside, and the Outside . . | 107 |
| 7 | Acknowledgements | 109 |
| 8 | Supplementary Material | 110 |
| 8.1 | Multiplication in Neurons via Permissive Gating | 110 |
| 8.1.1 | Models of Multiplicative Interactions - Network Level . | 110 |
| 8.1.2 | Models of Multiplicative Interactions - Single Neuron Level | 111 |
| 8.2 | Improvement of Tactile Perception by Meditation | 114 |
| 8.2.1 | Original Data - Sensory Focussing Group | 114 |
| 8.2.2 | Original Data - Control Group | 115 |
| 8.2.3 | Evaluated Two Point Discrimination Thresholds - Right Index Finger (r2) | 116 |
| 8.2.4 | Evaluated Two Point Discrimination Thresholds - Right Middle Finger (r3) | 116 |
| 8.2.5 | Evaluated Two Point Discrimination Thresholds - Left Index Finger (l2) | 117 |
| 8.2.6 | Evaluated Localization Performance - Right Index Fin- ger (r2) | 117 |
| 8.2.7 | Evaluated Localization Performance - Right Middle Finger (r3) | 118 |
| 8.2.8 | Evaluated Localization Performance - Left Index Finger (l2) | 118 |
| 9 | List of Contributions | 138 |

1 Summary

In this doctoral thesis, several aspects of information integration and learning in neural systems are investigated at the levels of single neurons, networks, and perception.

In the first study presented here, we asked the question of how contextual, multiplicative interactions can be mediated in single neurons by the physiological mechanisms available in the brain (chapter 3). Multiplicative interactions are omnipresent in the nervous system [Salinas and Sejnowski (2001)] and although a wealth of possible mechanisms were proposed over the last decades, the physiological origin of multiplicative interactions in the brain remains an open question [Koch (1999); Nezis and van Rossum (2011)]. We investigated permissive gating [Katz (2003); Gisiger and Boukadoum (2011)] as a possible multiplication mechanism. We proposed an integrate-and-fire model neuron that incorporates a permissive gating mechanism and investigated the model analytically and numerically due to its abilities to realize multiplication between two input streams. The applied gating mechanism realizes multiplicative interactions of firing rates on a wide range of parameters and thus provides a feasible model for the realization of multiplicative interactions on the single neuron level.

In the second study (chapter 4) we asked the question of how gaze-invariant representations of visual space can develop in a self-organizing network that incorporates the gating model neuron presented in the first study. To achieve a stable representation of our visual environment our brain needs to transform the representation of visual stimuli from a retina-centered coordinate system to a frame of reference that is independent of changes in gaze direction [Duhamel et al. (1997)]. In the network presented here, receptive fields and gain fields organized in overlaid topographic maps that reflected the spatio-temporal statistics of the training input stream. Topographic maps supported a gaze-invariant representation in an output layer when the network was trained with natural input statistics. Our results show that gaze-invariant representations of visual space can be learned in an unsupervised way by a biologically plausible network based on the spatio-temporal statistics of visual

stimulation and eye position signals under natural viewing conditions.

In the third study we investigated psychophysically the effect of a three day meditative Zen [Kapleau (2000)] retreat on tactile abilities of the finger tips. Here, meditators strongly altered the statistics of their attentional focus by focussing sustained attention on their right index finger for hours. Our data shows that sustained sensory focussing on a particular body part, here the right index finger, significantly affects tactile acuity indicating that merely changing the statistics of the attentional focus without external stimulation or training can improve tactile acuity.

In the view of activity-dependent plasticity that is outlined in this thesis, the main driving force for development and alterations of neural representations is nothing more than neural activity itself. Patterns of neural activity shape our brains during development and significant changes in the patterns of neural activity inevitably change mature neural representations. At the same time, the patterns of neural activity are formed by environmental sensory inputs as well as by contextual, multiplicative inputs like gaze-direction or by internally generated signals like the attentional focus. In this way, our environments as well as our inner *mental* states shape our neural representations and our perception at any time.

2 Main Introduction

As humans, we are in constant perceptual contact with our environment via our sensory organs that translate physical states into chemical and electrical signals which are meant to be the language of our nervous systems. Our nervous systems integrate these different signals coming from our multiple sensory organs and creates our percept of the environment. In the best case, the internally perceived environment and the external physical environment fit in a way that the organisms re-actions to mental phenomena in the internally perceived environment lead to results in the physical environment that enable the organism to survive. In the worst case they do not fit. If the canvas, the brushes, and the colors that create my internal representation of the environment are not adequate, my actions will lead to tremendous problems for me - and maybe also for the environment.

How does our nervous system gain the ability to fit our inner perceptual world to the external physical world so that I am able to survive by interacting properly with my environment? How does it select adequate brushes and colors to paint a picture onto the canvas of my inner conscious world that helps me to act adequately in the environment? How do these abilities emerge? Is our perceptual world fixed from the moment of our birth, an inception that empowers us with our skills? Are we equipped with a nervous system painting pictures on the white canvas of our conscious world with a fixed set of painting skills, sets of colors and only a few brushes? Are we genetically determined, prewired, and predefined in the way who we are and what we perceive? Or are we constantly developing beings, born as the white canvas of our conscious world and equipped with a nervous system that constantly adapts its painting skills and its artist's workroom with constantly changing sets of brushes, spatulas and color sets according to the very actual pictures it is asked to paint and that arranges its workroom due to the experiences we make throughout our lives? Furthermore, if the second is true: Is there a point, at which development stops or are we in a constant state of development and thus endowed with the opportunity to change ourselves, the way we see the world, and the way we act in it at any time?

2.1 Main Questions

Let us assume that our environments constantly change¹. In a constantly changing environment it is not beneficial for organisms to genetically pass on a fixed set of perceptual abilities from one generation to the next. This is because these fixed sets would quickly become obsolete when faced with the changing environment and next generations would no longer be able to interact with their environment in an adequate way.²

In contrast to genetically passing on a fixed set of perceptual abilities from one generation to the next is the idea of passing on the ability of the nervous system to *develop* and to *adapt* its perceptual and acting abilities according to that actual world that calls the organism to respond to it. The central idea of this developmental, adaptational view of the nervous system is a steady state of use dependent self-organization that serves to constantly match perceptual and acting abilities to the actual environment the organism is confronted with [Dinse and Merzenich (2002)]. In this view, perception is a circular process in which the world we perceive and in which we act, forms the way we perceive the world.

Viewing brains as self-organizing systems, the main driving force for development and adaptation of neural representations is neural activity [Singer (1986)]. Patterns of neural activity shape our brains during development and significant changes in the patterns of neural activity inevitably change mature neural representations. At the same time, the patterns of neural activity are formed by environmental sensory inputs as well as by contextual, multiplicative inputs like gaze-direction or by internally generated signals like

¹Two hundred years ago, there were no cars. Five years ago, cars looked different than today. My girlfriend left last year, a new one came, my neighbour has got new glasses, in summer, leaves are green, in winter there are no leaves. I do not own a cat nor a car, but I think about getting both, ten years ago I had five friends in my home town, today, I am supposed to have fivethousand on Facebook. I lived in Munich last year, now I live in Freiburg. It seems reasonable to assume that our environments constantly change.

²If you are interested in a funny but nevertheless serious statement of what may happen, if you approach a new environment with old sets of perceptual abilities and opinions, I recommend the book *Briefe in die chinesische Vergangenheit* by Herbert Rosendorfer, in which a chinese Mandarin from the 10th century is supposed to wake up in 20th century Munich after traveling in a time machine.

the focus of controlled attention. It all collapses into two questions:

- How does our environment shape our neural representations and the way we perceive the environment and which role do contextual influences play in this process?
- How do factors in our inner world, for example our interests, the way we pay attention to things and the way we are aware of phenomena, shape our neural representations and the way we perceive the environment?

This doctoral thesis will try to contribute scientific knowledge to these questions. Moreover, the results will support the adaptational, developmental view of the nervous system. But before I begin presenting the conducted studies, let me introduce you to a few fundamentals of neuroscience that are important in order to understand the presented studies and to classify them into the contemporary view of the nervous system.³

2.2 Outline

In the next chapters I will go deeper into the above mentioned topics and questions concerning learning and perception. I will briefly review the neuroscientific view of how physical stimuli in the environment are transformed into the language of the nervous system: chemical signals, electrical potentials, and action potentials. I will review the concept of receptive fields and topographic maps which lie at the core of the question of how the brain encodes and represents its environment. I will look at the ability of the nervous system to integrate signals originating from different sensory modalities into one neural response, a topic known as multimodal integration. Here, the interaction between primary sensory information and contextual information is especially relevant. The study "Multiplication in Neurons via Permissive Gating", which will be presented in chapter 3, is thematically rooted here, because contextual interactions are thought to be mediated by multiplicative interactions in

³Fundamentals of neuroscience will be presented densely and briefly in this introductory chapter. For further studies I recommend the extensive introductory material presented in the books "From Neuron to Brain" [Kuffler et al. (1984)], "Neuroscience" [Purves et al. (2004)] and "Gehirn oder Geist - Wer und was sind wir?" [Bauer (2008)].

neurons. Furthermore, I will discuss how neural representations are formed by stepping into the developmental, adaptational view of the nervous system, reviewing literature on learning and self-organization. This will form the basis for the study "Unsupervised Learning of Gaze-Invariance" presented in chapter 4 in which it is shown that gaze-invariant representations of visual space can be learned by a self-organizing network. However, once established, these neural representations are not static but are in a constant state of use dependent self-organization that keeps brain organization and functionality plastic for the whole lifetime of an organism. Reviewing the concepts of neural plasticity, perceptual learning and attention, I will form the basis for the study "Improvement of Tactile Perception by Meditation" which will be presented in chapter 5. In this study, I will present an experiment investigating the effects of sustained attention in adults on the perceptual abilities in the somatosensory area.

Regarding the above mentioned main questions of this thesis, the study "Multiplication in Neurons via Permissive Gating" can be seen as a preparatory investigation for the study "Unsupervised Learning of Gaze-Invariance", where the two studies "Unsupervised Learning of Gaze-Invariance" and "Improvement of Tactile Perception by Meditation" directly relate to the main questions.

After the introduction I will go on presenting the three studies separately and I will discuss the results of the three studies in chapter 6.

2.3 Sensory Organs and Neurons

2.3.1 Sensory Organs

Our sensory organs form the contact stage between our physical environment and our brain. Sensory organs are specialized modalities composed of even more specialized sensory receptors that act as measuring instruments projecting the wealth of physical states in the environment onto their respective state space. For example, our eye is specialized in detecting electromagnetic waves of wavelengths in a range between around 400nm and 800nm, whereas

our ear is specialized in detecting sounds in a frequency range between around 16Hz and 20000Hz. The huge part of the physical environment beyond those tiny ranges is not considered.

Sensory receptors in the eye are selective for special frequency bands of light and translate the frequency-dependent light intensity into chemical and electrical signals. Sensory receptors in the inner ear are mechanical receptors: Sound reaching the eardrum undergoes a frequency analysis in the inner ear resulting in deviations of the basial membrane where different sound frequencies lead to deviations at different positions of the basilar membrane. Frequency-selective sensory receptors detect those deviations and translate them into chemical and electrical signals. Sensory receptors in the skin detect different aspects of touch and also translate them into chemical and electrical signals. Our smell and taste receptors detect that specific aspects of the environment on which they are specialized on - odorants. All sensory receptors share one principle: physical states in the environment are transformed into chemical and electrical signals.⁴

Our sensory organs, confronted with an unthinkable wealth of physical states, measure those tiny aspects of these states that proved to be functionally meaningful in evolution. To me it feels like a miracle that our organisms are able to, first, effectively detect the specific information important for our survival and that, second, it creates from these different information sources a single, continuous and integrated internal representation of the environment on the canvas of our consciousness that feels so unbelievably real and overarching. The basis for this miracle is that the results of the measurements made by the sensory receptors can be transmitted into stages that are able to construct useful content from these measurements. This will be elaborated in the following.

2.3.2 Neurons, Synapses & Action Potentials

In the common neuroscientific view, the basic mediators of information content in the brain are neurons. The human brain contains about 10^{12} neurons,

⁴Statements in this paragraph are based on scientific views presented in textbooks such as [Purves et al. (2004)].

each forming several thousand synapses, the functional contacts between neurons. Physiologically, neurons are cellular components of the brain [Cowan and Sharp (1988); Ramon y Cajal (1911, 1984)] able to conduct electrical pulses rapidly over large distances.

Neurons. Typically, neurons are viewed as consisting of dendrites, a soma, an axon, and synapses. A dendrite is a short, branching process of cellular extensions specialized to act as the receptive network of the neuron receiving electrical and chemical stimulation from sensory receptors or other neurons and transmitting it to the soma. Each neuron has numerous dendrites with profuse dendritic branches. The soma is the cell body of a neuron and contains the nucleus and most of the metabolic machinery of the cell. The axon is the electrically active process of a neuron being able to transmit action potentials, the main mediator of the neural code [Hodgkin (1951); Hodgkin and Huxley (1952); Rieke et al. (1999)]. Neurons mostly have only one axon, but this undergoes extensive branching enabling communication with many target cells.

Synapses. The functional contacts between neurons are synapses. Synapses consist of a presynaptic terminal bouton separated by a narrow gap, called the synaptic cleft, from an area of postsynaptic membrane containing receptors. At a chemical synapse, a release of neurotransmitters from the presynaptic terminal triggered by changes in the membrane potential of the presynaptic neuron carries a signal to the receptors on the postsynaptic membrane. In this way, the electrical excitability in the postsynaptic neuron is influenced. Chemical synapses can mediate either excitatory or inhibitory effects. Here, excitation is the depolarisation of the membrane potential of a postsynaptic neuron, the electrical potential difference across a neuron's membrane. Excitation increases the likelihood of an action potential in the postsynaptic neuron to occur. Inhibition is the hyperpolarization of the membrane potential of a postsynaptic neuron, reducing the likelihood of an action potential in the postsynaptic neuron.

Action potentials. An action potential or spike is a large ($\approx 100\text{mV}$)

and short ($\approx 1\text{ms}$) electrical signal that is executed when the membrane potential of a neuron is strongly depolarized such that it exceeds a spiking threshold [Lapicque (1907); Brunel and van Rossum (2007); Adrian (1914); Hodgkin (1951); Hodgkin and Huxley (1952)].⁵ Action potentials propagate without failure, in an all-or-none fashion, along the neurons axon to its presynaptic terminal and evoke a response in a postsynaptic neuron [Eccles (1964)] in the form of a postsynaptic potential. When the membrane potential of the postsynaptic neuron exceeds its threshold due to input by synaptic potentials, another action potential is generated in the postsynaptic neuron.

The specificity of synaptic connections between neurons forms the basis for selectivities of neurons and for the development of neural representations as discussed in the next chapter.

2.4 Neural Representations

2.4.1 Receptive Fields

The receptive field of a neuron is defined as the region of sensory state space the stimulation of which leads to excitation or inhibition of the neuron. The receptive field in this way describes the selectivity of a neuron to specific stimuli [Sherrington (1909)]. In the special case of visual receptive fields in early stages of computation, the term refers to the spatial position in a respective coordinate frame (e.g. retinal position) and to the quality (e.g. color, spatial shape) a visual stimulus must have to cause a response in the neuron. The response of a neuron can be characterized by determining its average firing rate as a function of the stimulus parameter under consideration. The firing rate of a neuron is defined as the number of action potentials per second produced by a neuron. Other neural codes such as timing, latency or synchrony codes are possible [Theunissen and Miller (1995); Rieke et al. (1999); Vanrullen et al. (2005); Gollisch (2008); Brostek (2012)]. However, in this study I will focus on the firing rate code. Determining the firing rate for different stimuli allows to determine a response tuning curve [Dayan and Abbott (2002)], which specifies the selectivity of the neuron with respect to

⁵Other views on action potential generation are presented in [Izhikevich (2007)].

the parameters under consideration. For example, neurons in primary visual cortex (V1) of cats are tuned to bright or dark bars of certain orientations that are presented at specific retina-centered positions [Hubel and Wiesel (2005)]. Here, the retina-centered position of an object specifies the position of an objects image on the retina with respect to the center of the retina. The retina-centered position of objects changes when the direction of gaze changes. Objects positions can also be represented in other frames of reference: a head-centered and body-centered frame of reference is specified by an objects position with respect to the center of the head or the body, respectively (read more in chapter 4). Most visual neurons at early visual stages have receptive fields that are retina-centered. Selectivities for stimuli are mediated by specific patterns of connectivity in neural networks combining excitatory and inhibitory connections as well as other forms of synaptic and dendritic integration [Dayan and Abbott (2002)].

A feature of neural representations is the organization of selectivities in topographic feature maps.

2.4.2 Topographic Maps

Topographic maps are found in many areas of sensory and motor pathways [Kaas (1997); Swindale (2000); Brown et al. (2000); Chklovskii and Koulakov (2004); Thivierge and Marcus (2007)]. In a topographic map, neurons that are spatially close together encode similar stimulus properties [Thivierge and Marcus (2007)]. An example of topographic maps is found in visual area V1 [Hubel and Wiesel (1974); Hirsch and Gilbert (1991); McLaughlin and O’Leary (2005)]. Neurons in area V1 are retinotopically organized. This retinotopic organization is superimposed by an orientation topography, where neighbouring populations of neurons respond to edges of similar orientation [Hubel and Wiesel (1974)]. Topographic maps are not limited to the case of ordered mapping of visual content. For example, in somatosensory cortex, selectivities for skin regions are arranged in a topographic map that reflects the positions of the skin regions in the body.⁶

⁶In the cochlea, the organ of hearing in the inner ear, there is a tonotopic map ordered by frequency that projects to the auditory cortex [Weisz et al. (2004)]. In the olfactory

Before I will go on reviewing theories of how receptive fields and topographic maps develop, let me review the concept of multimodal integration.

2.5 Contextual or Multimodal Integration

Contextual or multimodal integration is the ability of a neuronal system to integrate information from different sensory sources into one neural response. Multimodal interaction is widespread in the brain [Hassenstein and Reichardt (1956); Reichardt (1961); Andersen and Mountcastle (1983); Andersen et al. (1985); Brotchie et al. (1995); Treue and Martinez-Trujillo (1999); McAdams and Maunsell (2000); Gabbiani et al. (2002); Freeman (2004); Womelsdorf et al. (2006)]. The benefit for an organism having the capability for this multimodal integration is that it must not only rely on one specific type of sensory modality in order to orient itself in the world but that it can combine information from different sensory modalities and form a more reliable percept of the environment.

A physiological mechanism that could underlie multimodal interactions is gain-modulation [Salinas and Sejnowski (2001)]. Here, primary sensory inputs and contextual inputs are combined in the output firing rate of one neuron. A primary sensory input elicits an output firing rate in a neuron due to its receptive field [Hubel and Wiesel (1962)]. The gain of this tuning function is modulated by a contextual input source in a nearly multiplicative way while the tuning concerning the primary sensory input is unaffected. Parallel to the concept of the receptive field, the selectivity of the gain-modulatory effect with regard to its sensory source can be called gain field. A prominent example of gain-modulation is the nearly multiplicative modulation of retina-centered tuning curves in parietal cortex of macaque monkeys by gaze direction [Andersen and Mountcastle (1983)] which will be a central aspect in the

system there is a map where functionally similar neurons (representing specific odorants) of the olfactory epithelium project onto specific modules of the olfactory bulb regardless of their spatial location [O'Leary et al. (1999)]. In area TE_d of the inferotemporal cortex, topography of complex features, even for characteristics of object views were found: different views of faces evoke activity in nearby populations of neurons [Wang et al. (1996)] which suggests that some features of high dimensional input space are mapped continuously in adjacent regions [Tanaka (1996, 2003)].

study "Unsupervised Learning of Gaze-Invariance" presented in chapter 4. In the study "Multiplication in Neurons via Permissive Gating" that is presented in chapter 3 we investigate permissive gating [Katz (2003); Kepecs and Raghavachari (2007); Gisiger and Boukadoum (2011)] as a possible physiological mechanism that could underlie gain modulation and contextual interactions.

Let us now focus on theories of how receptive fields and topographic maps develop.

2.6 Learning and Early Perceptual Development

One problem in neurophysiology has been to understand the origin of feature-sensitive neurons and their spatial order with regard to topographic representations: How are receptive fields, selectivities and topographic maps formed in sensory areas? How do they develop?

2.6.1 The Brain as a Self-Organizing System

Genetic information is insufficient to explain the huge amount of specific connectivity between the approximately 10^{12} neurons in a human brain [Singer (1986)]. In contrast to this is the view of the brain as a self-organizing system. Here, during the early phase of brain development, the detailed form and function of cells as well as the coarse connectivity between cells are shaped by biochemical signals that are communicated between nearby neurons and glial cells [Singer (1986)]. However, when neurons become electrically active, connections between nerve cells undergo a process of activity-dependent self-organization. In embryogenesis, basic connections in the nervous system are shaped by self-generated spontaneous activity [Singer (1986); Firth et al. (2004); Feller (2009)]. After this process, self-organization as a function of sensory experience becomes more and more important.

2.6.2 Sensory Experience and Development

Numerous experiments indicate that the detailed, specific connectivities in the brain are nurtured by sensory experience in a steady process of self-

organization. In visual cortex I of grown up cats, monkeys, and other species, neurons being selective for bars of different orientations can be found [Hubel and Wiesel (1962, 1968, 2005); Kuffler et al. (1984); Bosking et al. (1997)]. Orientation selectivities of different cells are distributed around the clock with each orientation appearing with equal probability [Hubel and Wiesel (1962); Blakemore and Cooper (1972)]. Restricting the early visual environment of cats to stripe patterns of one orientation biased this distribution of orientation selectivities towards the stripe patterns a cat was exposed to [Hirsch and Spinelli (1971); Blakemore and Cooper (1972); Pettigrew et al. (1973)]. If a cat was exposed to an environment with horizontal or vertical stripes, mostly cells could be found that were selective for horizontal or vertical stripes, respectively. The selectivity and organizational structure of neurons in early visual cortex seems to depend strongly on the environment an organism is exposed to during its early development. These representations seem to be shaped by experience.

2.6.3 Synaptic Plasticity

Developmental processes and learning processes in general are based on changes on the synaptic level. The first anatomical theory of learning goes back to 1885 where Alexander Bain proposed: "For every act of memory, every exercise of bodily aptitude, every habit, recollection, train of ideas, there is a specific grouping or co-ordination of sensations and movements by virtue of specific growths in the cell-junctions." [Bain (1855); Cooper (2005)] Phenomena of learning and memory are ascribed to groupings on the intracellular range, whereas the belief of a separate brain area that is responsible for learning and memory has taken a backseat since then. The idea that learning mechanisms are based on dependencies between single neurons can be seen as the basis for today's theories about learning. Today it is widely believed that activity-dependent plasticity of synaptic efficacies forms the basis for learning and memory [Dayan and Abbott (2002)].

2.6.4 Spike-Timing-Dependent Plasticity

In 1949, Donald Hebb supposed that if a presynaptic neuron A often contributed to the firing of a postsynaptic neuron B , the synapse from neuron A to neuron B would be strengthened [Hebb (1949)]. Indeed, experiments have shown that the temporal order of pre- and postsynaptic spiking determines the sign and amplitude of changes in the synaptic efficacy [Zhang et al. (1998)]. Within a window on the order of tenths of milliseconds between pre- and postsynaptic spike, the sign of long-lasting synaptic modification depends on the order of spiking: A presynaptic spike that precedes a postsynaptic spike produces long-term potentiation (LTP), the persistent strengthening of synapses lasting hours to days [Bliss and Lomo (1973)]. A presynaptic spike that follows a postsynaptic spike results in long-term depression (LTD) [Murkey and Malenka (1992); Kirkwood and Bear (1994)] of synaptic efficacies, a persistent weakening of synapses lasting hours to days. This mechanism is referred to as spike-timing-dependent plasticity (STDP) [Markram et al. (1997); Magee and Johnston (1997); Bell et al. (1997); Bi and Poo (1998); Dan and Poo (2004); Song et al. (2000)]. These changes in synaptic efficiency are able to shape receptive fields and the neurons selectivities. Hebb's postulate is in line with these findings as a synapse is strengthened only when a presynaptic spike precedes a postsynaptic spike and therefore can be interpreted as having contributed to it.

2.6.5 Self-Organization of Topographic Maps

The emergence of topographic maps can be explained by self-organizing networks. The emergence of topographic maps of feature-sensitive cells was first demonstrated in simulations by von der Malsburg (1973) and extended by Kohonen (1982, 1984). Those self-organizing networks rely on three main elements: Hebbian learning in forward connections, short range lateral excitation and long range lateral inhibition. This scheme of pattern formation by local self-activation and lateral inhibition occurs in many different developmental situations, from single cells to mammalian embryology [Meinhardt and Gierer (2000)]. In a process of self-organization where the system changes its synaptic

weights due to the activity in the network and the input layers, the feature maps form according to the interaction of stimuli, recurrent connections in the network and learning parameters.

Self-organizing networks can learn orientation maps similar to the ones found in visual cortex when they are trained with a stimulus set of oriented bars [Kohonen (1982, 1984); Choe and Miikkulainen (1998)]. In these models, spatial correlations (i.e. the spatial similarity between stimuli) are the crucial feature which enables the models to form topographic maps: Orientations that are highly spatially correlated are represented in nearby regions of the topographic map. The mapping of spatial statistics in the environment onto spatial relations in neural representations is a substantial feature of self-organization of topographic maps in the brain.

2.6.6 Temporal Invariance Learning

Not only spatial statistics, but also temporal statistics play a major role in the self-organizing process of the brain. These temporal statistics are especially important in the development of invariant object recognition: the ability to recognise familiar objects independent of the viewing conditions. Here, the problem is that a small change in viewing angle, viewing distance, illumination, and gaze direction can cause a dramatic change in the retinal image of an object. In order to achieve invariant object recognition, our visual system has to develop a representation which is insensitive to the dramatic changes in the retinal image; but which is sensitive to object-specific qualities of the sensory input. These relevant qualities provide a cue for object identity. In a natural scene object identities are largely temporally invariant on the time scale of changes in gaze direction, viewing angle or other parameters. Therefore a cue for learning object identities is temporal invariance.

Földiák (1991) proposed a modified Hebbian learning rule that serves as a model for explaining the development of temporally invariant representations. The so called *trace rule* changes synaptic weights according to the temporal correlation between pre- and postsynaptic spiking activity. Weight changes depend not on instantaneous correlations only as in the Hebb rule but also

on the postsynaptic spiking history, which is preserved in a memory trace and can be described as a temporal low pass filtering of the postsynaptic activity. This has the effect that activity at one moment influences learning at a later moment and allows for learning features in the environment that are invariant over time - e.g. object identities. Several other mechanisms were proposed for learning invariant representations through temporal correlations which explain the development of essential neural properties such as the phenomenon of invariant object recognition [Wallis (1996); Wallis and Rolls (1997); Einhäuser et al. (2005); Wallis et al. (2009); Stringer et al. (2006)], place cells [O'Keefe (1976); Wyss et al. (2006); Franzius et al. (2007)] or complex cells in visual cortex [Wiskott and Sejnowski (2002); Einhäuser et al. (2002); Berkes and Wiskott (2005)]. A crucial feature in these models is the extraction of temporal statistics under natural viewing conditions: the models learn invariances for slowly changing features in input streams which relate to slowly changing features under natural viewing conditions. Those systems adapt to the spatial and temporal correlations in the input streams they are presented to.

2.6.7 Invariance Learning in Self-Organizing Networks

A biologically plausible mechanism that combines self-organization via spatial and temporal statistics in input streams was proposed by Michler et al. (2009). They showed that it is possible to map spatio-temporal correlations in input signals onto a topographic map by combining the principles of short range lateral excitation and long range lateral inhibition with the concept of the trace-rule [Földiák (1991)]. The implementation of the trace rule is realized by synapses with long synaptic decay time constants that mediate the recurrent connections and serve as a memory trace due to their long time constants. These synapses have a physiological correlate in the binding period of glutamate in NMDA channels [Wallis and Rolls (1997)]. The network architecture will be described in detail in section 4. The network maps spatio-temporal correlations in the input sequence upon the topography of a self-organizing map, which has similar properties as the object feature

topography in the inferotemporal cortex [Gross et al. (1985); Rolls et al. (1985); Rolls and Baylis (1986); Rolls et al. (1987); Tovee et al. (1994); Ito et al. (1995); Tanaka (1996); Wang et al. (1996); Tanaka (2003)].

2.6.8 Self-Organization of Contextual Interactions

In this section the view of how sensory representations and receptive fields develop in resonance with sensory experience in young organisms was reviewed. Spatio-temporal statistics, synaptic plasticity and self-organizing networks are the main key-words to keep in mind here. By this it can be explained, how receptive fields and topographic maps are formed. However, it is still an open question how contextual interactions like gain fields develop. Attempts have been made to answer this question [Zipser and Andersen (1988); Mazzoni et al. (1991); Salinas and Abbott (1997); White and Snyder (2004); Davison and Fregnac (2006)]. However, these models are quite unphysiological. In chapter 4 we will present the study "Unsupervised Learning of Gaze-Invariance" in which a physiologically plausible model for the development of contextual gain fields in visual cortex is investigated which is based on the network presented by Michler et al. (2009).

In the last chapter we focussed on reviewing the neuroscientific view of neural development concerning the question of how neural representations are formed in young organisms. Let us now consider the question of how plastic cortical representations in adult brains are.

2.7 Neural Plasticity in Adults

In visual cortex I of normally grown up cats, columnar regions of neurons can be found that respond to inputs of either the right eye or the left eye [Hubel and Wiesel (1962); Bienenstock et al. (1982); Freeman (2004)]. In their pioneering experiments, Hubel and Wiesel [Hubel and Wiesel (1965)] found that by patching one eye in young kittens, most neurons in visual cortex I responded to inputs from the open eye. Only a few cells were found to be activated by inputs to the patched eye: the structure of ocular dominance

columns was strongly altered. Transferring the patch during a critical phase of the first few months of the kittens life to the open eye inverted the effect. After that critical phase, an inversion of the effects could not be observed any more. These experiments established a view of early sensory areas as being plastic during early development but being hardwired and static after a certain critical age in adult organisms [Fahle and Poggio (2002)].

2.7.1 Adult Sensory Representations Adapt to Significant Changes in the Environment

However, adult early sensory areas show a high degree of plasticity: Once developed, the neural representations in early sensory areas are not static but are in a constant process of use dependent adaptation [Dinse and Merzenich (2002)]. In their pioneering work, Jenkins et al. (1990) showed in a neurophysiological experiment with adult owl monkeys, that finger stimulation over about ten days altered the neural representation of the stimulated fingers in primary somatosensory cortex. Characteristics of receptive fields as well as topographic representations of fingers differed greatly from that recorded in control experiments. The results of Jenkins et al. (1990) showed a clear effect of training on early sensory representations in adult owl monkeys and were a milestone - if not the foundation stone - in the field of Neuroplasticity. Use dependent plasticity of somatosensory areas was also shown in adult humans. Comparing the cortical representation of fingers in professional string players and controls showed that the cortical representation of the left hand of string players was larger than that in controls [Elbert et al. (1995)]. A wealth of studies report similar effects of training on cortical reorganization [Godde et al. (1996); Jürgens and Dinse (1997); Dinse and Merzenich (2002); Dinse et al. (2003); Lissek et al. (2009)].

2.7.2 Perceptual Learning

Sensory experience or training specifically influences perceptual performance by changing the coding properties in primary sensory areas [Fahle and Poggio (2002)]. For example practicing to discriminate small orientation deviations

of a horizontally aligned visual stimulus leads to improvements in perceptual performance for horizontal stimuli but not for vertically aligned stimuli [Fiorentini and Berardi (1980)]. In the same way improvements of vernier discrimination are specific for stimulus orientation [Fahle (1997)]. Moreover, perceptual improvements of texture discrimination are highly eye-specific [Karni and Sagi (1995); Fahle and Morgan (1996)]. This has led to the assumption that the neural correlates of these types of perceptual learning are native to a relatively early stage of processing where cells are both monocular (unlike in areas beyond primary visual cortex) and orientation-specific (unlike in the retina) [Fahle and Poggio (2002)]. Physiological experiments in primary visual areas [Gilbert and Wiesel (1992); Fahle and Skrandies (1994)], primary auditory areas [Recanzone et al. (1993)], and primary somatosensory areas [Diamond et al. (1993); Wang et al. (1995); Godde et al. (2000)] inspired by Jenkins et al. (1990) support this view of the plasticity of adult primary sensory areas [Fahle and Poggio (2002)].

A crucial factor in perceptual learning is the phenomenon of attention [Ahissar and Hochstein (2002)] which will be introduced in the next section.

2.8 Attention

As organisms, equipped with multiple sensory organs, we are confronted with a tremendous wealth of messages from the environment that our brain is asked to process in a meaningful way in order to yield adequate information about the environment whereas most of the messages from the environment are behaviorally irrelevant at the moment [Treue (2001)]. Having finite processing resources, our cognitive system needs to select some behaviorally relevant messages or tasks and withdraw others [Broadbent (1956); Deutsch and Deutsch (1963); Strayer and Johnston (2001); Spence and Read (2003)]. By this top-down influence the brain optimizes its processing resources by concentrating processing on a very small portion of incoming messages [Treue (2001)]. William James, one of the founders of psychology, stated in his book *the principles of psychology* [James (1890)]:

”Everyone knows what attention is. It is the taking possession by

the mind in clear and vivid form, of one out of what seem several simultaneously possible objects or trains of thought. Focalization, concentration of consciousness are of its essence. It implies withdrawal from some things in order to deal effectively with others.”

The view of attention as a selecting mechanism is still up-to-date in psychology [Ahissar and Hochstein (2002); Ashcraft (2005)].

2.8.1 Input Attention and Controlled Attention

In cognitive psychology, mainly two forms of attention are distinguished: input attention and controlled attention [Ashcraft (2005)]. Input attention denotes a mostly input-driven, reactive, involuntary process. The orienting reflex, the immediate response of an organism to significant changes in the environment by directing attention to the novel phenomenon, is one example that can be captioned by the term input attention [Cowan (1995); Abrams and Christ (2003)]. In contrast to input attention, controlled attention denotes the act of voluntarily directing attention to phenomena that are of interest for an organism without the necessary condition of significant changes in the environment. ”I” control or select what I want to pay attention to and what I want to ignore instead. This is why the ability to attend to one phenomenon while ignoring another is also called selective attention. Here, phenomena can be physical objects in the environment as well as thought or ideas [Ashcraft (2005)].

Paying attention to a task has strong implications for perception and action. For example, without directing attention to a simple reporting task, false conjunctions are likely to be made between color and shape in an unattended region of the displayed stimuli [Treisman and Gelade (1980)]. By directing attention to a message spoken by one person, while being disturbed by other messages by many other speakers, we can reliably understand the selected message. This phenomenon is termed *cocktail party effect* and its reliability depends on the physical differences between the spoken messages [Cherry (1953); Cherry and Taylor (1954)].

2.8.2 Neural Correlates of Attention

The process of paying attention changes the neural responses of single neurons in the absence of changes in sensory inputs as reviewed in [Treue (2001)]. For example, when a monkey pays attention to a given stimulus, the neurons that encode the stimulus show enhanced responsiveness and selectivity as well as altered tuning curves [Spitzer et al. (1988); Mountcastle et al. (1987); Richmond and Sato (1987)]. The amount of arousal also has an effect on the responsiveness of single neurons in visual cortex of cats in a way that neurons of sleeping cats show a reduced signal-to-noise ratio compared to awake cats [Livingstone and Hubel (1981)]. Top-down attentional modulations of neural responses and neurons tuning curves go all the way back to the very primary sensory cortices [McAdams and Maunsell (1998); Roelfsema et al. (1998); Ito and Gilbert (1999); McAdams and Maunsell (1999); Lee et al. (1999); Gilbert et al. (2000); McAdams and Maunsell (2000); Corbetta et al. (1990); Brefczynski and De Yoe (1999); Gandhi et al. (1999); Martinez et al. (1999); Somers et al. (1999); Treue (2001)]. Here, directing attention on a stimulus seems to induce a gain-modulating effect in those neurons in primary sensory cortices that encode the specific stimulus [Treue (2001)].

2.8.3 Attention and Perceptual Learning

Psychophysical experiments indicate that attention is essential for the learning of simple tasks in perceptual learning [Ahissar and Hochstein (1993, 2002)]. Experimenters found a near absence of learning when subjects did not attend to the stimulus aspects that were relevant for the task. This indicates that the attentional focus may prevent the organism from learning irrelevant stimulus aspects [Ahissar and Hochstein (2002)]. Furthermore, the attentional focus increases the effectiveness of perceptual training in the auditory, visual, and somatosensory domain [Seitz and Dinse (2007)].

In chapter 5 I will present the study "Improvement of Tactile Perception by Meditation". Here, it is indicated that attention is not only an essential ingredient for learning but that it is also sufficient: perceptual learning occurs

in the absence of any external training only by paying sustained attention to a sensory phenomenon.

3 Multiplication in Neurons via Permissive Gating

3.1 Abstract

Multiplicative interactions in neurons are omnipresent in the nervous system [Salinas and Sejnowski (2001)]. However, the mechanisms that underlie these multiplicative interactions are unclear. In this study, we investigated permissive gating [Katz (2003); Kepecs and Raghavachari (2007); Gisiger and Boukadoum (2011)] as a possible multiplication mechanism. Permissive gating was modelled via two functionally different input pathways which interact in a specific manner: input from the *feeding* pathway F contributes to the somatic membrane potential of the neuron only if input from the *gating* pathway G exceeds a specific gating threshold γ .

The applied gating-mechanism realized multiplicative interactions of firing rates on a wide range of parameters and thus provides a feasible model for the realization of multiplicative interactions on the single neuron level.

3.2 Introduction

In 1907, Louis Lapicque proposed a classical model of action potential generation in neurons which today is called the *integrate-and-fire* model: whenever the *sum* over synaptic inputs exceeds a *spiking threshold*, an action potential is generated [Lapicque (1907)]. After more than one hundred years of scientific development, including the formulation of the Hodgkin-Huxley model which explains the generation of action potentials via the dynamical interaction of voltage dependent ion-channels [Hodgkin and Huxley (1952)], the integrate-and-fire model is still a valid working hypothesis for modelling single neurons [Dayan and Abbott (2002); Herz et al. (2006); Brunel and van Rossum (2007)]. In the view of the integrate-and-fire model an important characteristic of the cell is its output firing rate - the number of spikes per second - in relation to one input stream. The output firing rate is obtained by temporally *averaging* over a spike train. This allows to derive the classical receptive field of the

neuron which describes the selectivity of the neuron for a given stimulus space. The canonical computations in those kinds of models are *summation*, *thresholding*, and *averaging*. Studies published over the last decades suggest, that this view of a neuron as a simple summation and thresholding stage that provides an output firing rate should be revised.

In 1983 Anderson and Mountcastle found evidence for a *multiplicative* effect of gaze direction on the output firing rate of neurons in area 7a of parietal cortex of macaque monkeys that are selective for visual stimuli [Andersen and Mountcastle (1983)]. Additional to the well known properties of neurons showing selectivities for sensory stimuli, these neurons were found to include contextual information about gaze direction in a non canonical, *multiplicative* fashion. Such multiplicative interactions have turned out to be omnipresent in the nervous system. The most prominent examples are source-position estimations in the barn owl auditory system [Pena and Konishi (2001); Fisher et al. (2007)], looming stimulus detection [Gabbiani et al. (2002)], binocular interaction [Freeman (2004)], motion detection in the visual system [Hassenstein and Reichardt (1956); Reichardt (1961); Borst (2011)], gaze direction gain fields and coordinate transforms in the visual system [Andersen and Mountcastle (1983); Andersen et al. (1985); Brotchie et al. (1995); Ono et al. (2010)], and modulation of neurons output firing rates by attentional context [Treue and Martinez-Trujillo (1999); McAdams and Maunsell (2000); Womelsdorf et al. (2006)].

The ability of neurons to multiply inputs implies tremendous computational abilities for neural networks. The Stone-Weierstrass theorem [Stone (1948)] states that any continuous function can be accurately approximated by polynomials [Koch and Poggio (1992); Nezis and van Rossum (2011)]. Polynomials are compositions of variables and constants via summation, subtraction, and multiplication. Summation and subtraction are notorious features of neurons equipped with excitatory and inhibitory synapses. Including the ability to multiply inputs in this system thus allows it - in principle - to compute any function of its inputs. In computational modelling, prominent examples for this computational power are coordinate transformations via basis function networks [Pouget and Snyder (2000)]. Basis function networks can be seen

as the neural correlate of the Stone-Weierstrass theorem as they allow to compute a wealth of nonlinear functions of their inputs [Dayan and Abbott (2002)].⁷

Subsuming, multiplication is omnipresent in the nervous system and the ability to multiply inputs leads to a wealth of computational abilities and perceptual benefits. Multiplicative interactions can be modelled phenomenologically in black-box models of neurons without caring about the biophysical mechanisms that realize multiplication in the brain. This has led to many insights concerning the possibilities that the application of multiplicative mechanisms in neural networks allows for [Zipser and Andersen (1988); Salinas and Abbott (1995); Pouget and Snyder (2000)]. However, the biophysical basis of multiplicative interactions remains unclear.

A wealth of possible biophysical mechanisms has been proposed over the last decades in order to answer the question of how multiplication could in principle be realized by the physiological mechanisms available in the brain [Koch and Poggio (1992); Salinas and Sejnowski (2001)]. They differ with respect to two main approaches. One set of approaches focusses on the explanation of multiplicative mechanisms as an emergent property of neural networks composed of ordinary single neurons that themselves are not capable of mediating multiplicative interactions. Here, ordinary means that neurons do not need more functional properties than the traditional averaging, thresholding, summation, and subtraction to realize multiplication in the networks. Here, multiplication is mediated by specific feedforward networks [Nezis and van Rossum (2011)] as well as by recurrent network connectivities [Salinas and Abbott (1996); Salinas and Sejnowski (2000)]. The second approach focuses on the explanation of multiplicative interactions via biophysical mechanisms in single cells. Here, dendritic interactions [Tal and Schwartz (1997); Larkum et al. (2004)], coincidence detection [Srinivasan and Bernard (1976)], background synaptic activity [Chance et al. (2002); Brostek

⁷Chapter 4 deals with the computational power of basis function networks: the described network transforms retina-centered to head-centered coordinates - which implies massive benefits for perception and action in an organism.

(2012)], or nonlinear properties of ion channels [Mel (1992, 1999); Schiller et al. (2000)] are taken into account in order to explain multiplicative interactions. The above mentioned mechanisms that propose answers to the question of how multiplication could in principle be mediated by the physiological mechanisms available in the brain are presented in detail in the supplementary materials (chapter 8.1.1 and 8.1.2). In the following I will focus on a mechanism called *permissive gating* which is another such candidate mechanism and serves as the basis for the multiplicative interactions in the model neuron presented in this study.

3.2.1 Permissive Gating

In permissive gating, the presence of the gating-input A opens a gate for input B and thus allows input B to pass and contribute to the membrane potential of the neuron. By this, input B can only contribute to the membrane potential of the neuron, if the gating-input A is present. However, the gating-input A does not directly contribute to the membrane potential but only input B does. This permissive form of gating can be thought of as being a basis for gain-modulation and multiplicative interactions as it implements a sort of AND gate.

Gating is commonly understood to be a mechanism for *excluding* synaptic input - the ability to close gates that are open and thus to forbid signals to pass [Katz (2003)] also known as *shunting*. In this view, the presence of the gating-input A would forbid signal B to pass. Primary afferent depolarization is a classical example of exclusive gating: Here, central locomotor circuits (gating-input A) prevent sensory input (B) from arriving during inappropriate phases of the locomotor cycle by inhibiting the release of neurotransmitters from sensory afferents [Rudomin (1999); Büschges and El Manira (1998)]. But gating can also be understood in the above mentioned permissive fashion. Many possible biophysical mechanisms that may serve as a basis for permissive gating were investigated over the last years. One candidate mechanism for the biophysical basis of permissive gating is neuromodulation. Studies in the mollusc *Aplysia* have shown that serotonin selectively enhances the

amount of neurotransmitters released from sensory neurons [Byrne and Kandel (1996)] leading to permissive gating. Other candidate mechanisms that could realize permissive gating involve ionotropic receptors [MacDermott et al. (1999); Vitten and Isaacson (2001)] or intrinsic neuromodulation [Katz and Frost (1996)]. Other studies focus on explaining permissive gating via the interaction between resting membrane potentials and integrative electrophysiological properties of neurons [Ivanov and Calabrese (2003); Evans et al. (2003); Herberholz et al. (2002); Katz (2003)]. Last but not least, *bistable* or *up/down* neurons that oscillate between silent *down* states and firing *up* states are thought to be a basis for gating information in the cortex [Gisiger and Boukadoum (2011)] and are meant to be common in the brain [MacLean et al. (2005)]. Here, the *down* state names a situation with hyperpolarized membrane potentials, the *up* state names a situation where the neurons membrane potential is just below the neurons firing threshold. Furthermore, the *down* state is accompanied with the complete absence of action potential generation by the neuron, whereas in the *up* state action potentials can be observed.⁸

3.2.2 Permissive Gating and Multiplicative Interactions

In 2007 Kepecs and Raghavachari examined the roles of NMDA-receptors in postsynaptic integration and found that NMDA-receptors may serve to gate the flow of information as well as control the gain of information transfer [Kepecs and Raghavachari (2007)]. The authors proposed a biophysical model that realizes the phenomena of an *up/down* neuron via two input pathways with different AMPA/NMDA receptor content. The proposed model is a detailed two-compartmental Hodgkin-Huxley like model [Hodgkin and Huxley (1952)] composed of a spike-initiation zone and an active dendrite.

⁸For example, neurons in the nucleus accumbens (NAC) show these transitional *up/down* properties [O'Donnell and Grace (1995)]. Here, stimulation of the prefrontal cortex triggers almost no action potentials in NAC neurons when they are in a *down* state, where stimulation of hippocampal neurons leads to a shift of NAC neurons from a *down* to an *up* state - without invoking spike initiation in NAC neurons. However, stimulation of prefrontal cortex reliably leads to spikes in NAC neurons when those neurons are in an *up* state. Hippocampal input to NAC neurons can thus be understood as being a gatekeeper [Katz (2003)] for prefrontal-cortex input in NAC neurons.

Here, the NMDA-rich pathway gates the spike generation of the AMPA-rich pathway: the AMPA-rich pathway can not trigger an up-state and alone can not generate enough current to generate an action potential. However, sufficiently strong input to the NMDA-rich pathway can trigger an up-state and allow input to the AMPA-rich pathway to elicit a spike. Once in the up-state, a further increase in input to the NMDA-rich pathway changes the gain of the neuron by realizing a multiplicative increase in the output firing rate of the neuron without changing its selectivity resulting from inputs to the AMPA-rich pathway. These gain-modulatory properties correspond to physiological findings [Andersen and Mountcastle (1983)]. The results of Kepecs and Raghavachari (2007) suggest that permissive gating mechanisms in principle are capable of realizing multiplicative interactions between two input streams.

3.2.3 Scope of this study

Multiplicative mechanisms as well as mechanisms of permissive gating are common in the brain [Katz (2003)]. The study by Kepecs and Raghavachari (2007) showed that permissive gating may lead to multiplicative interactions in a detailed biophysical model neuron. However, in simulations of learning mechanisms in large networks, computational time has to be kept as small as possible from a practical point of view. Here, simple integrate-and-fire models are more feasible than detailed biophysical models, as they skip the time-consuming process of calculating the detailed generation of action potentials. In this study we investigate a simple implementation of a permissive gating mechanism due to its ability to realize multiplicative interactions between two input streams in an integrate-and-fire model neuron [Eckhorn et al. (1990)].

3.3 Methods

We investigated a phenomenological implementation of a permissive gating mechanism due to its ability to realize multiplicative interactions in a spiking neuron model. Incoming spikes are modelled as delta pulses and elicit excitatory postsynaptic potentials (EPSPs) as an impulse response in two separate

dendritic regions. The time course of the feeding (F) and gating (G) EPSPs (measured in mV) is modeled by an instantaneous jump in the postsynaptic potential followed by an exponential decay

$$F(t) = w_f \cdot e^{-dt/\tau_f} \quad G(t) = w_g \cdot e^{-dt/\tau_g} \quad (3.1)$$

where t is an integer time-step with duration $dt = 0.25\text{ms}$. The amplitude of the impulse response is specified by the synaptic weights w_f and w_g (in mV). The permissive gating mechanism is implemented by a specific interaction between the two dendritic regions: EPSPs from the *feeding* stream F only contribute to the somatic membrane potential of the neuron if EPSPs from the *gating* stream G exceed a specific gating threshold γ . By this, the gating stream permissively gates the feeding input stream. Successive EPSPs elicited in the same dendritic region superimpose linearly. The feeding input stream represents junctions in the main stimulus driven pathway of a neuron where the gating stream represents junctions receiving contextual signals that are meant to modulate the feeding inputs influence on the output firing rate.

The somatic membrane potential of a neuron at time step t thus computes as

$$U(t) = F(t) \cdot \Theta(G(t) - \gamma) \quad (3.2)$$

where $\Theta(x)$ is the Heaviside step function and γ (in mV) is the gating-threshold. The resting membrane potential is 0mV.

To allow for a preliminary investigation of the gating mechanism, mechanisms of spike thresholding in the soma will be skipped in a *simplified neuron model*. In this situation the output spike train is a simple copy of the feeding input stream if the gate is opened all the time. The output firing rate of the model neuron decreases when the opening probability of the gate is lowered. This skipping of thresholding mechanisms in the soma allows us to investigate the influence of the gating mechanism with regard to the opening probability of the gate independent of nonlinear interactions in the somatic region. This neuron model will be called *simplified neuron model* in the following.

A skipping of somatic thresholding mechanisms is useful for the investigation of the gating mechanism but is biologically implausible with regard to the

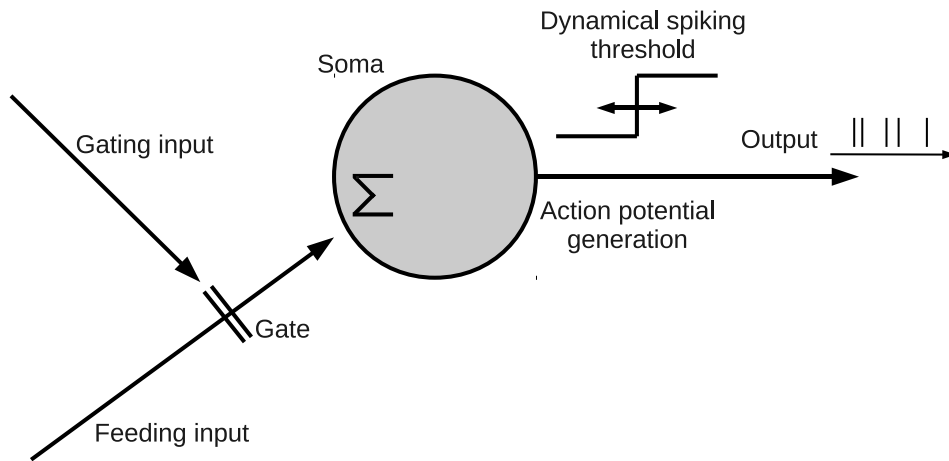


Figure 1: **Gating model neuron.** The figure displays the signaling pathway in the gating model neuron. Feeding inputs $F(t)$ contribute to the somatic membrane potential $U(t)$ only when gating inputs $G(t)$ are large enough to open the gate by crossing the gating-threshold γ . Inputs are integrated in the soma. When the somatic membrane potential $U(t)$ crosses the dynamical threshold $\Gamma(t)$, an action potential is generated. In the simplified model, somatic mechanisms are skipped in order to investigate the gating mechanism independent of somatic nonlinearities: the dynamical spiking threshold and synaptic decay time constants in the feeding stream are set to zero. Thus, in the simplified model, each spike in the feeding stream elicits a spike in the output stream if the gate is open ($G(t) > \gamma$). For the mathematical formulation see equation 3.2.

dynamical integrate-and-fire nature of action potential generation. Thus, we set up a second model neuron which will be called *complete model neuron* in the following. We extended the simplified model neuron with skipped somatic mechanisms by a somatic thresholding mechanism similar to the one used in the *Marburg Model Neuron* proposed by Eckhorn et al. in 1990 [Crair and Malenka (1995); Eckhorn et al. (1990); Pauly (2000)]. Synaptic decay time constants are chosen to be $\tau_f = \tau_g = 7\text{ms}$ initially. An action potential is generated when the somatic membrane potential $U(t)$ exceeds a dynamical threshold $\Gamma(t)$. This dynamical threshold consists of a baseline threshold $\Gamma_{base} = 1\text{mV}$ and a threshold potential $\Gamma_\xi(t)$.⁹ When a spike is generated at time step t_s , the threshold potential is increased by a fixed value $\xi = 1\text{mV}$ and then exponentially decays with time constant $\tau_\xi = 10\text{ms}$. The dynamical threshold at time step t thus computes as

$$\Gamma(t) = \Gamma_{base} + \Gamma_\xi(t) \quad (3.3)$$

$$\Gamma_\xi(t) = \xi \cdot \sum_{t_s} \exp(-dt \cdot (t - t_s)/\tau_\xi). \quad (3.4)$$

This kind of thresholding serves as a simulation of the absolute and relative refractory period in real neurons [Eckhorn et al. (1990)]. The model neuron is illustrated in figure 1.

Input spike trains to the model neuron are modelled as a homogeneous Poisson process which is often used as an approximation of stochastic neural firing [Dayan and Abbott (2002)]. Evaluation methods will be described in the respective passage in the results section. Simulations were executed on a *Lenovo x61s* laptop running Ubuntu 10.04 LTS. Simulation software was written in the programming language *Python* (version 2.6.5) using standard scientific libraries (*Scipy*, *Numpy* and *Pylab*). Each parameter set was simulated for 10s with a sampling rate of $dt = 0.25\text{ms}$.

⁹All voltage-related units in the theoretical studies presented in this thesis (chapters 3 and 4) are gauged in relation to the arbitrarily chosen value of the dynamical spiking threshold $\Gamma_{base} = 1\text{mV}$.

3.4 Results

In this section the model neurons will be investigated focussing on the effect of the gating mechanism on the neurons output. We will first consider the generation of single spikes in the complete model neuron that incorporates the interaction between the gating and the feeding input stream as well as somatic spike thresholding. After that we consider the influence of the gating mechanism on the average output firing rate of the simplified model neuron with skipped somatic thresholding mechanisms. We will analytically derive a relationship between parameters of the gating input stream and the opening probability of the gate and relate it to the output firing rate of the simplified model neuron. Simulations with the simplified and complete model neuron show that the gating mechanism realizes multiplicative interactions on a wide range of input parameters.

3.4.1 Generation of Single Spikes - Complete Model Neuron

Typically, integrate-and-fire neurons elicit a spike when the sufficient condition that the sum over synaptic input currents exceeds a spiking threshold is met [Lapicque (1907); Eckhorn et al. (1990)]. Only one condition has to be met here to allow the model neuron to elicit a spike. In the model neuron presented here, two conditions have to be met to allow the input streams to elicit a spike. First, the gating potential $G(t)$ has to be larger than the gating threshold γ in order to let the Heaviside function $\Theta(G(t) - \gamma)$ become 1 and thus to let feeding inputs pass on to the somatic thresholding mechanism (equation 3.2). Second, the feeding potential $F(t)$, that determines the membrane potential $U(t)$ when the gate is open, has to be larger than the dynamical spiking threshold $\Gamma(t)$. Only when these two conditions

$$(G(t) > \gamma) \text{ AND } (F(t) > \Gamma(t))$$

are met, can a spike be elicited. This mechanism is illustrated in figure 2 and implements an AND gate between the feeding and the gating input-stream which is known to be a basis for multiplicative interaction [Mel (1999)].

If nonlinear spike thresholding mechanisms in the soma are skipped in the

simplified model neuron, an output spike is elicited in the model neuron if (1) a spike in the feeding input stream and (2) an open gate ($G(t) > \gamma$) occur simultaneously.

3.4.2 Influence of the Gating Mechanism on Output Firing Rates - Simplified Model Neuron

The concept of gain modulation assumes a modulatory input stream to multiplicatively modulate the output firing rate of a neuron with respect

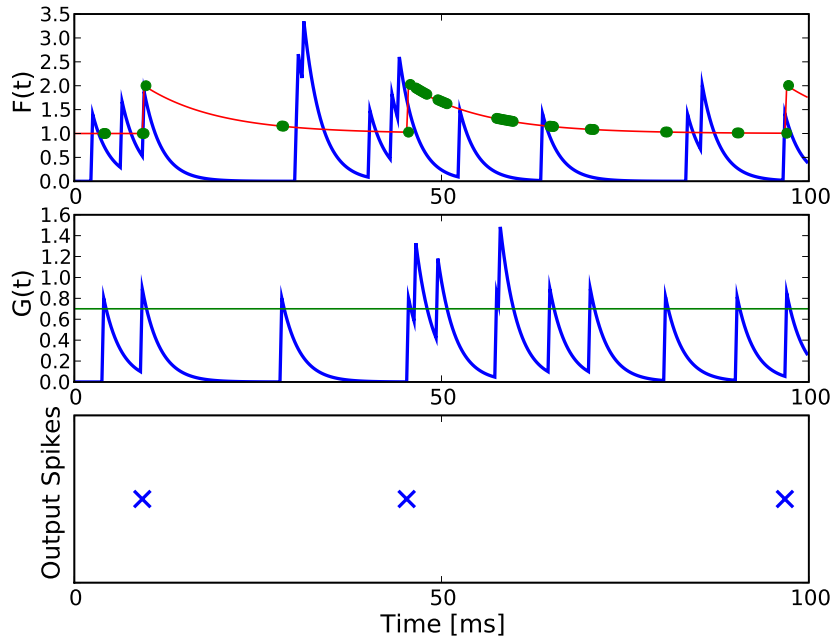


Figure 2: **Generation of output spikes in the complete gating model neuron.** The upper panel shows feeding EPSPs $F(t)$ as an impulse response to incoming spikes at feeding synapses (blue trace) and the dynamical spiking threshold $\Gamma(t)$ (red trace). The middle panel shows gating EPSPs $G(t)$ elicited by gating inputs (blue trace) and the static gating threshold $\gamma = 0.7\text{mV}$ (green trace). Whenever $G(t) > \gamma$ feeding potentials $F(t)$ are allowed to contribute to the membrane potential (green dots in the upper panel). A spike is generated (lower panel), when the two necessary conditions that (1) the gating potential is larger than the gating threshold ($G(t) > \gamma$) and (2) the feeding potential is larger than the dynamical threshold $F(t) > \Gamma(t)$ are met. One of these two conditions alone is not sufficient to elicit a spike.

to a sensory input stream [Andersen and Mountcastle (1983); Salinas and Sejnowski (2001)]. To investigate if the gating mechanism presented here is a feasible model for mediating gain modulation we test how inputs to the gating input stream influence output firing rates of the model neuron with respect to the feeding input stream. We first skip the spike thresholding mechanism in the soma of the model neuron setting $\Gamma(t) = 0\text{mV}$ and $\tau_f = 0\text{ms}$ as described in the methods section for the *simplified model neuron*. Thus, each spike in the feeding input stream elicits one output spike if the gate is open ($G(t) > \gamma$). When the gate is open all the time, the output stream is a copy of the feeding input stream and the output firing rate r_o equals the feeding inputs firing rate r_f . If the gate is closed all the time, no output spike is elicited at all ($r_o = 0\text{Hz}$). In between these two extreme situations, we expect the gating mechanism to modulate the output firing rate r_o between 0Hz (gate closed all the time) and the firing rate of the feeding input stream $r_o = r_f$ (gate open all the time). We express the output firing rate r_o as the product of the opening probability of the gate p_{open} and the feeding input frequency r_f :

$$r_o = r_f \cdot p_{open} \quad (3.5)$$

We then analytically describe the opening probability of the gate p_{open} as a function of the gating input firing rate r_g , the gating decay time constant τ_g and the gating input weight w_g . When the input weight w_g is larger than the gating threshold γ , one spike in the gating input stream opens the gate and it takes a time of t_c milliseconds until the gate closes again. The closing time t_c can be calculated via the time it takes until the exponentially decaying gating EPSP with amplitude w_g relaxes to the gating threshold value of γ :

$$w_g \cdot e^{-t_c/\tau_g} = \gamma \quad (3.6)$$

$$\Leftrightarrow t_c = \tau_g \cdot \ln\left(\frac{w_g}{\gamma}\right) \quad (3.7)$$

When average inter spike intervals $isi_g = 1/r_g$ are much larger than the closing time t_c then overlapping gating EPSPs can be neglected. In this situation the probability p_{open} that the gate is open can be estimated by the

product of t_c and the input firing rate r_g :

$$p_{open}(r_g, \tau_g, w_g, \gamma) = r_g \cdot t_c \quad (3.8)$$

This suggests that the opening probability p_{open} is proportional to the gating input firing rate with proportionality factor t_c given that $isi_g \gg t_c$ and $w_g > \gamma$. Under these conditions the combination of equation 3.5 and equation 3.8 suggests that the output firing rate r_o with respect to r_f is modulated multiplicatively by the gating firing rate r_g with proportionality factor t_c :

$$r_o = r_f \cdot p_{open} = r_f \cdot r_g \cdot t_c \quad \text{when } isi_g \gg t_c \text{ and } w_g > \gamma. \quad (3.9)$$

Figure 3 illustrates this for a feeding firing rate of $r_f = 150\text{Hz}$ and $t_c =$

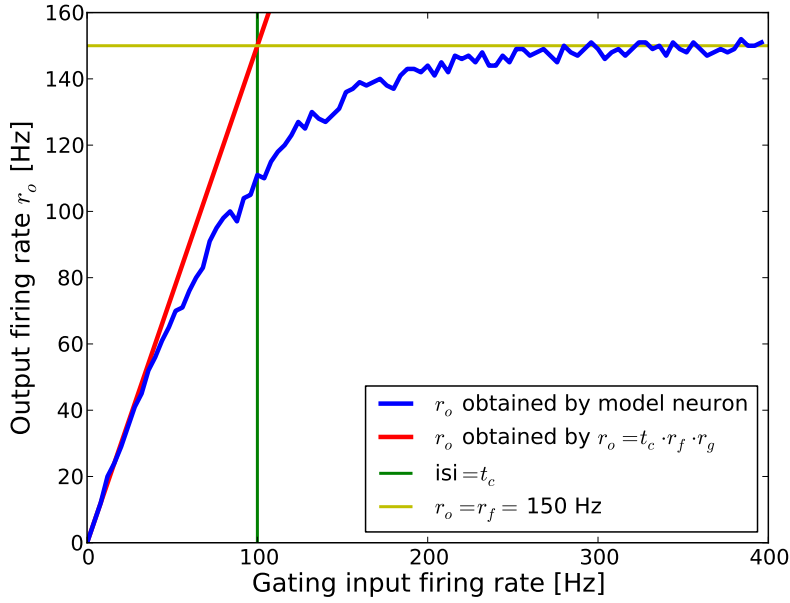


Figure 3: **Output firing rate as a function of gating input firing rate in the simplified model neuron.** Output firing rates r_o of the simplified model neuron are shown in the blue trace as a function of gating input firing rates. The red trace shows output firing rates as predicted by equation 3.9. The predicted output firing rate deviates from the models output firing rate when the claim $isi_g \gg t_c$ is violated. Inter spike intervals equal the closing time t_c when $r_g = 100$ Hz (green trace $isi = t_c$). The yellow trace illustrates the saturation frequency $r_o = r_f = 150$ Hz which is reached when the gate is opened all the time.

10ms ($w_g = 3.0\text{mV}$, $\tau_g = 7\text{ms}$). Output firing rates of the model neuron are well described by equation 3.9 when $isi_g \gg t_c$ (which corresponds to $r_g \ll 100\text{Hz}$) but not when interspike intervals are in the range of t_c . When the gating firing rate is $r_g = 100\text{Hz}$ average interspike intervals equal the closing time ($isi_g = t_c$). Here, equation 3.9 predicts an output firing rate of 150Hz that should equal the feeding input firing rate because the gate should be opened all the time. Nevertheless, the saturation frequency of 150Hz was foremost reached at much higher gating input firing rates due to overlapping gating EPSPs which decrease the opening probability. This is not considered in the analytical description of the model. Output firing rates deviated from predicted firing rates at a gating input frequency larger than approximately 50Hz. Thus, in the following we simulated the model neuron in a range where $isi_g > 2t_c$.

We tested the model for different feeding and gating input firing rates $r_f = [0, \dots, 150]\text{Hz}$ and $r_g = [0, \dots, 150]\text{Hz}$ with a closing time of $t_c = 2.5\text{ms}$ ($w_g = 1.0\text{mV}$, $\tau_g = 7\text{ms}$). As the smallest average inter spike intervals in the gating input stream were larger than the closing time $isi_{min} = \frac{1}{150\text{Hz}} = 6.7\text{ms} > 2t_c$ we expected the output firing rate to be the weighted product of the feeding and the gating input firing rates under the assumption that the analytical equation 3.9 describes the model neuron sufficiently. Figure 4 shows the 2-d-matrix of output firing rates as a function of feeding and gating input firing rates. Here, it can be seen that gating inputs modulated the output firing rate for a wide range of feeding input firing rates. To quantify the type of interaction between the feeding and the gating inputs, the 2d-array of output firing rates was fit based on a multiplicative and an additive model as done in previous studies [Pena and Konishi (2001); Fisher et al. (2007); Kepecs and Raghavachari (2007)]:

$$r_{mult}^{out} = a_m \cdot r_f \cdot r_g \quad (3.10)$$

$$r_{add}^{out} = a_s \cdot r_f + b_s \cdot r_g. \quad (3.11)$$

a_m , a_s and b_s were fitting parameters. Analytical models were fit to the data by a least square method. The multiplicative analytical model corresponds to

equation 3.9 with the fitting parameter a_m representing the closing time t_c . Correlations between the multiplicative analytical model and the output of the gating neuron model were high $r^2 = 0.987$ (figure 5). The additive

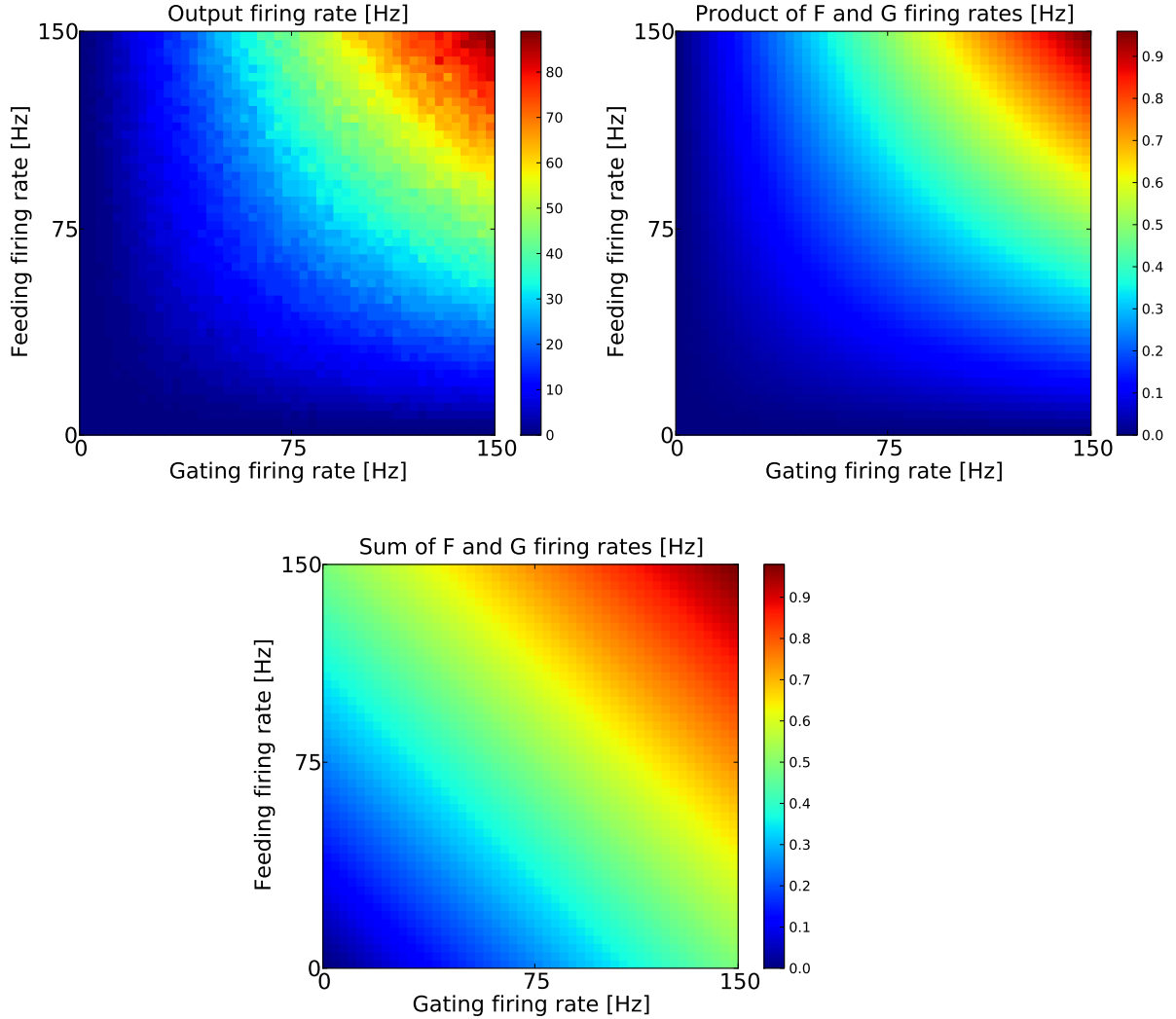


Figure 4: **Output firing rates of the simplified model neuron as a function of feeding and gating input firing rates.** Upper left panel: output frequency of the simplified gating model neuron as a function of feeding input firing rates and gating input firing rates. Gating inputs modulated the output firing rate for different feeding input firing rates. Upper right panel: normalized exact product of the feeding and gating input firing rates. Lower panel: normalized exact sum of feeding and gating input firing rates. Visual inspection indicates that the model neuron showed multiplicative rather than additive behaviour.

model showed a lower correlation value $r^2 = 0.668$. Moreover, the fitting parameter a_m of the multiplicative analytical model reflected the constant closing time factor t_c in equation 3.9: $t_c = 2.5\text{ms}$ and $a_m = 2.3\text{ms}$. Repeating the simulations for parameters that violate the condition $isi_g > 2t_c$ with $r_g = [0, \dots, 400]\text{Hz}$ with a minimal inter spike interval of $isi_{min} = \frac{1}{400} = 2.5\text{ms}$ and a closing time of $t_c = 10\text{ms}$ ($w_g = 3.0\text{mV}$, $\tau_g = 7\text{ms}$) yielded relatively small correlation values of $r^2 = 0.8$ for the multiplicative and $r^2 = 0.6$ for the additive model. This is as overlapping gating EPSPs and saturation effects that appear when $isi_g \not> t_c$ are not considered in the analytical models.

To test equation 3.9 for different parameters, we did two experiments. First, we varied the gating input weights between $w_g = [1.0, \dots, 10.0]\text{mV}$ while mutually varying τ_g to keep t_c constant. Here, we also kept the gating threshold $\gamma = 0.7\text{mV}$ constant; second, we varied gating input weights be-

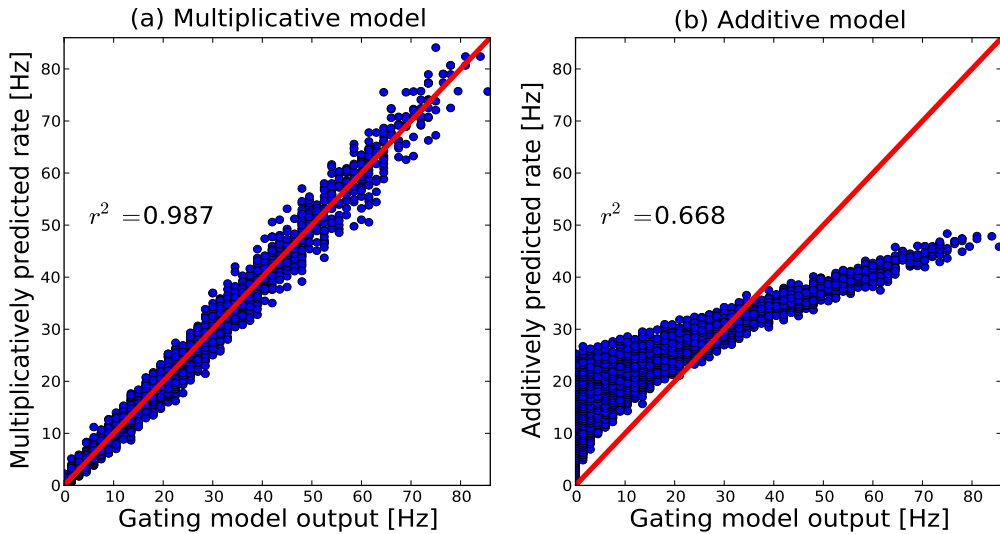


Figure 5: **Correlations between the responses predicted by analytical models and the data obtained with the gating threshold model.** Firing rates obtained by fitting the multiplicative (eq. 3.10) and the additive analytical model (eq. 3.11) are plotted against the output of the gating model neuron. The red line denotes the diagonal with correlation value 1. Analytical models are explained in the main text. (a) Correlation between data and multiplicative model r_{mult}^{out} with $r^2 = 0.99$. (b) Correlation between data and additive model r_{add}^{out} with $r^2 = 0.67$.

| | | | | | |
|---------------|------|------|------|------|------|
| w_g [mV] | 1.0 | 2.0 | 5.0 | 10 | 20 |
| τ_g [ms] | 8.0 | 2.7 | 1.4 | 1.07 | 0.85 |
| r_{mult}^2 | 0.99 | 0.99 | 0.99 | 0.99 | 0.99 |
| r_{add}^2 | 0.66 | 0.65 | 0.67 | 0.67 | 0.67 |
| fit a_m | 2.6 | 2.6 | 2.38 | 2.33 | 2.31 |

Table 1: **Correlation values** between the multiplicative analytical model and the output of the simplified gating neuron model r_{mult}^2 and correlation values between the additive analytical model and the output of the simplified gating neuron model r_{add}^2 . Gating weights w_g and gating time constants τ_g were varied mutually in order to keep $t_c \approx 2.8$ ms constant (eq. 3.7 with constant gating threshold $\gamma = 0.7$ mV). Correlation values were high for the multiplicative analytical model and low for the additive analytical model. The multiplicative fitting parameter a_m was in the range of the closing time t_c .

tween $w_g = [1.0, \dots, 20.0]$ mV while mutually varying the gating threshold $\gamma = [0.35, \dots, 7.0]$ mV to keep t_c constant. Here, we kept $\tau_g = 5$ ms constant. We varied feeding and gating input firing rates $r_f = [0, \dots, 150]$ Hz and $r_g = [0, \dots, 150]$ Hz and calculated t_c with a supposed saturation firing rate of $r_g = 350$ Hz in order to fulfill $isi_g > 2t_c$. By this, every parameter in equation 3.9 was varied in a broad range. Table 1 shows that changing w_g and τ_g mutually while keeping γ constant did not influence the correlation values. Moreover, the closing time $t_c \approx 2.8$ ms was in the range of the fitting parameter a_m . Changing w_g and γ mutually while keeping τ_g constant also did not influence correlation values as shown in table 2. Here, the closing time t_c was also in the range of the fitting parameter a_m (eq. 3.10). Correlation values were high for the multiplicative analytical model invariant of mutual changes in gating input weights w_g , gating time constant τ_g or gating threshold γ . This confirms that the output firing rate of the model neuron is sufficiently described by $r_o = t_c \cdot r_f \cdot r_g$ under conditions $isi_g > 2tc$ and $w_g > \gamma$ (eq. 3.9) in the tested range. The model neuron is reliably described by a multiplicative interaction between the feeding and the gating input streams.

| | | | | | |
|---------------|------|------|------|------|------|
| $w_g[mV]$ | 1.0 | 2.0 | 5.0 | 10 | 20 |
| $\gamma [mV]$ | 0.35 | 0.7 | 1.75 | 3.5 | 7.0 |
| r_{mult}^2 | 0.99 | 0.99 | 0.99 | 0.99 | 0.99 |
| r_{add}^2 | 0.65 | 0.66 | 0.66 | 0.65 | 0.67 |
| fit a_m | 2.6 | 2.5 | 2.6 | 2.6 | 2.6 |

Table 2: **Correlation values** between the multiplicative analytical model and the output of the simplified gating neuron model r_{mult}^2 and correlation values between the additive analytical model and the output of the simplified gating neuron model r_{add}^2 . Gating weights w_g and gating thresholds γ were varied mutually in order to keep $t_c \approx 2.8$ ms constant (eq. 3.7 with constant gating time constant $\tau_g = 5$ ms). Correlation values were high for the multiplicative analytical model and low for the additive analytical model. The fitting parameter a_m was in the range of the closing time t_c .

3.4.3 Gating Mechanism in the Complete Model Neuron

We now transfer the findings obtained with the simplified model neuron to the model neuron that incorporates dynamical thresholding of feeding EPSPs. The influence of the gating mechanism on the output firing rate of the simplified model neuron was described by the opening probability. Analytical equations concerning the opening probability of the gate are still valid here. Equation 3.9 describes the conditions that have to be met for the gating stream to have a multiplicative influence on the output firing rate of the model neuron. In the last chapter it was shown that this equation describes the gating mechanism invariant of mutual changes in gating parameters. Thus, in the following gating parameters are fixed to one set of parameters which fullfils equation 3.9 for gating firing rates between 0 and 150 Hz ($w_g = 1.0$ mV, $\tau_g = 8.0$ ms, $\gamma = 0.7$ mV). We hypothesize that with these parameters a multiplicative interaction between the feeding and the gating input stream is obtained.

To quantify the type of interaction between the feeding and the gating input stream, we fitted the multiplicative (eq. 3.10) and additive (eq. 3.11) analytical models to 2d-arrays of output firing rates obtained by varying feeding and gating input firing rates between 0Hz and 150Hz. In the feeding input stream we varied parameters $w_f = [0.5, \dots, 25]$ mV and $\tau_f = [1, \dots, 50]$ ms

| $\frac{r_{o,max}[Hz]}{r_{mult}^2/r_{sum}^2}$ | $\tau_f = 2ms$ | $\tau_f = 5ms$ | $\tau_f = 10ms$ | $\tau_f = 25ms$ |
|--|-------------------------|-------------------------|-------------------------|-------------------------|
| $w_f = 0.5mV$ | $\frac{1}{-/-}$ | $\frac{4}{0.79/0.49}$ | $\frac{9}{0.85/0.57}$ | $\frac{28}{0.87/0.64}$ |
| $w_f = 0.75mV$ | $\frac{4.5}{0.9/0.54}$ | $\frac{9}{0.92/0.61}$ | $\frac{17}{0.92/0.65}$ | $\frac{47}{0.91/0.67}$ |
| $w_f = 1.0mV$ | $\frac{9}{0.96/0.7}$ | $\frac{15}{0.96/0.69}$ | $\frac{30}{0.97/0.69}$ | $\frac{69}{0.92/0.68}$ |
| $w_f = 1.25mV$ | $\frac{14}{0.96/0.73}$ | $\frac{21}{0.98/0.71}$ | $\frac{35}{0.95/0.71}$ | $\frac{92}{0.93/0.69}$ |
| $w_f = 5.0mV$ | $\frac{60}{0.97/0.72}$ | $\frac{94}{0.96/0.73}$ | $\frac{150}{0.95/0.72}$ | $\frac{372}{0.95/0.72}$ |
| $w_f = 10.0mV$ | $\frac{104}{0.98/0.72}$ | $\frac{171}{0.96/0.73}$ | $\frac{267}{0.95/0.73}$ | $\frac{650}{0.96/0.74}$ |

Table 3: **Correlation values** r_{mult}^2 and r_{sum}^2 and maximum output firing rates $r_{o,max}$ of the complete model neuron for different feeding time constants τ_f and different feeding input weights w_f . Gating parameters were kept constant: $w_g = 1.0mV$, $\tau_g = 8.0ms$, $\gamma = 0.7mV$.

in a broad range to check for parameter ranges in which multiplicative interaction is achieved. Correlation values between the output firing rates and the analytical models as well as the rounded maximum output firing rates are displayed in table 3. Correlation values between the data and the multiplicative analytical model were lower than the values obtained with the simplified model neuron. This is because the multiplicative analytical model does not account for nonlinearities in the feeding input stream caused by the spike-thresholding mechanism. For example, in the integrate-and-fire neuron, a spike is elicited if the membrane potential is at least greater than the baseline of the spiking threshold $\Gamma_{base} = 1mV$. If feeding weights are less than $w_f = 1mV$, only consecutive spikes that overlap in the temporal range of the feeding decay time constant can elicit an output spike. For low feeding firing rates this is very unlikely even when the gate is open all the time: a certain input firing rate is needed to elicit output spikes. This is displayed in figure 6 for the parameter set $w_f = 0.5mV$ and $\tau_f = 5ms$. Here, feeding input firing rates below 30Hz led to an output firing rate of 0Hz even at high gating firing rates. Qualitatively, this is in line with input-output nonlinearities in biological neurons where a certain input to neurons dendrites is needed to elicit an output spike [Koch and Poggio (1992); Dayan and Abbott (2002)]. However, the multiplicative analytical model does not account for such kinds of nonlinearities and thus yielded low correlation values.

To account for these nonlinearities, another analytical model which we will call multiplicative-exponential model, was fit to the data:

$$r_{mult-exp}^{out} = a_m \cdot r_f^{b_m} \cdot r_g^{c_m} \quad (3.12)$$

where a_m , b_m , and c_m are fitting parameters. By mutually scaling the r_f and the r_g axis the multiplicative-exponential analytical model captures the non-linear behaviour of the feeding input stream together with the multiplicative interaction between both streams (figure 6). To account for nonlinearities in the additive model, we fitted a similar additive-exponential model to the data:

$$r_{add-exp}^{out} = a_s \cdot r_f^{b_s} + c_s \cdot r_g^{d_s} \quad (3.13)$$

where a_s , b_s , c_s , and d_s are fitting parameters. We calculated correlation values between the two models and the data values obtained with feeding weights and feeding decay time constants used above (except for the parameter pair $w_f = 0.5\text{mV}, \tau_f = 2\text{ms}$). Correlation values for the multiplicative-exponential

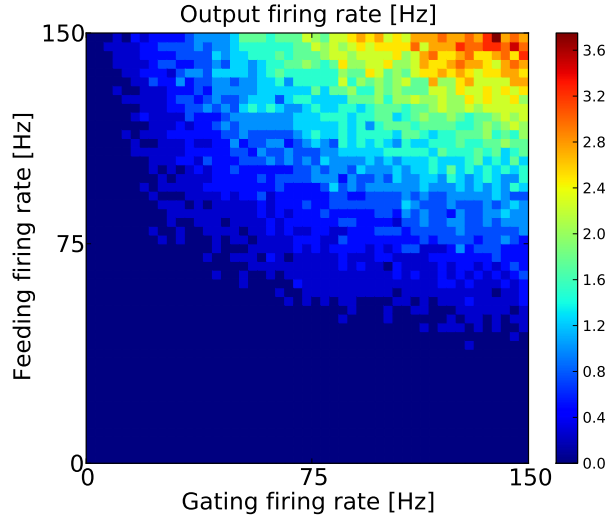


Figure 6: **Output firing rates** for low feeding weight $w_f = 0.5\text{mV} < \Gamma_{base} = 1\text{mV}$ and low synaptic decay time constant $\tau_f = 5\text{ms}$ (complete model neuron). At feeding input firing rates below 30Hz no output spikes were elicited in the model - not even at high gating firing rates.

analytical model were high on average ($\bar{r}_{mult-exp}^2 = 0.985 \pm 0.007$, lowest value: 0.97) and comparable to correlation values obtained with the simplified model neuron. Correlation values for the additive-exponential analytical model were low on average ($\bar{r}_{add-exp}^2 = 0.76 \pm 0.03$, highest value: 0.79). We conclude that in the tested range the output firing rate of the integrate-and-fire neuron can be explained by the product - but not by the sum - of the gating firing rate and a nonlinearly transformed feeding firing rate.

3.4.4 Effects of Input Synchrony

In the model neurons a main prerequisite for an output spike to occur is a temporal overlap between feeding spikes and periods where the gate is open. Moreover, synchronicities and correlations between input spike trains are known to have influences on neurons gains [Srinivasan and Bernard (1976)].¹⁰ To see how synchronies between feeding and gating input streams influence the output firing rate of the model neuron we simulated the simplified model neuron with two identical input spike trains with input frequencies $r_f = r_g = [5, 25, 50, 75, 100]$ Hz. Reduced synchrony was realized by jittering the spike times of the gating input stream. Here, an average jitter of x ms corresponded to a modulation in the timings of each spike according to a uniform distribution of jitters between $-2 \cdot x$ to $2 \cdot x$ ms. Figure 7 shows the output firing rate of the simplified model neuron as a function of average jitter while $w_g = 1.0$ mV, $\tau_g = 7$ ms and $\gamma = 0.7$ mV. Synchronization in input spike trains led to a strong increase in the output firing rate when the jitter is in the range of the gating time constant. At an average jitter around 10 ms the output firing rate was comparable to that obtained with statistically independent input streams. For an input firing rate of 75Hz we calculated the gain factor in the output firing rate which was obtained by dividing the

¹⁰In general, in addition to the average firing rate, the precise timing of action potentials seems to be relevant for information coding [Theunissen and Miller (1995); Rieke et al. (1999); Vanrullen et al. (2005); Gollisch (2008)]. A typical example for this type of neural coding is the *synchrony code* in which groups of neurons synchronize their activity [Gollisch (2008)]. For example, visual cortical neurons synchronize their responses as a function of how coherent features in the visual field are [Eckhorn et al. (1988, 1990); Engel et al. (1992); Damasio (1990)]

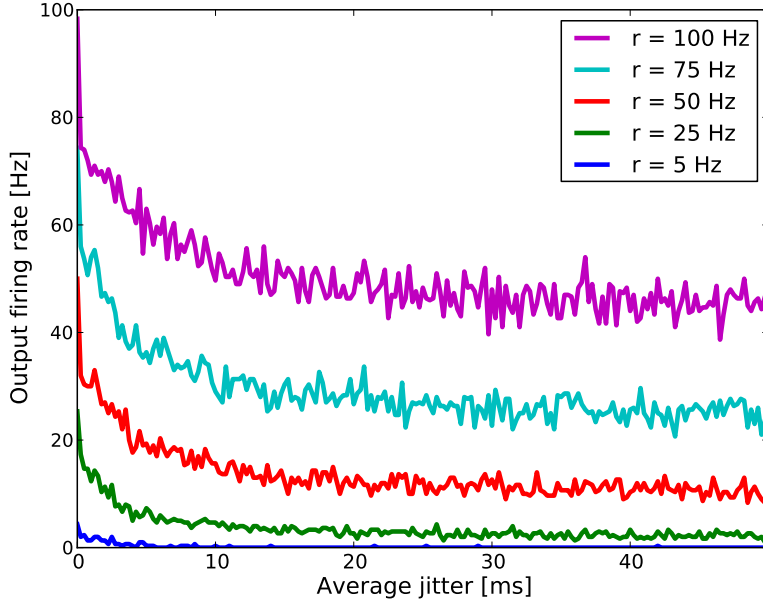


Figure 7: **Effects of input synchrony on output firing rates for four different input firing rates.** Output firing rates of the simplified model neuron are shown as a function of average jitter between identical feeding and gating input streams for five different input firing rates. When the average jitter was zero, the two input streams were identical and thus perfectly synchronized.

maximum output firing rate with zero jitter by the average output firing rate between a jitter of 40 to 50ms. We calculated this factor for different gating input weights between $w_g = [0.5, \dots, 10]$ mV while keeping all other parameters constant (table 4). With increasing gating weights the gain factor got smaller, being very high at gating weights smaller than the gating threshold (table 4).

At high gating weights, successive gating EPSPs are likely to overlap and the opening probability of the gate is high. Thus, synchronization does not have a big effect on the output firing rate here. When the gating weight is in the order of magnitude of the gating threshold ($\gamma = 0.7$ mV), synchrony becomes an important modulation factor. Nevertheless in the brain it is difficult to imagine that a sensory input stream and a contextual input stream that most likely originate in two different cortical areas are synchronized as precisely as claimed here.

| | | | | | | | | | | | |
|-------------|-----|-----|-----|-----|-----|-----|-----|-----|-----|-----|-----|
| w_g [mV] | 0.4 | 0.5 | 0.6 | 0.7 | 0.8 | 0.9 | 1.0 | 2.0 | 3.0 | 4.0 | 10 |
| gain factor | 8.9 | 7.3 | 4.8 | 4.8 | 4.3 | 3.2 | 2.8 | 1.8 | 1.5 | 1.4 | 1.2 |

Table 4: **Gain factors** calculated by dividing the maximum output firing rate with zero jitter by the average output firing rate between a jitter of 40 to 50 ms for an input firing rate of 75Hz. Gain factors are shown for different gating input weights w_g .

3.5 Discussion

We investigated the multiplicative properties of a simple implementation of a permissive gating mechanism in a leaky integrate-and-fire model with a feeding and a gating input pathway. Feeding and gating input pathways interacted multiplicatively on a wide range of parameters.

3.5.1 Comparison to a Detailed Biophysical Model

As shown previously in a detailed biophysical model, permissive gating mechanisms seem to be capable of implementing multiplicative behaviour between two input streams. In the detailed biophysical model of Kepecs and Raghavachari [2007] the interaction of two input streams via a permissive gating mechanism was investigated. This model yielded high correlation values for the multiplicative analytical model $r^2 = 0.99$ and lowered correlation values for the additive model which were identical to the analytic models used here. The correlation values are comparable to the simplified neuron model investigated here where spike thresholding mechanisms in the soma are skipped. It remains an open question as to how the multiplicative properties of the biophysical model neurons [Kepecs and Raghavachari (2007)] change when parameter values are changed by e.g. learning mechanisms.

3.5.2 Multiplicative Interactions with Small Gating Weights

The influence of the gating mechanism on the output firing rate of the model neurons was described via the opening probability of the gate $r_o = r_f \cdot p_{open}$. An important claim for the analytical description of the opening probability of the gating mechanism was that gating weights w_g have to be larger than

the gating threshold γ . Under these conditions the opening probability of the gate was well described by equation 3.8. In the case where gating weights w_g are smaller than the gating threshold γ , the opening probability can not be described by equation 3.8 any more. When $w_g < \gamma$, two or more spikes that produce overlapping EPSPs in the gating stream are necessary to open the gate. This introduces nonlinearities in the analytical description of the opening probability. Where equation 3.5 ($r_o = r_f \cdot p_{open}$) is still valid in that case, the opening probability can not simply be described by $p_{open} = r_g \cdot t_c$ anymore as it considers $w_g > \gamma$. An analytical description of p_{open} will not be given here for $w_g < \gamma$. We hypothesize that feeding and gating input streams interact in a way where nonlinearly modulated gating firing rates are multiplied with the feeding input firing rates as captured by the multiplicative-exponential analytical model. To test this, we fitted the four analytical models to 2d-matrices of output firing rates obtained by varying r_f and r_g between 0 and 500Hz. Maximum input firing rates were chosen to be high in order to raise the probability of overlapping gating EPSPs. Parameters in the gating input stream were varied between $w_g = [0.5, \dots, 0.9]$ mV and $\tau_g = [2, \dots, 25]$ ms while keeping the gating threshold fixed at a value of $\gamma = 1.0$ mV. In the simplified model neuron, correlation values for the multiplicative and the additive analytical model as well as in the additive-exponential model were low on average ($r_{mult}^2 = 0.87 \pm 0.09$, $r_{add}^2 = 0.71 \pm 0.04$, $r_{add-exp}^2 = 0.75 \pm 0.01$). Correlation values in the multiplicative-exponential model were very high on average ($r_{mult-exp}^2 = 0.99 \pm 0.008$). In the complete integrate-and-fire model neuron correlations values were qualitatively similar ($r_{mult}^2 = 0.84 \pm 0.1$, $r_{add}^2 = 0.7 \pm 0.05$, $r_{add-exp}^2 = 0.74 \pm 0.01$, $r_{mult-exp}^2 = 0.99 \pm 0.007$). We conclude that when $w_g < \gamma$ the model neuron is sufficiently described by a product of the feeding input firing rate and a nonlinearly modulated gating firing rate.

3.5.3 Exact and Nearly Multiplicative Interactions

The model neuron showed exact multiplicative behaviour when the assumptions in equation 3.9 were followed which was quantified by calculating

correlation values between the model output and an analytical multiplicative model (eq. 3.10). For exact multiplication, gating weights are assumed to be larger than the gating thresholds ($w_g > \gamma$) in order to be able to derive the closing time t_c which serves as a scaling factor for the multiplication of feeding and gating firing rates ($r_o = r_f \cdot r_g \cdot t_c$). Furthermore, interspike intervals in the gating input stream are assumed to be larger than the closing time so that overlapping gating EPSPs can be ignored. Under those conditions, the output of the model neuron is well described by a multiplication of the scaled feeding and the gating input firing rates. If these conditions are ignored, nonlinearities that distort the exact multiplicative interaction are observed. In the complete model neuron with somatic spike thresholding, the output of the model neuron is better described by a multiplication of two nonlinearly modulated feeding and gating input firing rates, $r_o = a_m \cdot n(r_f) \cdot m(r_g)$, where n and m are nonlinear functions. In the study presented here, simple exponential nonlinearities $r_o = a_m \cdot r_f^{b_m} \cdot r_g^{c_m}$ were sufficient to fit the output of the neuron model on a wide range of tested parameters. Moreover, the model was not well approximated by a summation of nonlinearly modulated feeding and gating firing rates $r_o = a_s \cdot r_f^{b_s} + c_s \cdot r_g^{d_s}$. For biological neurons this implies that a physiological implementation of the presented gating mechanism is well suited for realizing nearly multiplicative interactions between two input streams on a wide range of parameters. This was previously suggested by Kepecs and Raghavachari (2007).

3.5.4 Robustness of Models that Explain Multiplicative Interactions via a Network Approach

In previous studies [Salinas and Sejnowski (2001); Nezis and van Rossum (2011); Salinas and Sejnowski (2000)], multiplication was explained as an emergent property of a network of ordinary single neurons. Here, ordinary means that neurons do not need more functional properties than the traditional averaging, thresholding, summation, and subtraction to realize multiplication in the networks. These mechanisms do not provide an answer to multiplicative interactions on the cellular level but treat multiplicative interactions as

emergent properties in networks. In all these models, the ability of the network to realize multiplicative interactions depends on the specific connectivity in the network. However, connectivities in biological networks show a large amount of plasticity due to long term potentiation, [Siegelbaum and Kandel (1991); Dan and Poo (2004)], short term synaptic plasticity [Tsodyks et al. (1998)] and other adaptational effects [Miller and Mackay (1994)]. By this, the connectivity and functionality in biological networks changes at any time. It is not known if models that explain multiplication via network interactions are feasible when plasticity mechanisms are taken into account. To our knowledge, investigations of the applicability of those mechanisms in self-organizing networks that incorporate synaptic plasticity mechanisms remain open.

3.6 Outlook to Chapter 3

In the next chapter, the integrate-and-fire neuron model presented here will be implemented in a self-organizing network that learns gaze-invariant representations of visual space in an unsupervised way. The robustness and applicability in this self-organizing networks that will be shown in the next chapter makes permissive gating a feasible candidate mechanism as a mediator of gain field phenomena observed in biological neurons [Andersen and Mountcastle (1983); Salinas and Sejnowski (2001)].

4 Unsupervised Learning of Gaze-Invariance

4.1 Abstract

To achieve a stable representation of our visual environment, for perception and goal-based action, our brain needs to transform the representation of visual stimuli from a retina-centered coordinate system to a frame of reference that is independent of changes in gaze direction [Duhamel et al. (1997)]. Here we present a model that learns these coordinate transformations via a biologically plausible learning mechanism [Michler et al. (2009)]. In contrast to previous studies [Zipser and Andersen (1988); Mazzoni et al. (1991); Salinas and Abbott (1997)], the network model develops gaze-invariant representations of visual stimuli in an unsupervised way from the statistics of visual inputs under natural viewing conditions only. Gaze-invariance is achieved by a coordinate transformation by neurons that are gain-modulated by gaze direction [White and Snyder (2004)]. Our model provides a possible explanation for the functional relevance of topographic maps and the development of retina-centered neurons in parietal cortex that are gain-modulated by gaze direction.

4.2 Introduction

Every second, we make several saccadic eye movements to bring objects of interest into our visual and attentional focus. These rapid jumps in gaze direction shift the image of the environment on our retina, disrupting the spatio-temporal contiguity of the neuronal representation of the visual world [Bremmer and Krekelberg (2003)]. Many postretinal stages of the visual system are retinotopically organized and are similarly affected by saccades. In order to achieve a stable representation of visual space, our brain must represent information about visual space in a frame of reference that is invariant to changes in gaze direction [Duhamel et al. (1997)]. Here, a representation of the visual environment denotes a set of topographically arranged neurons with each neuron encoding the luminosity at a specific position in a respective coordinate frame. Thus, a retina-centered representation refers to response

strengths of topographically arranged neurons, where each neuron encodes the luminosity value of the retinal image at a position of a specific photoreceptor on the retina. Such a representation is called retinotopic.

Think of the process of finding this doctoral thesis on the desk and grabbing it for reading. After having localized the thesis by scanning the visual environment, one has to reach for it. This is not a trivial problem, since the reference frame in which the thesis is encoded - the retina - is different from the effectors reference frame - the hand. Encoding of the position of objects requires a frame of reference and different sensory modalities are coded in different frames of reference. A retinal frame of reference specifies an objects position with respect to the center of the retina, a head-centered and body-centered frame of reference is specified correspondingly. A head-centered representation is invariant to changes in gaze direction and therefore is a candidate for providing the information necessary to achieve a stable perception of the visual environment.

Physiological findings indicate, that visual information at early visual stages is represented in a retina-centered frame of reference [Boussaoud and Bremmer (1999)], the auditory system uses a head-centered frame of reference that arises from the early computations in the auditory system [Pena and Konishi (2001)], and arm movements are generated with respect to the body [Georgoulous et al. (1986)]. Our ability to interact with objects in our environment depends on the ability to execute reliable arm, hand, finger movements and movements of the lower extremities and on the ability to coordinate all these movements. The execution of arm movements with reference to visual information requires a transformation of an objects position from a retina-centered into a body-centered frame of reference: The representation of the image of an object on the retina must be combined with gaze direction, which leads to a head-centered representation. To achieve a body-centered representation, this head-centered representation must be combined with the position of the head relative to the body. In this process, the first stage is the transformation from retina-centered to head-centered coordinates.

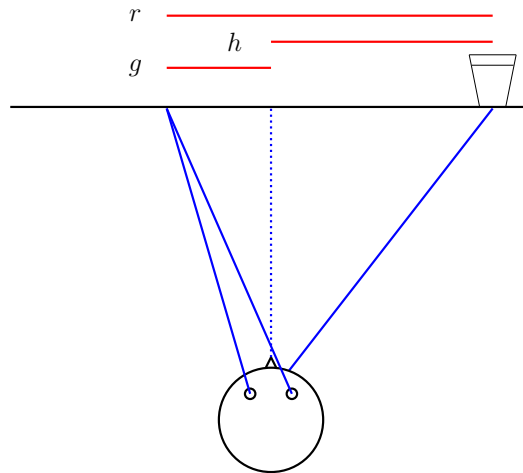


Figure 8: **Coordinate transformation from retina-centered to head-centered coordinates.** The position of an object in head-centered coordinates h is determined by adding the direction of gaze g to the position of the object in retinal coordinates r .

4.2.1 Coordinate Transformations and Basis Function Networks

What must be done to determine the position of an object relative to the head on the basis of visual cues? The coordinates of the object in a head-centered coordinate frame must somehow be extracted from the retinal image, which however depends on gaze direction and thus changes when our eyes move. The determination of the position of an object relative to the head is possible by the combination of information about gaze direction with the retinal position of the object, as illustrated in figure 8. The position of an object in head-centered coordinates h is determined by adding the direction of gaze g to the position of the object in retinal coordinates r which is the head-centered position of the object related to the direction of gaze $r := h - g$. Thus, the head-centered position can be determined from retinal position and gaze direction by

$$h = (h - g) + g = r + g. \quad (4.1)$$

As the position h is not influenced by a change in gaze direction, it is called gaze-invariant. However, this position summation is only the transformation

of one retinal position. A head-centered representation that contains information about every position in head-centered space requires a transformation from every position in retina-centered space to the respective position in head-centered space. For a pixel representation, this corresponds to the transformation of a retinal pixel representation to a head-centered pixel representation, i.e. the transformation of the represented positions with their corresponding luminosities. It is known from theoretical studies on neural networks [Pouget and Sejnowski (1997)], that a head-centered representation of the visual environment can be achieved by combining information about gaze direction with information about the retinal image in a multiplicative way.

Neurons in parietal cortex of macaque monkeys have been found to combine information about visual stimuli with information about gaze direction. Those neurons encode stimuli in a retina-centered frame of reference while being gain-modulated by gaze direction [Andersen and Mountcastle (1983)]: The direction of gaze modulates the activity of these neurons in a nearly multiplicative way while selectivities for visual stimuli, characterized by the neurons receptive field, remain largely unchanged. Parallel to the concept of the receptive field, the interaction between visual responses and gaze directions is called a *gain field* [Andersen and Mountcastle (1983); Salinas and Sejnowski (2001)].

Such gain-modulated neurons may be involved in the coordinate transformation from retina-centered to head-centered coordinates [Andersen and Mountcastle (1983); Pouget and Snyder (2000); Pouget et al. (2002)]: In the framework of *basis function networks*, information about the position of an object relative to the head can be constructed by reading out nonlinear combinations of retinotopic responses with information about the direction of gaze [Pouget and Snyder (2000)]. So far, however, it is unclear how such mechanisms can develop in the visual system.

4.2.2 Development of Gaze-Invariant Representations

Zipser and Andersen (1988) showed that coordinate transformations from a retina-centered to a gaze-invariant, head-centered frame of reference can be learned in an artificial neural network. Neurons in the network showed gain-modulation properties similar to those found in parietal cortex [Andersen and Mountcastle (1983)]. However, it is unlikely that the applied backpropagation learning algorithm is used in the brain. Attempts have been made to improve the biological plausibility of methods to learn coordinate transformations [Mazzoni et al. (1991); Salinas and Abbott (1997); White and Snyder (2004); Davison and Fregnac (2006)] but in all cases supervised learning via teaching signals was applied, whereas it is thought that the brain would have to learn the processing of visual information in an unsupervised way [Barlow (1989)]. Here we propose a model of unsupervised learning for how the brain might learn the coordinate transformations necessary to represent visual space in a gaze-invariant frame of reference by taking into account the statistics of natural viewing conditions. Under natural viewing statistics, when a visual scene is explored by saccadic eye movements, the position of an objects image on the retina changes on a faster time scale than the objects position in the environment [Einhäuser et al. (2007)]. In our network model (figure 9) we exploit this temporal asymmetry to learn gaze-invariant representations. The basis for our model is a self-organizing network model proposed by Michler et al. [2009] that develops representations of an input signal in which neurons are selective for slowly varying features and invariant for fast changing features of a retinotopic input signal. We extended this model by a second input layer representing the direction of gaze and trained the network with inputs whose spatio-temporal statistics were in accordance with natural viewing conditions: mimicking saccadic eye movements, the position of an objects image on the retina changes in a faster time scale than the objects position in the environment. Training stimuli consisted of idealized visual scenes with slowly moving objects, represented by Gaussian luminance blobs, that were scanned by frequent horizontal saccadic eye movements.

Inputs from neurons representing retinal and gaze direction information are

nonlinearly combined via a permissive gating mechanism [Katz (2003)]: Retinal inputs are added to the membrane potential of neurons in a self-organizing layer only when excitatory postsynaptic potentials (EPSPs) from the gaze direction layer cross a certain gating threshold. This nonlinear combination is implemented in order to allow for a nearly multiplicative - gain field like - interaction of retinal and gaze direction inputs (see chapter 3).

Our model explains the unsupervised development of gain-modulation properties [Andersen and Mountcastle (1983); Duhamel et al. (1997)] on the basis of a new neuron model of nonlinear interactions between retinal and gaze direction inputs (chapter 3). The network model learns coordinate transformations to a gaze-invariant frame of reference by biologically plausible neural mechanisms that take into account the statistics of visual inputs under natural viewing conditions.

4.3 Methods

4.3.1 Network Architecture

The network model consists of four layers, each with toroidal topology (figure 9): a retinotopic input layer R (15 horizontal \times 5 vertical neurons) representing the position of an object in retinal coordinates; a gaze direction layer G (15 \times 5) representing the direction of gaze; a recurrently connected map formation layer M (50 \times 50) which receives input from layers R and G ; an output layer O (10 \times 10) receiving convergent input from neurons in layer M via a Gaussian kernel ($w_{o,max} = 1.0\text{mV}$, $\sigma = 3$ where 1 is the distance between two neighbouring neurons). Neurons in the output layer have localized receptive fields in the map layer in order to represent invariant features of the input signal [Michler et al. (2009)]. Connections from neurons in layer R and G to neurons in layer M were initially connected all-to-all with equal weights ($w_r = w_g = 0.02\text{mV}$). The map formation layer is recurrently connected with short-range excitatory connections to NMDA synapses via a Gaussian kernel ($w_{max} = 0.035\text{mV}$, $\sigma = 1.2$) and inhibitory connections ($w_i = 0.04\text{mV}$) to GABA synapses [von der Malsburg (1973); Kohonen (1982); Choe and Miikkulainen (1998); Michler et al. (2009)]. Each map layer neuron receives

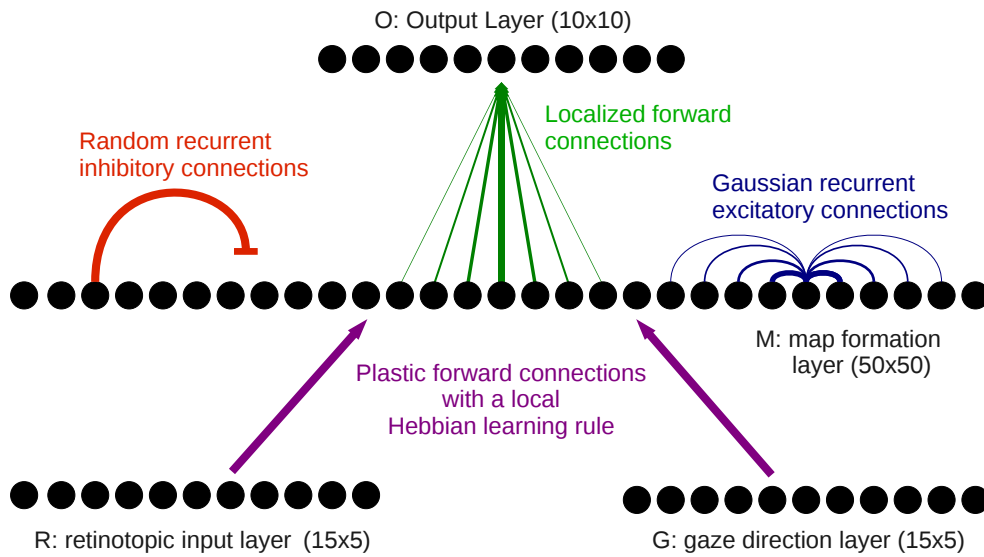


Figure 9: **Network architecture.** The model consists of four layers of neurons. The retinotopic input layer R encodes the position of a two dimensional objects image on the retina; gaze direction layer G encodes gaze direction. The map formation layer M combines inputs from layers R and G in a nonlinear way (see section 4.3.2). Forward connections are plastic and synaptic weights are changed according to a local Hebbian learning rule (see section 4.3.3). The map formation layer is recurrently connected via random inhibitory connections and Gaussian excitatory connections in order to implement the principles of topographic map formation [Kohonen (1982)]. Excitatory recurrent connections elicit responses in synapses with long decay time constants in order to realize a memory trace [Földiák (1991)] that supports invariance learning [Michler et al. (2009)]. The output layer O receives convergent input from neurons in layer M.

inhibitory connections from 250 randomly chosen presynaptic neurons in the map layer.

4.3.2 Neuron Model & Synapse Types

Neurons are modeled as leaky integrate-and-fire units with a dynamical voltage threshold and biologically plausible time constants [Lapicque (1907); Eckhorn et al. (1990)]. The multiplicative-like gain modulation of map layer neurons is modeled by a permissive gating mechanism: excitatory postsynaptic potentials (EPSPs (in mV)) from the retinal layer contribute to the membrane potential of the neuron only if EPSPs from the gaze direction layer exceed a gating-threshold value. The multiplicative properties of this permissive gating mechanism and its biophysical basis was extensively described in chapter 3. Incoming spikes are modelled as delta pulses and elicit postsynaptic potentials as an impulse response. The membrane potential of a neuron (in mV) in the map layer at time step t is computed by

$$U_M(t) = R(t) \times \Theta(G(t) - \gamma) + E(t) - I(t) + \Omega(t) \quad (4.2)$$

where $R(t)$ and $G(t)$ are retinal and gaze direction EPSPs originating from incoming retinal and gaze direction spikes, respectively; $\Theta(x)$ is the Heaviside step function; $\gamma = 0.4\text{mV}$ is a gating-threshold; $E(t)$ and $I(t)$ are EPSPs from excitatory and inhibitory recurrent connections, respectively; Ω is Gaussian noise with zero mean and standard deviation 0.25mV . The resting membrane potential is 0mV and successive EPSPs superimpose linearly.

Postsynaptic potentials are increased by the synaptic weight $w_{i,j}$ assigned to the connection between pre- (j) and postsynaptic (i) neuron each time a spike arrives at the postsynaptic neuron. After a spike arrives at the synapse, postsynaptic potentials decay exponentially with corresponding time constants $\tau_{AMPA} = 2.4\text{ms}$ (retinal and gaze direction inputs), $\tau_{NMDA} = 100\text{ms}$ (excitatory recurrent connections) and $\tau_{GABA} = 7\text{ms}$ (inhibitory recurrent

connections) [Crair and Malenka (1995)]:

$$R(t) = w_r \cdot e^{-t/\tau_{AMPA}} \quad (4.3)$$

$$G(t) = w_g \cdot e^{-t/\tau_{AMPA}} \quad (4.4)$$

$$E(t) = w_e \cdot e^{-t/\tau_{NMDA}} \quad (4.5)$$

$$I(t) = w_i \cdot e^{-t/\tau_{GABA}}. \quad (4.6)$$

When the overall membrane potential $U_M(t)$ exceeds a dynamical threshold $\Gamma(t)$, an action potential is assigned to this time step. The dynamical threshold consists of a baseline threshold $\Gamma_{base} = 1\text{mV}$ and a threshold potential. When a spike is generated at time-step t_s , the threshold potential is increased by a fixed value $\xi = 1\text{mV}$ and then exponentially decays with time constant $\tau_\xi = 10\text{ms}$ [Eckhorn et al. (1990)]. The total threshold is thus computed by

$$\Gamma(t) = \Gamma_{base} + \sum_{t_s} \xi \cdot \exp(-(t - t_s)/\tau_\xi). \quad (4.7)$$

The dynamical threshold serves as a simulation of the relative and absolute refractory period in real neurons.

Recurrent excitatory *NMDA* synapses exhibit short term synaptic depression [Tsodyks et al. (1998); Michler et al. (2009)]. The synaptic efficacy $e_{i,j}(t)$ of the synapse between neuron j and i decreases after a presynaptic spike at time t_{sj} and recovers exponentially with time constant $\tau_{rec} = 250\text{ms}$. The time course of the synaptic efficacy is

$$\frac{d}{dt}e_{i,j} = \frac{1 - e_{i,j}(t)}{\tau_{rec}} - U_{se} \cdot e_{i,j}(t) \cdot \delta(t - t_{sj}), \quad (4.8)$$

where $U_{se} = 0.3$ is the fraction of available transmitter that is released during a presynaptic action potential.

The membrane potential of neurons in the retinotopic input layer (U_R), the

gaze direction layer (U_G), and the output layer (U_O) is computed by

$$U_R(t) = In_R(t) + \Omega(t) \quad (4.9)$$

$$U_G(t) = In_G(t) + \Omega(t) \quad (4.10)$$

$$U_O(t) = M(t) + \Omega(t) \quad (4.11)$$

where $M(t)$ are EPSPs originating from incoming spikes from the map formation layer, $In_R(t)$ and $In_G(t)$ are EPSPs originating from input stimuli (section 4.3.4), and Ω is Gaussian noise with zero mean and standard deviation 0.25. $M(t)$, $In_R(t)$, and $In_G(t)$ decay exponentially with time constant $\tau_{AMPA} = 2.4\text{ms}$. Dynamical thresholding mechanisms are identical to the one described for $U_M(t)$. Synaptic delays between 1 and 10ms were assigned randomly to each synapse in the network.

4.3.3 Learning Rule

A Hebbian learning rule similar to those proposed by other authors [Gerstner et al. (1996); Saam and Eckhorn (2000); Michler et al. (2009)] is used. The synaptic weights $w_{i,j}$ from neuron j to i of the forward connections from layers R and G to the map layer are modified simultaneously according to the learning rule

$$\frac{d}{dt}w_{i,j} = \delta_i \cdot \alpha \cdot L_{pre,j}L_{post,i} \quad (4.12)$$

$$L_{pre,j} = \sum_{t_{sj}} \exp\left(-\frac{t - t_{sj}}{\tau_{pre}}\right) \quad (4.13)$$

$$L_{post,i} = \sum_{t_{si}} \exp\left(-\frac{t - t_{si}}{\tau_{post}}\right). \quad (4.14)$$

δ_i is 1 when a spike occurs in the postsynaptic neuron. t_{sj} and t_{si} denote the times of the past pre- and postsynaptic spikes. When a spike occurs, the pre- and postsynaptic learning potentials $L_{pre,j}$ and $L_{post,i}$ are increased by 1. They exponentially decay with time constants $\tau_{pre} = 20\text{ms}$ and $\tau_{post} = 10\text{ms}$ [Michler et al. (2009)]. $\alpha = 0.0007$ is a constant that corresponds to the learning rate.

To prevent synaptic weights from growing infinitely, a homeostatic mechanism is implemented in the model. Each time the firing rate of a postsynaptic neuron in the map formation layer exceeds a threshold $\Gamma_{firingrate} = 40\text{Hz}$, its input weights are multiplied by a normalization factor $f = 0.999$ [Michler et al. (2009); Miller and Mackay (1994); Bienenstock et al. (1982)]. There is evidence for such kind of synaptic weight normalization in the brain [Royer and Pare (2003)].

4.3.4 Stimuli, Training & Testing Procedure

Training stimuli mimicked the typical viewing situations when a visual scene is explored by saccadic eye movements, with gaze direction changing on a faster time scale than object positions in space. We trained the network with two two-dimensional Gaussian stimuli ($\sigma = 0.75$) normalized to a maximum value of 0.2mV. Gaussians were presented to the two 15×5 dimensional input layers and were centered vertically while the 15 horizontal positions in each layer changed systematically. The stimulus set represented 15×15 combinations of retinal position and gaze direction, corresponding to 15 object positions in head-centered space and 15 different gaze directions. Horizontal gaze directions changed randomly each 300ms, corresponding to the exploration of a visual scene by saccades (figure 10). Head-centered object positions changed continuously every 6s, corresponding to the continuously varying position of a slowly moving object in the environment. The position of the retinal Gaussian was determined by a projection of the position of the object in the head-centered environment onto the retina considering the actual gaze direction. Numerical voltage values of stimuli were added to the input potentials $In_R(t)$ and $In_G(t)$ at each time step (section 4.3.2).

The same stimuli were used for testing. Each stimulus combination of the 15 retinal positions and 15 gaze directions was presented five times for 2s in order to account for noise-variability of stimulus responses. From the average response we determined receptive fields and selectivities for retinal- and head-centered object positions. Selectivities for retinal- and head-centered positions were quantified using selectivity indices. To determine how well

stimulus positions were encoded we calculated estimation errors. Simulation software was written in *C++*. Simulations were executed on the *German Neuroinformatics Node (G-Node)* with a sampling rate of 0.25ms. Evaluation software was written in *IDL* (version 6.2).

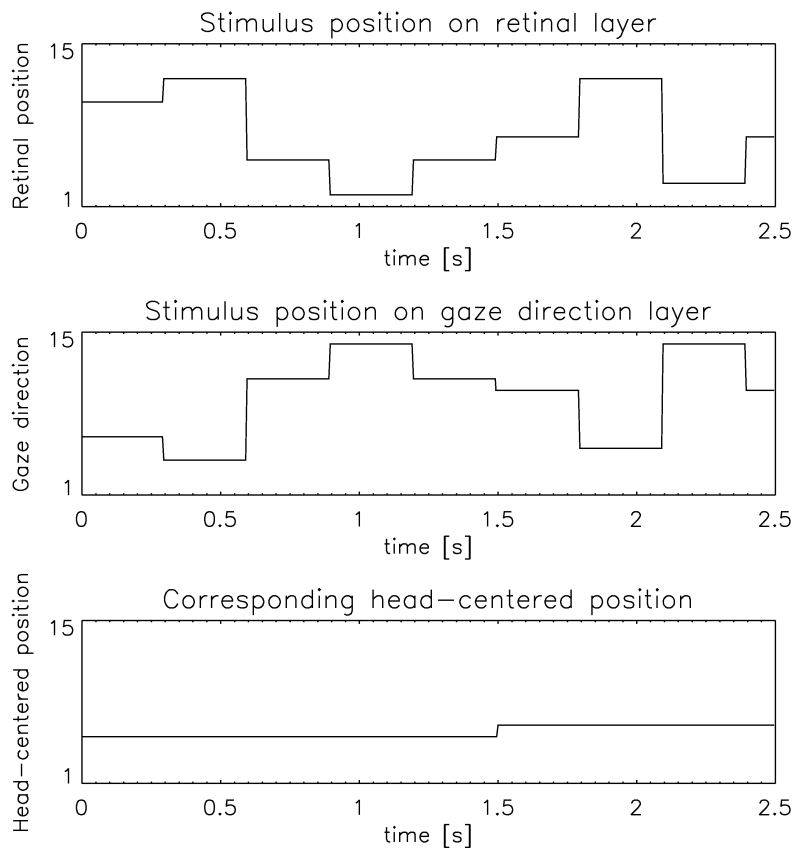


Figure 10: **Training protocol.** Horizontal positions of Gaussian stimuli on the retinal and gaze direction layers changed systematically during training. Corresponding positions in head-centered coordinates changed slowly and smoothly (lower panel) compared to changes in gaze direction (middle panel). Changes in gaze direction lead to jumps in the position of the head-centered objects image in retinal coordinates (upper panel). Statistics of inputs during training mimicked the situation where a visual scene with a slowly moving object is explored by saccadic eye movements, with gaze direction changing at a faster time scale than object positions in visual space.

4.4 Results

4.4.1 Receptive Fields and Topographic Maps in Map Formation Layer Neurons

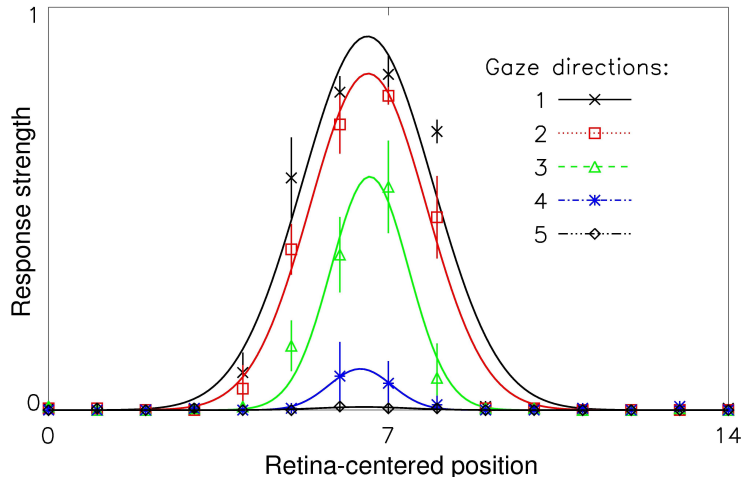


Figure 11: **Learned receptive fields in the map formation layer.** Response strength of one typical map layer neuron as a function of retinal stimulus position of the stimulus for five adjacent gaze directions (1-5). Each stimulus was presented five times, error bars show the standard deviation in response strengths. The neuron has a localized retina-centered receptive field. Response gain is modulated by gaze direction [Andersen and Mountcastle (1983)].

After training, neurons in the map layer showed an organized pattern of selectivities with respect to both input layers. A typical neuron in the map formation layer received input from a localized region in the retina layer, corresponding to a retina-centered receptive field. The activity of map layer neurons was modulated by inputs from the gaze direction layer (figure 11). Changes in gaze direction did not change the selectivity of the neuron but multiplicatively scaled the neurons tuning curves. This is in agreement with gain modulation properties of neurons in parietal cortex of macaque monkeys [Andersen and Mountcastle (1983)].

Selectivities for positions of objects in the visual environment were organized topographically in the map formation layer (figure 12). Neighboring neurons were selective both for neighboring retina-centered positions and for neighboring gaze directions, and topographic maps showed a pinwheel-like

organization structure [Obermayer and Blasden (1993)]. In addition, neurons with similar head-centered selectivities were clustered in larger regions that contained neurons with different retina-centered receptive fields and gain-fields. We quantified this by calculating the peak spatial frequencies of the topographic maps: When head-centered object positions changed after every 20th saccade, which is in accordance with natural viewing conditions

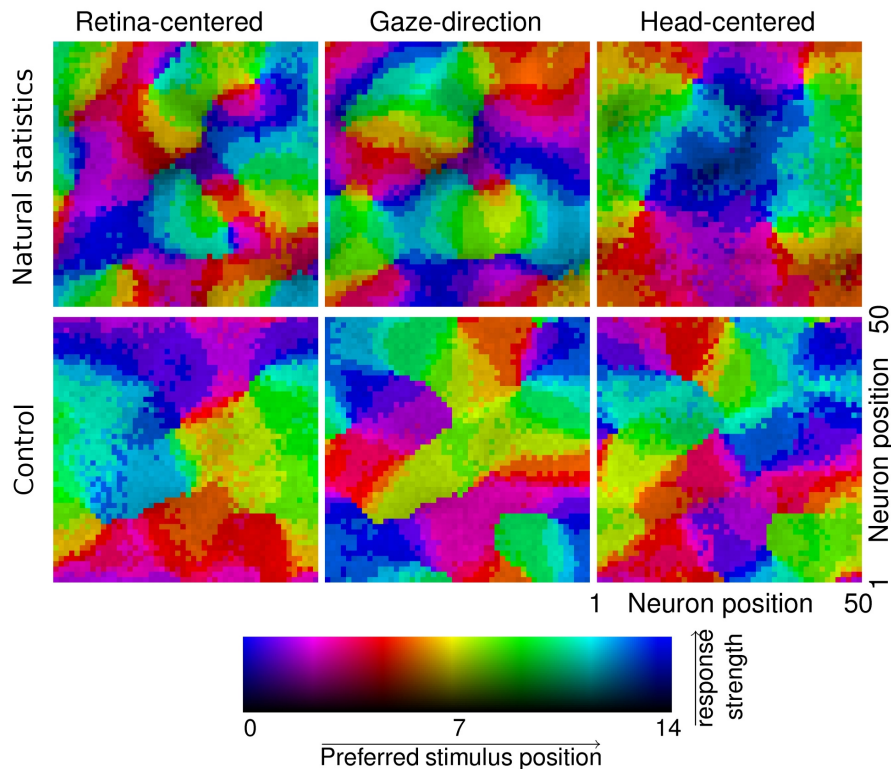


Figure 12: **Topographic maps.** Topographic organization of preferred retina-centered (left panel), gaze direction (middle panel) and head-centered (right panel) selectivities in the map formation layer. Color encodes preferred stimulus position in the respective coordinate frame, brightness encodes relative response strength. In the upper panels (natural statistics), head-centered object position changed 20 times slower than gaze directions during training which mimics natural viewing statistics [Einhäuser et al. (2007)]. Patches of similar head-centered preferred positions are larger than the patches of retina-centered positions. In the lower panels (control), equal time scales for changes in head-centered object positions and gaze directions were used during training which does not correspond to natural viewing statistics [Einhäuser et al. (2007)]. Patches of similar retina-centered preferred positions are larger than patches of head-centered positions.

[Einhäuser et al. (2007)], frequencies of head-centered maps are lower than those of retinal or gaze direction maps ($f_h = 0.98$, $f_r = 2.2$, $f_g = 1.98$ periods per map length). However, when head-centered object positions changed on the time scale of saccades¹¹, neurons with similar retina-centered receptive fields were clustered in larger regions ($f_h = 2.2$, $f_r = 0.98$, $f_g = 2.2$). This difference in spatial frequencies of topographic maps argues for a major role of viewing statistics in the self-organization process of the model.

These topographic distributions of selectivities determined the properties of output layer neurons with localized receptive fields in the range of the large head-centered regions (width of Gaussian kernel: $\sigma = 3$).

4.4.2 Receptive Fields and Coding Properties of Output Layer Neurons

After training the network with statistics of natural viewing conditions, neurons in the output layer were selective for stimuli at specific head-centered positions and head-centered selectivities showed a high degree of invariance to changes in gaze direction (figures 13 and 14) similar to receptive fields of neurons in area VIP of macaque monkeys [Duhamel et al. (1997)]. Retina-centered selectivities were not invariant to changes in gaze direction (figure 15).

To quantify the selectivity of output layer neurons for head-centered and retina-centered positions, respectively, we calculated selectivity indices. Each output layer neuron's selectivity index was calculated from the minimum and the maximum of its retinal (t_r) and head-centered averaged tuning curve (t_h) (figure 13). Head-centered and retinal selectivity $s_{h/r}$ was calculated by $s_{h/r} = \frac{\max(t_{h/r}) - \min(t_{h/r})}{\max(t_{h/r}) + \min(t_{h/r})}$ where $\max(t_{h/r})$ is the maximum of the averaged head-centered or retina-centered tuning curve, respectively, and $\min(t_{h/r})$ is the minimum of the averaged head-centered or retina-centered tuning curve, respectively. The selectivity index thereby measures the relative difference in responses to different stimuli.

When the network was trained with natural viewing statistics, output layer neurons had high selectivity indices in the head-centered coordinate frame

¹¹Under control statistics the network was trained with gaze directions and head-centered positions changing every 300ms.

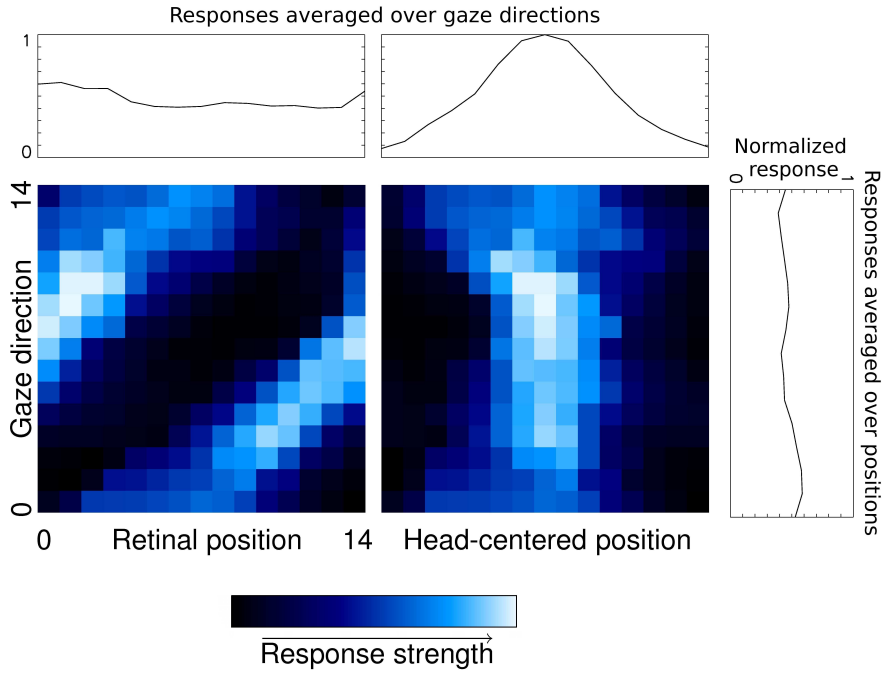


Figure 13: **Receptive fields of a largely gaze invariant output layer neuron.** Response strengths for different retina-centered (left) or head-centered (right) positions and gaze directions. The output layer neuron is located at the center for the map formation layer. The line plots on top show spatial tuning curves derived by averaging across gaze directions. Responses of output layer neurons are fairly invariant to changes in gaze direction in a head-centered frame of reference [Duhamel et al. (1997)]. Receptive fields of other neurons are shown in figures 14 and 15.

($s_h = 0.59 \pm 0.17$) and low selectivity indices ($s_r = 0.31 \pm 0.12$) in the retina-centered coordinate frame (figure 16). When the network was trained with control statistics where head-centered stimulus positions changed on the time scale of saccades output layer neurons had low selectivity indices in the head-centered coordinate frame ($s_h = 0.36 \pm 0.18$) and high selectivity indices in the retina-centered coordinate frame ($s_r = 0.6 \pm 0.16$) (figure 16). The difference between joint selectivity indices in the two training conditions is due to the differences in the structure of topographic maps in the map formation layer. When trained with natural viewing statistics, patches of similar preferred head-centered positions were larger than patches of similar preferred retina-centered positions. Due to the convergent connectivity from map layer neurons to output layer neurons, neurons in the output layer tended to be

selective for head-centered positions invariant to changes in retinal position or gaze direction in the natural training condition. When trained with control statistics, neurons in the output layer tended to be selective for retina-centered positions invariant to changes in gaze direction due to the reciprocal structure of topographic maps where patches of similar preferred retina-centered posi-

Head-centered response characteristics of output layer neurons

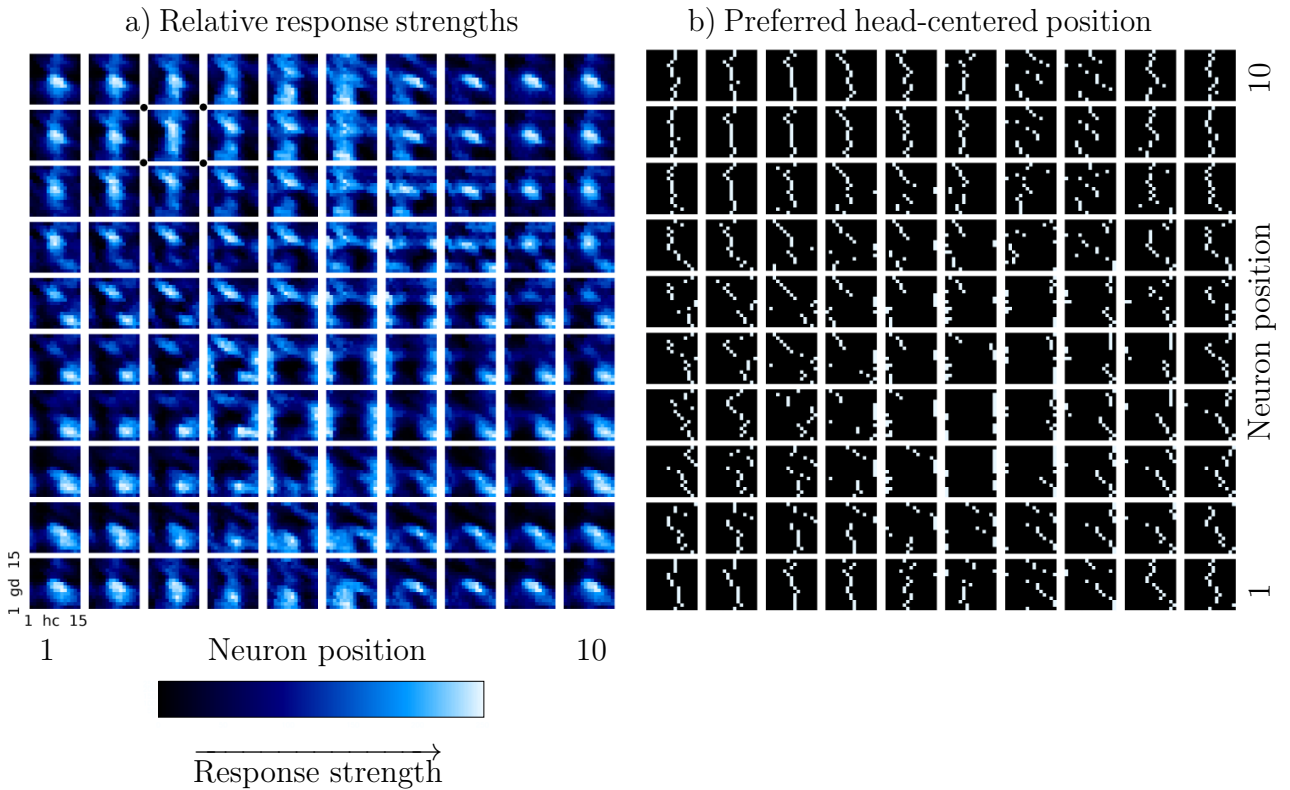


Figure 14: **Head-centered receptive fields and preferred head-centered positions of output layer neurons trained with natural viewing statistics.** Each square shows the response characteristics of one of the 10×10 neurons in the output layer. The horizontal axis of each square denotes the 15 head-centered positions and the vertical axis denotes the 15 gaze directions analogous to the right panel in figure 13. **a)** Response strengths of the 10×10 output layer neurons to different head-centered positions (horizontal axis) and gaze directions (vertical axis). The neuron shown in figure 13 is marked with black dots. **b)** The preferred head-centered position (horizontal axis) is shown for each neuron and each gaze direction (vertical axis). Preferred head-centered positions are largely invariant to changes in gaze direction.

tions were larger than patches of similar preferred head-centered positions.

To determine how well the response of output layer neurons predicts head-centered or retina-centered positions of stimuli we calculated estimation errors. For each stimulus combination of retinal position and gaze direction, we determined the population response of the output layer by taking the sum

Retina-centered response characteristics of output layer neurons

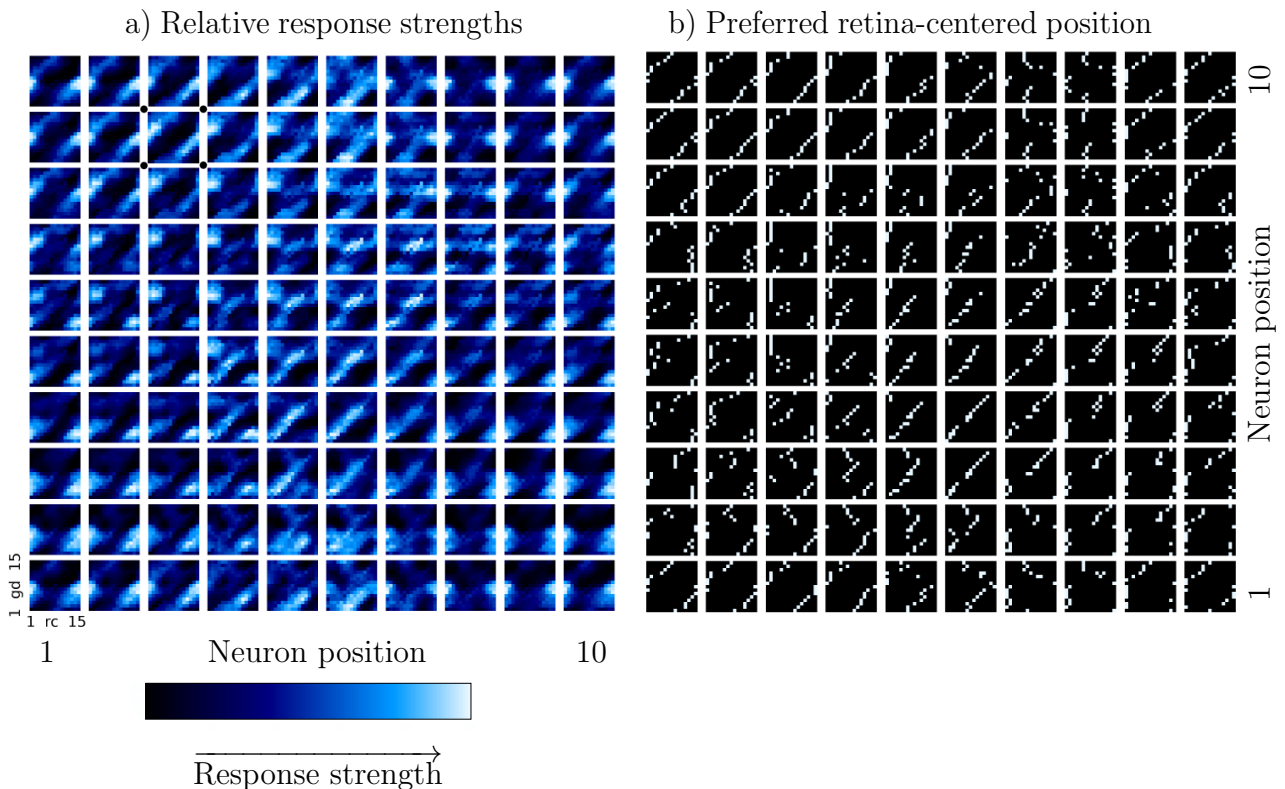


Figure 15: **Retina-centered receptive fields and preferred retina-centered positions of output layer neurons trained with natural viewing statistics.** Each square shows the response characteristics of one of the 10×10 neurons in the output layer. The horizontal axis of each square denotes the 15 retina-centered positions and the vertical axis denotes the 15 gaze directions analogous to the left panel in figure 13. **a)** Response strengths of the 10×10 output layer neurons to different retina-centered positions (horizontal axis) and gaze directions (vertical axis). The neuron shown in figure 13 is marked with black dots. **b)** The preferred retina-centered position (horizontal axis) is shown for each neuron and each gaze direction (vertical axis). Preferred retina-centered positions are not invariant to changes in gaze direction.

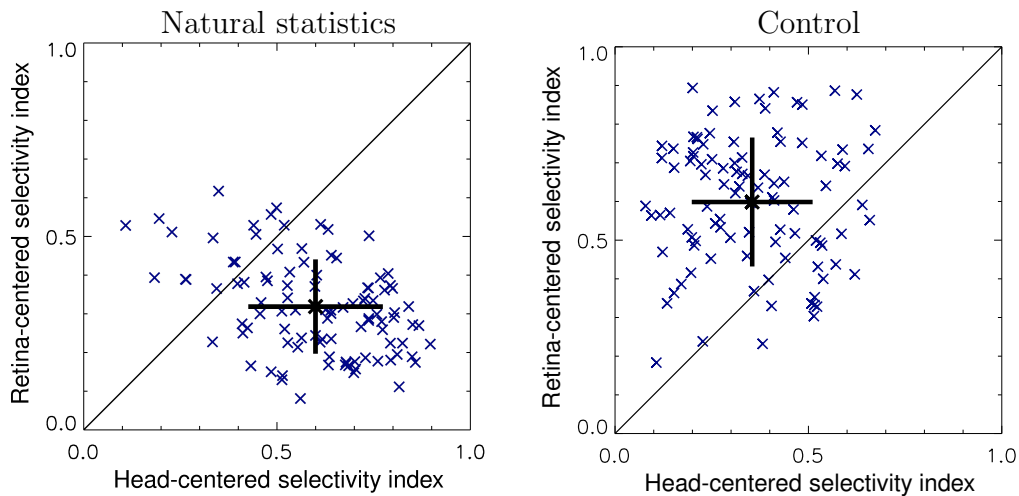


Figure 16: **Selectivity indices of output layer neurons for natural and control statistics.** Selectivity indices for retina-centered position plotted against selectivity indices for head-centered position for all 100 output layer neurons. Crossed black lines indicate mean and standard deviation of selectivity indices. The left panel (natural statistics) shows selectivity indices for the representation trained with natural statistics where head-centered object positions changed after every 20th saccade. Here, selectivity indices for head-centered stimulus position (s_h) tend to be higher than selectivities for retina-centered stimulus position (s_r). The right panel (control) shows selectivity indices for the representation trained with control statistics where head-centered stimulus positions changed on the time scale of saccades. Here, selectivity indices for retina-centered stimulus position (s_r) tend to be higher than selectivities for head-centered position (s_h).

over each neuron’s head-centered or retina-centered tuning curve weighted by each neuron’s output firing rate as a response to the given stimulus. The maximum of the population response was taken as the decoded head-centered or retina-centered position for the specific stimulus combination. Estimation errors were determined by calculating the differences between the decoded head-centered or retina-centered position and the actual head-centered or retina-centered position of a presented stimulus for each stimulus combination. When the network was trained with natural statistics estimation errors were low for head-centered positions and were higher for retina-centered positions (figure 17). Estimation errors show that the neural activity in the output layer contained reliable information about the spatial stimulus position of a presented object and little information about the retinal stimulus position

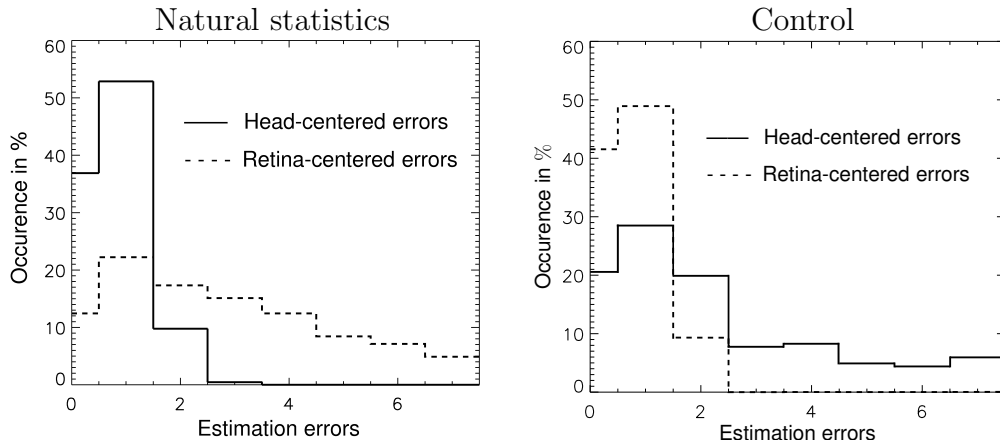


Figure 17: **Histogram of estimation errors for natural and control statistics.** Distributions of estimation errors derived from the responses of output layer neurons for retina-centered (dotted line) and head-centered (solid line) positions. When the network was trained with natural statistics (left panel) head-centered estimation errors were lower than retina-centered estimation errors. When the network was trained with control statistics (right panel) retina-centered estimation errors were lower than head-centered estimation errors.

when the network was trained with natural statistics. When trained with control statistics, estimation errors for head-centered positions were higher than those for retina-centered positions.

We conclude that under natural viewing conditions where gaze direction changes on a faster time scale than head-centered object positions the population of output layer neurons achieves a representation of the visual environment that is consistent with a head-centered frame of reference. However, when we neglect statistics of natural viewing conditions, training the network with head-centered object positions changing on the time-scale of saccades, the population of output layer neurons tends to represent visual space in a retina-centered frame of reference. This argues for a major role of natural viewing statistics for learning gaze-invariant, head-centered representations of visual space.

4.4.3 Reduction of the Dimension of the Map Formation Layer

After learning, the network of gain-modulated neurons is functionally similar to a basis function network [Pouget and Snyder (2000)]. Retinal and gaze direction inputs are combined in the map formation layer in a nonlinear way and form a basis set that spans the head-centered space. These basis functions are organized in topographic maps (figure 12) according to the spatio-temporal statistics in the inputs only [Michler et al. (2009); Einhäuser et al. (2007)]. This yields a head-centered representation in the output layer with receptive field properties similar to those of neurons in area VIP [Duhamel et al. (1997)]. According to the theory of basis function networks [Pouget and Snyder (2000)] the map formation layer should contain at least 15×15 neurons in order to transform 15 horizontal object positions accurately. This assumption implies a tremendous number of neurons needed in the map formation layer when more horizontal positions or horizontal and vertical positions need to be transformed. However, reduction of the number of neurons in the map formation layer after learning hardly affected decoding performance (figure 18). We simulated this by randomly erasing single neurons in the map formation layer after the learning process until the desired reduced number of neurons was reached. The decoding performance for each reduced network was quantified by averaging the head-centered estimation errors over the whole stimulus set. Reducing the map layer from 50×50 to 15×15 neurons did not at all reduce decoding performance, as with 15×15 neurons the full stimulus space is still combinatorially represented. A reduction to 10×10 neurons reduced performance to 83% (fit data¹²), with 5×5 neurons a performance of 56% was achieved and even with 15 neurons a performance of 47% was achieved.

We suggest that this robustness is due to the advantages of representing information in population codes. Due to overlapping retinal tuning curves and gain fields of individual neurons in the map formation layer, many neurons respond to a given stimulus combination and a specific position can be encoded

¹²Original data was fit via a least square method by a root function $a \cdot \sqrt[b]{N} - c$ where a,b, and c are fitting parameters and N is the number of neurons in the map layer.

without a neuron being specifically selective for only this position.

4.4.4 Stable Head-Centered Representations and Choice of Model Neurons

Results presented in the last paragraphs were obtained by simulating nonlinear interaction between retinal (R) and gaze direction (G) input via a permissive gating-mechanism (see chapter 2). However, other approaches to realize nonlinear interactions in the framework of the presented network model are possible as presented in Philipp (2009). We tested the performance of the network with three map layer model neurons which differed in the nonlinear interaction between retinal (R) and gaze direction (G) inputs and

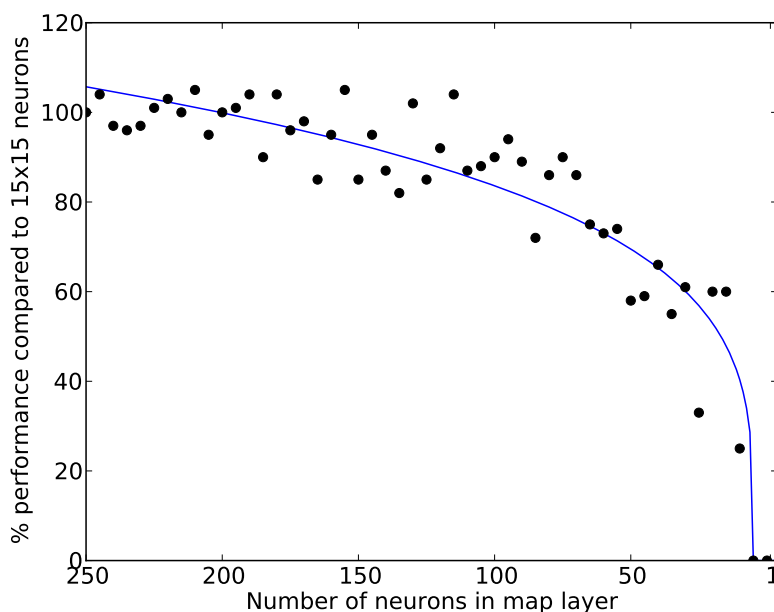


Figure 18: **Decoding performance with reduced map formation layer.** Relative decoding performance of the network with a reduced map formation layer compared to a network with 15×15 neurons in the map formation layer (see text). Relative performance is shown as a function of the number of neurons in the map formation layer. Black dots show original data; the blue solid line is a fit root function.

were identical otherwise concerning modeling of synaptic dynamics and spike generation as described in the methods section. In the gating model neuron, nonlinear interactions were realized by a thresholding mechanism

$$U(t) = R(t) \times \Theta(G(t) - \gamma) + Rec(t) \quad (4.15)$$

where $U(t)$ is the membrane potential of a map layer neuron, γ is the gating threshold, $R(t)$ and $G(t)$ are retinal and gaze direction EPSPs, $\Theta(x)$ is the Heaviside step function, and $Rec(t) = E(t) - I(t) + \Omega(t)$ are the additional recurrent inputs.

In the second model neuron, nonlinear interactions were modeled as a direct product of the retinal and gaze direction EPSPs

$$U(t) = R(t) \times G(t) + Rec(t). \quad (4.16)$$

In the third neuron model, nonlinear interactions were modeled by a more modulatory than multiplicative combination of retinal and gaze direction EPSPs as proposed by Eckhorn et al. (1990):

$$U(t) = R(t) \times (1 + G(t)) + Rec(t) = R(t) + R(t) \times G(t) + Rec(t). \quad (4.17)$$

However, in our self-organizing network only the gating-mechanism led to stable head-centered representations in spite of extensive parameter scans. The multiplicative interactions in the $R \times G$ approach resulted in uncontrollable learning dynamics and representations that showed undefined salt and pepper-like topographic maps [Koulakov and Chklovskii (2001)] without gaze-invariant receptive fields of output layer neurons. We suggest that the problem of the $R \times G$ multiplicative model is that the effect of the gaze direction inputs does not saturate with increasing gaze direction input - as it does in the gating model neuron (see figure 3 in chapter 2). In the gating model neuron, the influence of the gating inputs is bounded. The maximum influence is achieved in the situation where a neurons gate is opened all the time. In this case the membrane potential is determined by the retinal EPSPs only $U(t) = R(t) \times 1$, because $\Theta = 1$. Here, a further increase in gaze direction inputs has no more

influence on the membrane potential of the postsynaptic neuron. However, in the multiplicative $R \times G$ model the effect of gaze direction inputs increases unbounded. This can have unwanted effects on the network dynamics as with increasing synaptic weights unrealistically high firing rates can be obtained which may not be compensated for by the implemented homeostatic synaptic mechanisms [Miller and Mackay (1994)].

The modulatory $R \times (1 + G)$ approach led to retina-centered topographic maps independent of viewing statistics where head-centered and gaze-direction maps showed an undefined salt and pepper structure [Koulakov and Chklovskii (2001)]. Selectivities in the map formation layer developed for retinal inputs only whereas changes in gaze direction had no influence on the neuron's gain. It seems as if gaze direction inputs had no influence on the outcome of the process of self-organization. We suggest that this is due to the fact that in the $R \times (1 + G)$ model, the presence of a gaze direction input is not a necessary condition to produce an output spike - which it is in the gating model neuron (see figure 2 in chapter 3). Retinal inputs are sufficient to produce output spikes and thus the network organizes itself with respect to the retinal inputs and neglects gaze direction inputs.

4.5 Discussion

We presented a neural network model that explains how gaze-invariant representations of the visual environment can be learned on the basis of the statistics of natural viewing conditions where a slowly changing scene is scanned by frequent saccades. To our knowledge this is the first model to explain how gaze-invariant representations of the visual environment can be learned in a biologically plausible, unsupervised way. Previous models used supervised learning mechanisms [Zipser and Andersen (1988); Mazzoni et al. (1991)] such as backpropagation which are unlikely to be used in the brain. Our model provides a possible explanation for the development of retina-centered neurons in parietal cortex that are gain-modulated by gaze direction [Andersen and Mountcastle (1983)].

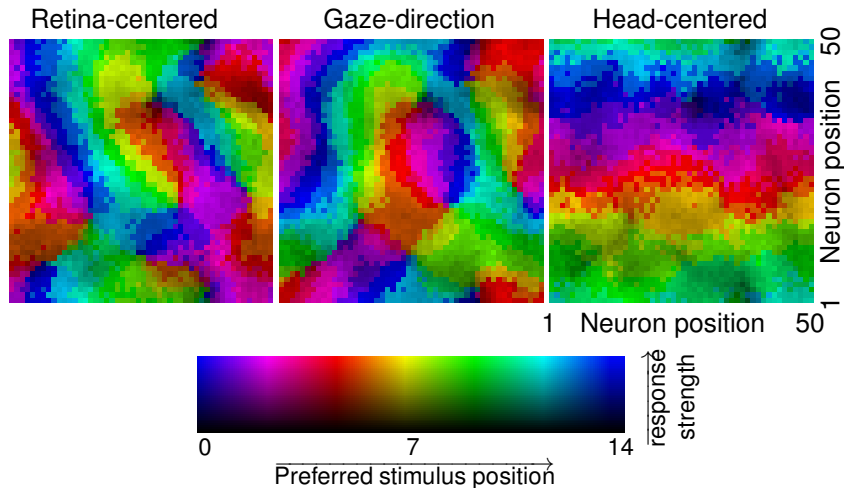


Figure 19: **Topographic maps with a striped pattern in head-centered coordinated.** Topographic organization of preferred retina-centered (left panel), gaze direction (middle panel) and head-centered (right panel) selectivities in the map layer. Color encodes stimulus position in the respective coordinate frame, brightness encodes relative response strength. Simulation parameters were identical to simulations with natural viewing conditions (see figure 12). Head-centered preferred positions are organized in a stripe structure. Patches of similar retina-centered preferred positions show a pinwheel-like organization structure.

4.5.1 Gain Fields and Structure of Topographic Maps

In an experiment using the technique of optical imaging, a topographic organization of gaze direction selectivities was found in parietal cortex [Siegel et al. (2003)]. Our model predicts a topographic organization of gaze direction selectivities that is superimposed by topographic maps for retinal and head-centered selectivities (figure 12) yielding a transformation to a head-centered frame of reference. The detailed structure of the topographic maps that were obtained in our simulations differ with respect to two main organization structures: One structure shows pinwheel-like organization in each coordinate frame (see figure 12), the other structure shows pinwheel-like organization patterns in the maps displaying retinal and gaze direction selectivities and shows a striped pattern in the head-centered map (see figure 19). Selectivity indices, estimation errors and receptive fields of output-layer neurons are qualitatively similar in both organization structures. This indicates that the two

organization structures are functionally similar with regard to head-centered selectivities and gaze-invariance. Surprisingly, both structures appear in simulations that are identical concerning all simulation parameters except for the precise noise-values which differ between individual simulations ($\Omega(t)$ in equation 4.2). Thus, the appearance of the two structures could be an emergent property of the process of self-organization that depends on slight deviations in noise values. However, it is unclear which mechanism determines the pinwheel-like or stripe-like organization structure. Further studies are required to answer the question of the origin of the two different organization structures.

Koulakov and Chklovskii [2001] proposed a model that explains the formation of the different organization structures observed here. The model is based on an evolutionary strategy that serves to minimize the recurrent connection length between neurons that encode similar stimulus properties. In the model it is assumed that evolution was likely to select for developmental rules that produce orientation maps which are optimized according to wire length. By varying the width of the recurrent interaction kernels in the map layer, the authors can induce the development of the resulting organization structures. However, it is unclear how these results transfer to the model presented here. The occurrence of stripe and pinwheel patterns was also observed in another model for the optimization of cortical maps [Keil and Wolf (2011)].

4.5.2 Coordinate Transformations and Eye Velocity Gain Fields

We investigated the development of gaze-invariant representations on the basis of gaze direction gain fields which are known to support coordinate transformations [Zipser and Andersen (1988); Mazzoni et al. (1991); Salinas and Abbott (1997); Pouget and Snyder (2000); White and Snyder (2004)]. The self-organizing network presented here learned a gaze-invariant representation of visual space from a nonlinear combination of retinal and gaze direction input. Neurons in the dorsal subpart of the medial superior temporal cortex (MSTd) in posterior parietal cortex are also thought to compensate for self-generated

eye or head movements [Brostek (2012)]. Area MSTd processes visual motion stimuli as well as information about eye movements [Newsome et al. (1988)] and neurons in MSTd nonlinearly combine information about the retinal image with information about eye velocity during tracking eye movements like smooth pursuit [Newsome et al. (1988)] or optokinetic response rather than information about gaze direction [Bradley et al. (1996); Bremmer et al. (2010); Brostek (2012)]. Model simulations suggest that the distribution of eye velocity gain fields in MSTd allows for a transformation from retinal image velocity to head-centered stimulus velocity during tracking eye movements [Brostek (2012)]. The authors suggest that eye velocity gain fields that developed during a process of supervised learning form a basis set that allows to generate numerous visual motion related variables, for example an estimate of head position or self-motion velocity [Brostek (2012)]. However, it is unknown, how such networks can develop in an unsupervised way. In the study presented here, we showed that gaze-invariant representations can develop in an unsupervised way in a network that is trained with statistics of natural viewing including saccadic eye movements. Our network could be a starting point to explain the development of eye velocity gain fields for coordinate transformations as studied by Brostek (2012). By training the network with input data that encodes retinal inputs and eye movements that mimic the statistics of natural viewing during tracking eye movements, the network could in principle learn coordinate transformations like those obtained by Brostek (2012) in an unsupervised way.

4.5.3 A General Mechanism for Information Integration?

The applied learning mechanism of exploiting spatio-temporal statistics of natural viewing conditions to form superimposed topographic maps and invariant representations was suggested by Michler et al. (2009). When the model was trained with a stimulus set in which the identity of objects changed on a slower time scale than the viewing angle under which an object was presented, the model developed a representation that was selective for object identity and invariant to viewing angle. Such neurons can be found in the

ventral path of the visual system. Here we presented a model of learning gaze-invariant representations of visual space - associated with the dorsal path of the visual system [Andersen and Mountcastle (1983)]. We conclude that the applied learning mechanism could be a general mechanism of information integration in the brain - not only coordinate transformations - applicable to all kinds of invariances - not only gaze- and viewing angle-invariance.

4.6 Outlook to Chapter 4

The presented model argues for a strong influence of natural statistics and contextual interactions on the development of neural representations: The combination of natural viewing conditions with contextual information about gaze direction that interacts nonlinearly with retinal information allows for the development of a gaze-invariant representation. From the input perspective, three main aspects are important for the developmental process of self-organization: (i) primary sensory input, (ii) contextual input that influences the sensory input, and (iii) natural joint statistics in both input streams. Those aspects also occur in a modified form in the next study presented in this thesis. In the next chapter the influence of the contextual entity of attention on somatosensory perception will be investigated. Here, adult Zen-meditators altered the natural statistics (iii) of the attentional context (ii) by focussing attention on their right index finger for hours. External somatosensory input (i) was prevented during the meditative intervention by the rigid meditation posture in Zazen. With psychophysical markers that measure perceptual abilities, we observed the effects of this intervention.

5 Improvement of Tactile Perception by Meditation

5.1 Abstract

Neuroplasticity typically describes the effects of a bodily training paradigm on neural representations [Jenkins et al. (1990); Merzenich and Jenkins (1991); Fahle and Poggio (2002)]. We here investigated the effect of a three day Zen retreat, a purely mental intervention, on somatosensory perception. Discrimination performance in the right index finger improved in the absence of any bodily training only by focussing sustained attention on the tip of the right index finger. Our findings indicate that the framework of neuroplasticity has to be extended to incorporate the observation that intrinsic brain activity created without external events can alter neural representations and perception.

5.2 Introduction

In neuroscience, neural representations are commonly characterized by single neurons receptive fields and topographic maps of selectivities for sensory stimuli. These neural representations build up during development and are in a constant process of adaptation in order to gain a dynamically maintained steady state that reflects the adaptation of the neural system to the statistics of an average environment [Barlow (1961); Dinse and Merzenich (2002); Simoncelli and Olshausen (2001)]. Environmental changes induce adaptational mechanisms in the brain aiming at a neural representation that fits the present environmental statistics and situations in order to gain maximal viability in perception and action with respect to the requirements of the actual environment.

There is a wealth of evidence that cortical maps and neural representations are in this above described state of permanent use- and experience-dependent fluctuation [Dinse and Merzenich (2002)]. The core of these studies is that alterations in afferent input statistics strongly influence the neural representation of the respective sensory entity: Our brain adapts to profound changes

in our sensory environment. The first studies concerning plasticity of cortical maps were conducted in the somatosensory area of higher mammals where selectivities for skin areas are represented in ordered topographic maps that reflect adjacencies on the body surface [Dinse and Merzenich (2002)]. In their pioneering work, Jenkins et al. (1990) showed in a neurophysiological experiment with adult owl monkeys, that finger stimulation over about ten days altered the neural representation of the stimulated fingers in primary somatosensory cortex. After training, the stimulated skin surface was represented over an expanded cortical region with receptive fields of individual cells being unusually small in these expanded areas. Topographic representations of fingers also "differed greatly from that recorded in control experiments": Representational discontinuities emerged in these map regions and borders between representations of individual fingers shifted. These results showed a clear effect of altered external inputs on cortical representations and were a milestone - if not the foundation stone - in the field of *Neuroplasticity*.

5.2.1 Neural Plasticity Without External Stimulation

The common view of neuroplasticity is that changes in the statistics of the environment lead to adaptational changes in neural representations. Considering the brain and its cortical maps as a self-organizing system, one can hypothesize that changes in the internal state of the brain can induce equally profound adaptational mechanisms in the brain as changes in the statistics of the external environment do.

Recent studies argue for this hypothesis: alterations of cortical representations and perceptual abilities can be induced without emphasis on external training. It seems that neural plasticity can be triggered merely by *changing the internal state of the subject* by mental imagery of stimuli [Tartaglia et al. (2009, 2012)] or by induction of activity patterns via neurofeedback [Shibata et al. (2011); Scharnowski et al. (2012)]. Furthermore, it is known that the attentional focus strongly increases the efficiency of perceptual training [Seitz and Dinse (2007)].

In the visual domain, Tartaglia et al. (2009) showed that imagining a crucial part of a bisection stimulus was sufficient for perceptual learning in a discrimination task in the absence of external training via repetitive stimulus presentation. The authors conclude that the neural processes underlying perceptual learning, which were usually assumed to be primarily dependent on stimulus processing, could be equally based on mentally generated signals. Similar results of mental imagery on perceptual performance were obtained investigating visual discrimination of motion directions [Tartaglia et al. (2012)]. In another study, an effect of visual attentional training with only minimal use of a visual stimulus enhanced visual spatial acuity [Dupuis-Roy and Gosselin (2007)].

In the study presented here we investigated the effect of a three day Zen retreat on the tactile abilities of the finger tips. During the retreat, subjects had to focus attention on the spontaneously arising percepts in their right index finger. In the instructions given to the subjects concerning the meditative intervention, there was no focus on any kind of external training, stimulation or movements.

5.3 Methods

5.3.1 Measures of Tactile Abilities

As markers of tactile abilities we measured 2-point discrimination (2pd) thresholds and localization performance on the tip of digit 2 and 3 of the right hand ($r2$ & $r3$) and digit 2 of the left hand ($l2$) via standard procedures. 2pd thresholds were assessed by using a custom-made device. Localization performance was measured using a forced choice paradigm, where subjects had to report the absolute position where they perceived a touch sensation within quadrants of a square that was printed on the skin of the fingertip.

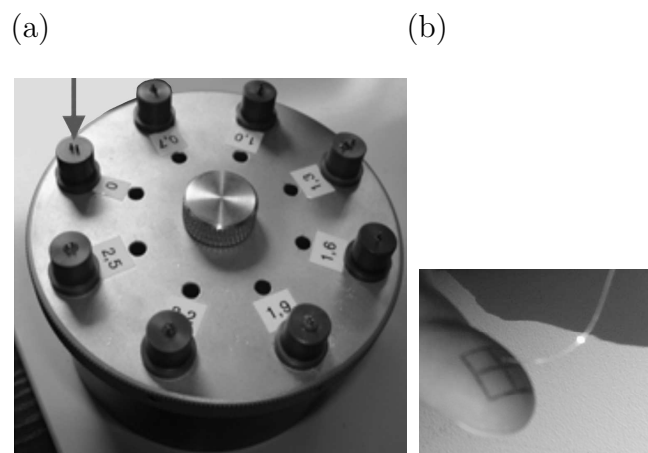


Figure 20: **Equipment to assess measures of tactile abilities.**(a): custom made device to assess 2pd thresholds. The arrow points to the stimulus with 1.6mm distance which is denoted at the opposite side of the wheel. (b): quadrants printed on the finger tip to assess localization performance. The subject is stimulated via a von Frey filament.

5.3.2 2-Point Discrimination Thresholds

The 2-point discrimination (2pd) threshold is a reliable marker of discrimination performance in humans. The 2pd thresholds were assessed by using the method of constant stimuli [Godde et al. (2000); Dinse et al. (2005)]. A custom-made device was used to assess the 2pd thresholds on a fixed position on the skin of the fingertips by rapidly switching between stimuli (figure 20 a). The stimuli consisted of 7 pairs of brass needles with different distances (ranging from 0.7 to 2.5mm in increments of 0.3 mm or from 1 to 4mm in increments of 0.5mm) and a single needle as 0 distance (control condition). The needles were 0.07mm in diameter with blunt ends that were approximately $200\mu m$ in diameter. Tactile stimuli were applied for approximately 1s; application forces of 150 to 200mN are applied when the custom made device is used appropriately. The subjects were instructed to place their finger on the support and to maintain the initial position of the finger. The stimuli were presented 10 times in randomized order resulting in 80 trials per session. Subjects were not informed about the ratio of needle pairs and single needles, which was 7:1. Subjects had to decide immediately after stimulus application

if they had the sensation of 1 or 2 needles by reporting the percept of a single needle or of a doubtful stimulus as "1", but the distinct percept of 2 stimuli as "2". All responses were plotted against needle distances resulting in a psychometric function, which was fitted by a sigmoid function (figure 21).¹³ The 2pd threshold was taken from the fit where 50% probability was reached. All subjects had to accomplish one training session to become familiar with the testing procedure.

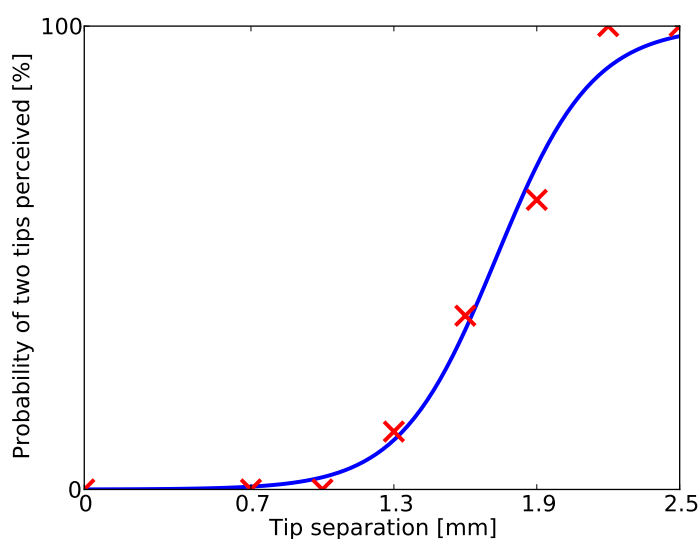


Figure 21: **Sigmoidal curve fit to determine 2-point discrimination threshold.** 2pd stimuli consisted of 7 pairs of brass needles with different distances and a single needle of 0 distance (80 trials per session). The probability that two tips were perceived was plotted against needle distances resulting in a psychometric function (red crosses), which was fitted by a sigmoidal function (blue trace). The 2pd threshold was taken from the fit where 50% probability was reached (1.68mm). The figure exemplary shows 2pd data and fit of one session done with a subject from the sensory focussing group (s9) on day 0 (see table supplementary table 1).

5.3.3 Localization Performance

Localization performance on the tip of the fingers was measured using a forced choice paradigm, where subjects had to report the absolute position on the tip

¹³2pd threshold data was fit by a sigmoidal function $a \cdot \tanh(b \cdot (x - c) + 1)$ via a least square method where a,b, and c were fitting parameters and x was the needle distance.

of a finger where they perceived a touch sensation without visual inspection [Dinse et al. (2005)]. A small square (1 cm²) was printed on the skin of the fingertip (figure 20 b), which contained four quadrants of equal size (5x5 mm each). The center of each quadrant was touched in a pseudorandomized order 40 times with a von Frey filament (Marstocknervtest, Marburg, Germany) with a buckling force of 1.4mN or 2.0mN, respectively, that was above threshold and clearly detectable at each of the four quadrants [Bell-Krotoski et al. (1995); Desrosiers et al. (1996)]. Subjects were instructed to report the number of that quadrant, where they felt the sensation. To facilitate this procedure, subjects were allowed to see a drawing of the fingertip with 4 quadrants identified by numbers 1 to 4. Average localization performance is given for each finger by the rate of correct quadrant identifications.¹⁴

5.3.4 Subjects, Measurement Protocol & Meditative Intervention

Before the first measurement on day 0 subjects were assigned to one of two groups: a *sensory focussing group* and a *control group* (all right handed). The groups' names were not told to the subjects. Subjects in both groups were told that we investigate the effects of a meditation retreat on somatosensory perception. Each subject was asked the following question:

”In group A you will have to take part in three measurements on day 0, 3 and 4. In group B, you will have to come to these measurements and spend additional two hours per day on a special meditation technique. Which group do you want to be in? If you are not willing to spend effort on the special meditation technique, please choose group A!”

We asked this to be secure that subjects in the sensory focussing group were motivated to practice the special meditation technique of focussing attention on their right index finger. The group assignment was done based on the subjects decisions and based on the objective to have age and gender-matched

¹⁴As a possible third marker of tactile abilities we assessed touch thresholds by probing the fingertips with von Frey filaments ranging from 0.08 mN to 10 mN in logarithmic scaling using a staircase procedure. However, as problems with this specific method for the assessment of touch thresholds were indicated recently, this data set will not be presented here.

groups. The mean age of the ten subjects in the sensory focussing group (4 female) was $49.9 \pm 5.7(\text{std})$ years. The mean age of the 10 subjects in the control group (5 female) was $51.7 \pm 4.2(\text{std})$ years. We asked subject to estimate the amount of hours per week they spend meditating in everyday life. Subjects in the sensory focussing group estimated $3.8 \pm 1.7(\text{std})$ meditation-hours per week, subjects in the control group estimated $3.9 \pm 1.4(\text{std})$ meditation-hours per week. Average meditation experience in the sensory focussing group was $14.7 \pm 7.5(\text{std})$ years and $9.5 \pm 7.13(\text{std})$ years in the control group. Subjects of both groups were paid and naive concerning the experimental hypothesis (control group: 30€; sensory focussing group: 70€. Subjects did not know about different payments. Difference in payment is due to effort that subjects in the sensory focussing group are supposed to put into the sensory focussing meditation technique.). Physical stimulation of the finger tips did not occur due to the rigid meditation posture in Zazen.

Measures of tactile abilities (chapter 5.3.1) were taken on day 0 - before

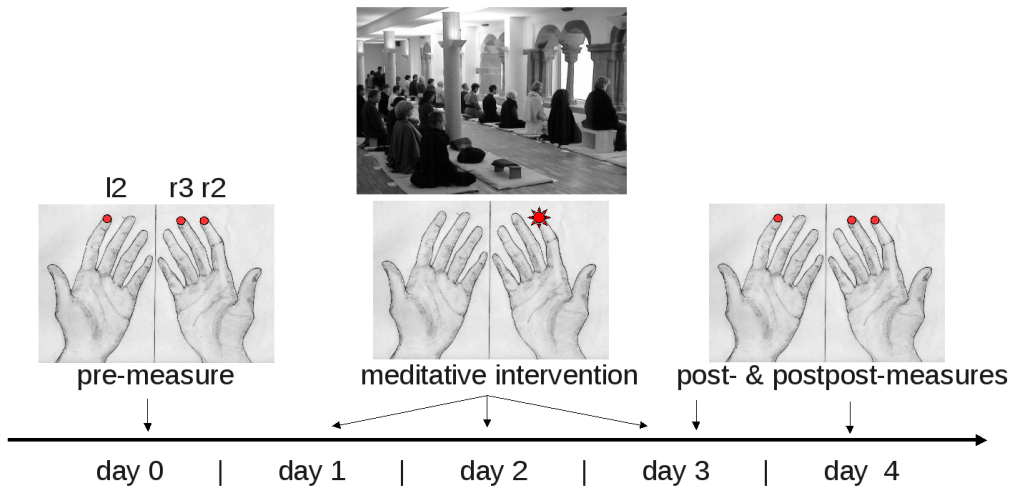


Figure 22: **Timeline of measurements and meditative intervention.** Measures of tactile abilities were taken on day 0, 3 and 4 on the finger tips of digits r2, r3 and l2 (pre-, post- and postpost-measures). On day 1, 2 and 3, subjects in the *sensory focussing group* were asked to focus attention on the finger tip of the right index finger (meditative intervention). Subjects in the *control group* kept their normal meditative practice for the whole time.

the beginning of the retreat - and on days 3 and 4 (figure 22). One set of measurements took about 45 minutes. The Zen retreat was held in total silence with long meditation periods (> 8 hours per day). During the total meditation period of 3 days, subjects in the *sensory focussing group* were asked to be completely aware of the spontaneously arising sensory percepts in their right index finger for 2 hours per day; while keeping their normal meditative practice (focussed attention on breath) for the rest of the day (6 hours). Subjects' tactile performance was measured again after the 3 day meditation period (day 3) and also after a 4th day of normal meditation without focussing on somatosensory percepts (day 4). Subjects in the control group kept their normal meditative practice for the whole 4 days without focussing on somatosensory percepts.

5.3.5 Data Acquisition, Software, and Investigator

During the measurements data was directly entered into a *Lenovo R61* laptop equipped with self written software in the programming language *Python 2.5*. Software for data evaluation was also self written and uses open source scientific standard packages *Scipy*, *Numpy* and *Matplotlib* for fitting functions and graphical illustrations and *IBM SPSS Statistics* for statistical evaluation. The measurements were performed by Sebastian Philipp. The problem of a non-blind experimentator will be elaborated in the Discussion section at the end of this chapter.

5.4 Results

Original data values, the responses of subjects on each individual stimulus, were analyzed as described in the methods section. Analysis yielded one 2pd threshold and one localization performance value for each day 0, 3, and 4, and each finger r2, r3, and l2 for each subject. These values are presented in a tabular view in the supplementary material (section 8.2.1 and 8.2.2).

The meditative intervention practiced by the sensory focussing group was a sustained direction of attention on the spontaneously arising percepts in the right index finger (r2). Therefore the presentation of results will focus on

changes of tactile abilities in the right index finger. Results concerning the development of tactile abilities in the right middle (r3) and the left index finger (l2) are treated as control measurements for the specificity of the observed effects. The central questions are:

- Does focussing attention on r2 influence tactile abilities in r2?
- Does it also influence performance in the neighbouring finger r3?
- Does it even influence performance in l2 which is represented in the contralateral primary somatosensory cortex?

5.4.1 2pd Thresholds

The meditative intervention of focussing attention on the right index finger strongly altered psychometric 2pd curves and 2pd thresholds (figure 23). Individual measures of r2 2pd thresholds on different days are presented in figure 24. 2pd thresholds in the right index finger were lowered for 8 of 10 subjects of the sensory focussing group on day 3 after the meditative intervention. Individual improvements of 2pd performance in r2 on day 3 ranged from -6% to 63% . Two subjects decreased slightly in r2 performance on day 3 (-6% and -1%) and 8 subjects increased performance in r2 (7% to 63%). On day 4, after one day of conventional meditation, 9 of 10 subjects of the sensory focussing group showed lowered r2 2pd thresholds compared to day 0. Individual improvements of 2pd performance in r2 on day 4 ranged from -7% to 72% compared to day 0.

As a sample size of 10 subjects per group is too small for a parametric test, a *non-parametric related-samples Wilcoxon signed rank test* was used for statistical analysis. Grouped data is presented in figure 25. For the sensory focussing group, Wilcoxon's test indicates a probability of $p_{r2} = 0.013$, $p_{r3} = 0.025$, and $p_{l2} = 0.086$ that the median of differences in 2pd thresholds between day 0 and day 3 was zero. Thus, the null hypothesis that the median of differences between day 0 and day 3 was zero can be rejected for r2 and r3 but not for l2 on a significance level of $p < 0.05$. 2pd performance on day 3

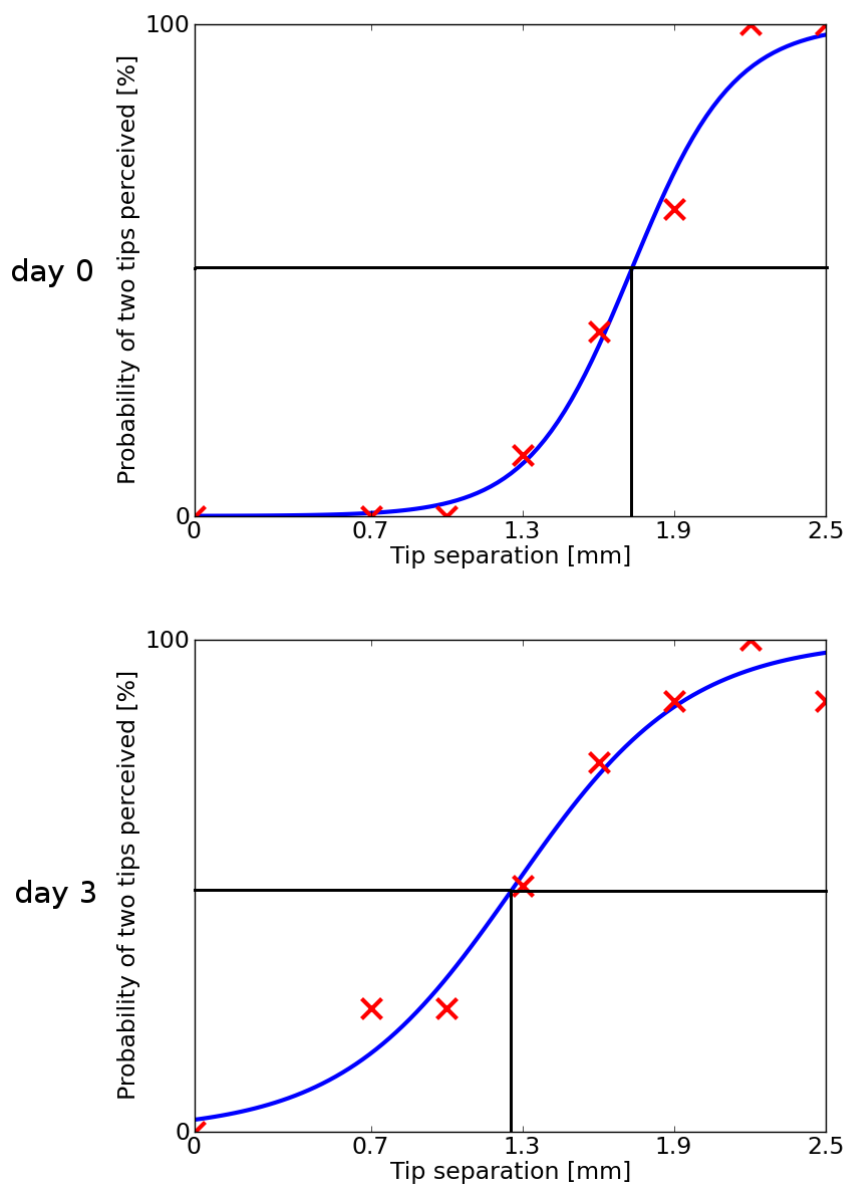


Figure 23: **Psychometric 2pd curves on day 0 and day 3.** The figure exemplary shows psychometric curves of subject s9 in the sensory focussing group on day 0 and day 3. The 2pd threshold was taken from the sigmoidal fit where 50% probability was reached. On day 0, subject 9 showed a 2pd threshold of 1.68mm. On day 3, subject 9 showed a lowered threshold of 1.27mm which relates to an improvement in 2pd performance of 24%.

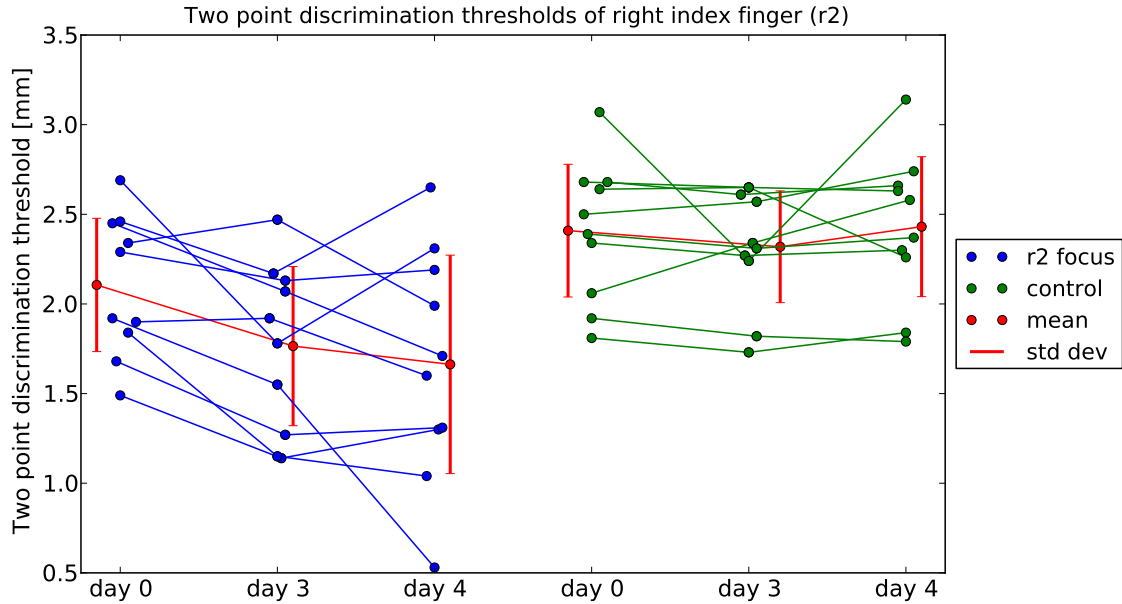


Figure 24: **Two point discrimination thresholds for r2.** Figure shows measured two point discrimination thresholds on day 0, 3 and 4 of individual subjects from the sensory focussing (blue) and control group (green) for the right index finger. 2pd thresholds in r2 were lowered for 8 of 10 subjects of the sensory focussing group on day 3 and for 9 of 10 subjects of the sensory focussing group on day 4.

improved on average by $17 \pm 13\%$ in r2 and by $12 \pm 16\%$ in r3.¹⁵ Furthermore, Wilcoxon's test indicates that medians differ between day 0 and day 4 for r2 and r3 ($p_{r2} = 0.014$, $p_{r3} = 0.022$) but not for l2 ($p_{l2} = 0.26$). A prolonged effect of the meditative intervention is thus indicated for fingers r2 and r3. 2pd performance on day 4 improved by $22 \pm 21\%$ in r2 and by $15 \pm 17\%$ in r3 compared to day 0. Wilcoxon's test indicates that medians of differences between day 3 and day 4 equal zero for each finger ($p_{r2} = 0.65$, $p_{r3} = 0.88$, and $p_{l2} = 0.33$). This indicates that the amounts of performance improvements were persistent for each finger.

The statistical analysis indicates an improvement in 2pd performance of the sensory focussing group on day 3 and day 4 for fingers r2 and r3 of the right hand. In the control group, average 2pd thresholds remained unchanged in

¹⁵Averaged over individual improvements.

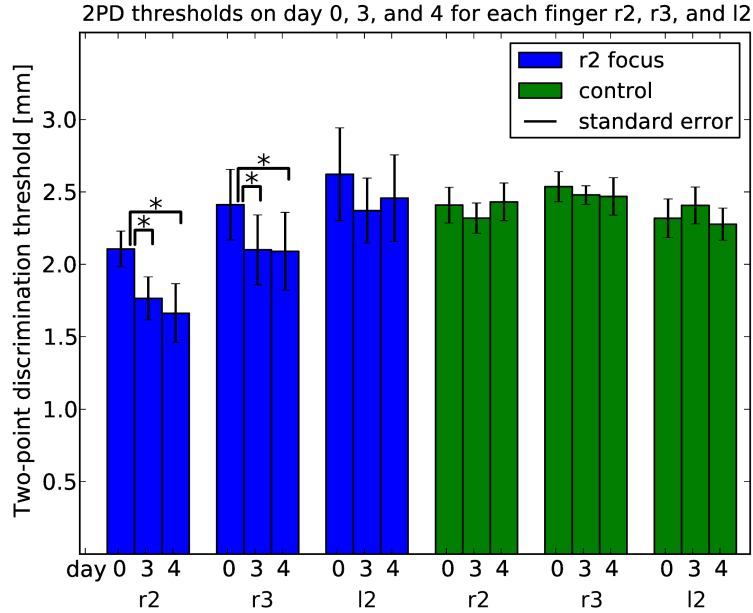


Figure 25: **Changes in average two point discrimination thresholds.** For each finger and each group average touch two point discrimination thresholds measured on day 0, day 3 and day 4 are shown. Two point discrimination thresholds in the sensory focussing group were lowered significantly for r2 on day 3 (Wilcoxon's test $p < 0.05$). Controls showed no significant changes.

each finger on day 3 (r2: $3 \pm 10\%$, r3: $1 \pm 10\%$, l2: $-6 \pm 19\%$) and day 4 (r2: $-1 \pm 10\%$, r3: $2 \pm 10\%$, l2: $0.7 \pm 11\%$). This is indicated as changes in distributions were not significant on day 3 ($p_{r2} = 0.12$, $p_{r3} = 0.45$, and $p_{l2} = 0.58$) and day 4 ($p_{r2} = 0.92$, $p_{r3} = 0.67$, and $p_{l2} = 0.96$).

5.4.2 Localization Performance

Individual localization performance was altered unspecifically in both groups (see figure 26 for r2). Individual localization performance was averaged over subjects for both groups for each finger and each day (figure 27). Wilcoxon's test for the sensory focussing group indicates no alterations in performance on day 3 ($p_{r2} = 0.92$, $p_{r3} = 0.81$, $p_{l2} = 0.57$) and day 4 ($p_{r2} = 0.48$, $p_{r3} = 1.0$, $p_{l2} = 0.94$) for each each finger. Statistical analysis of the control group also indicates no alterations on day 3 ($p_{r2} = 0.33$, $p_{r3} = 0.36$, $p_{l2} = 0.13$) and day

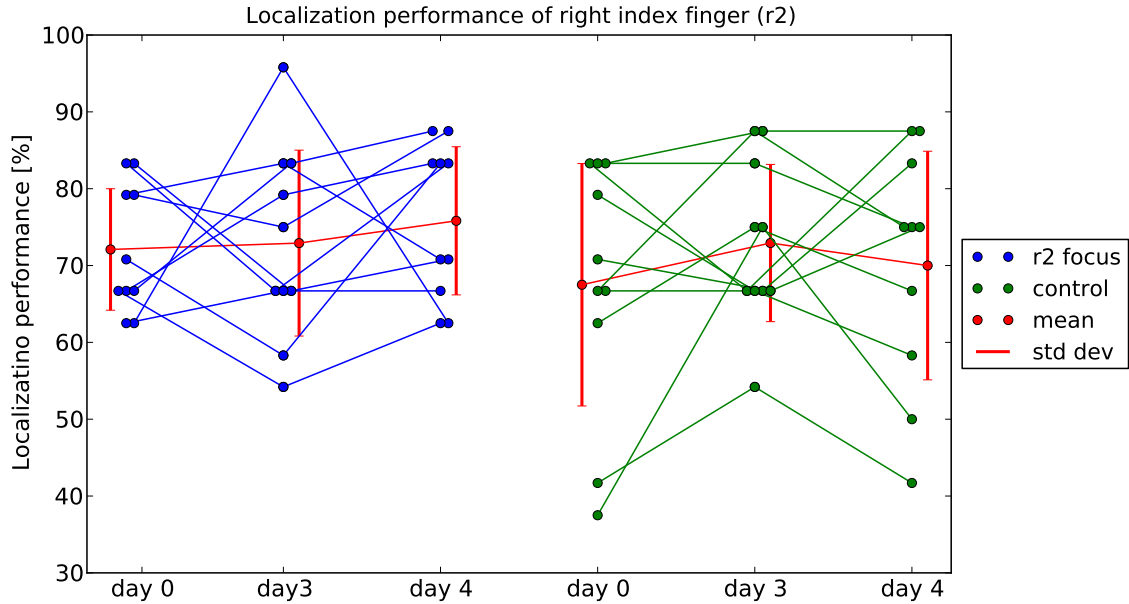


Figure 26: **Localization performance for r2.** Figure shows measured localization performance on day 0, 3 and 4 of individual subjects from the sensory focussing and control group for the right index finger

4 ($p_{r2} = 0.34$, $p_{r3} = 0.51$, $p_{l2} = 0.28$). Neither the meditative intervention of focussing attention on the right index finger, nor the intervention of conventional meditative practice had an effect on localization performance.

5.5 Discussion

Our data shows that focussing attention on a particular body part, here the right index finger, significantly affects discrimination performance (2pd thresholds) indicating that merely being aware, without external stimulation or training, can improve tactile abilities. Focussing attention on the right index finger resulted in significant improvements in 2pd performance in the right index finger (r2) and the neighboring right middle finger (r3) with no improvement in the left index finger (l2) which is represented in the contralateral primary somatosensory cortex. Such changes in stimulus processing are likely to be accompanied by changes in early cortical stages of sensory

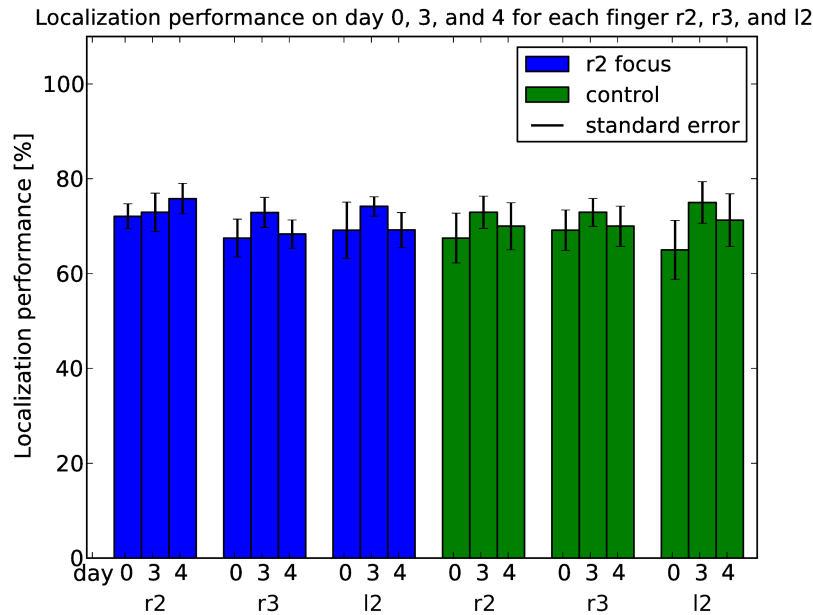


Figure 27: **Changes in average localization performance.** For each group and each finger average localization performance measured on day 0, day 3 and day 4 are shown.

processing [Godde et al. (1996); Pleger et al. (2001); Lissek et al. (2009); Shibata et al. (2011); Scharnowski et al. (2012)]. In the somatosensory area, primary somatosensory cortex (S1) contains a unilateral representation of the fingers whereas second somatosensory cortex (S2) contains a bilateral representation of the fingers. As significant changes in 2pd performance were found for r2 and r3 but not for l2, the results indicate an involvement of S1 in the learning process and no involvement of higher bilateral somatosensory areas (S2 and beyond). Furthermore, the improvement of 2pd performance in r2 and r3 argues for a non-locality of the effect of r2-focussing on the level of S1.

On day 4, after one day of conventional meditation, changes in r2 and r3 were still significant compared to day 0. Thus, a long-term effect of the meditative intervention is indicated. 2pd thresholds were not influenced by conventional meditation practiced by subjects in the control group. In both groups, no changes in localization performance were observed. Due to the rigid meditation posture in Zazen, where meditators are completely motionless, physical

stimulation of the finger tips can be ruled out.

5.5.1 Learning Mechanisms that Could Underlie the Observed Effects

A hypothesis that could explain how sensory focussing can create neural plasticity would be that focussing attention on the right index finger may elicit brain activity in the somatosensory area of the finger by enhancing the input gain of the respective neurons [Treue (2001)]. Focussing attention could thereby induce an asymmetry in spontaneous activity in somatosensory cortex leading to enhanced activity in the region of the respective body part where attention is focussed on which in turn implies activity-dependent self-organization processes. In visual cortex, directing attention to a peripheral location in visual space while expecting a stimulus produced increased activity in visual cortex in the absence of visual stimulation [Kastner et al. (1999)]. Such an increase in activity could also be induced in somatosensory cortex when attention is directed on the right index finger without somatosensory stimulation and could induce neural plasticity.

Another explanation for the observed effects is possible. It is known that changes in the peripheral properties of the fingers such as temperature and circulation influence tactile abilities [Stevens (1989); Stevens et al. (2003)]. This is as the effectiveness of sensory receptors and peripheral signaling cascades in the autonomous nervous system can have an influence on tactile abilities. Thus, changes in perceptual measures induced by training must not only be due to changes in cortical organization structures but can also be due to changes in the sensory periphery. Focussing sustained attention on the fingers during a meditative intervention could in principle induce changes in the autonomous nervous system and in the peripheral physiology of the fingers. To test this hypothesis we are currently conducting experiments where we monitor temperature, circulation and other appropriate measures in the hand before, during, and after a meditative intervention.

5.5.2 Joint Changes in Perceptual Measures and Immobilization

The observed changes after meditation were selective for the two different tasks, but the pattern of joint changes were different from those observed after external training or stimulation [Sterr et al. (1998); Godde et al. (2000); Lissek et al. (2009)]. Subjects that were treated with repetitive external stimulation [Godde et al. (2000); Ragert et al. (2004); Lissek et al. (2009)] showed lowered 2pd thresholds and worse localization performance in the trained fingers. In the study presented here, subjects in the sensory focussing group showed lowered 2pd thresholds and no changes in localization performance in r2. Differences in joint changes between the meditative intervention and external training argue for different mechanisms of neural plasticity in the two interventions.

Reducing the use of a limb for brief periods is known to have strong effects on somatosensory representations [Lissek et al. (2009)]. Lissek et al. (2009) showed that a few weeks of hand and arm immobilization by wearing a cast reduced hand use and strongly impaired tactile abilities. As the use of limbs is strongly reduced during a Zen-retreat where it is common to sit completely motionless for more than eight hours per day, an impairment in tactile abilities could be expected in the presented study although a period of four days of immobilization is quite short compared to periods of wearing a cast [Lissek et al. (2009)]. In our study, in both groups no impairments in tactile abilities were observed. We suggest that the potential for immobilization-impairments was compensated for by the intense awareness training practiced during the Zen-retreat by subjects in both groups [Walach et al. (2011)].

5.5.3 Possible Experimenter Effects

The experimenter (Sebastian Philipp) had to know, which subject belonged to the sensory-focussing or the control group from the beginning of the experiment for organizational reasons. Expectancies that could result from such a knowledge about groups are known to have the potential to influence the outcome of experiments [Rosenthal and Rubin (1978); Sheldrake (1998); Walach (2011)]. Possible experimenter effects can only be ruled out completely

by repeating the experiment under double-blind conditions.

5.5.4 Relation to Other Studies

Improvements in 2pd performance induced by external training and by sensory focussing are in the same order of magnitude [Godde et al. (2000)]. Two hours of external training by repetitive stimulation (*coactivation*) resulted in an improvement in 2pd performance by 16%. In our study, six hours of sensory focussing resulted in a significant improvement in 2pd performance of 17% in the right index finger where attention was focussed on and to a complementary improvement of 12% in the neighboring right middle finger. When the external coactivation protocol was applied for only 30 minutes, discrimination thresholds remained unaffected indicating a critical lower boundary for the induction of coactivation-induced changes [Godde et al. (2000)]. For future experiments it would be interesting to also measure a probable lower boundary for the induction of changes by sensory focussing. Godde et al. (2000) also measured the detailed recovery time course of coactivation effects: 4 hours after finishing the training protocol subjects showed a complete recovery. In the study presented here, 2pd improvements were still strong one day after sensory focussing, which indicates a possible long term effect. However, between day 3 and day 4 subjects in the sensory focussing group continued with their normal meditative practice of focussing attention on their breath. This intense awareness training may have compensated for recovery of 2pd thresholds. For organizational reasons we were not able to measure recovery effects over a longer period without the involvement of meditative practice.

Experiments conducted by other authors also dealt with the effect of mental states on sensory processing. In 2009 it was shown that imaging a crucial part of a visual bisection stimulus induces perceptual learning [Tartaglia et al. (2009)]. Subjects were asked to imagine an offset to the left or right of an imaginary line centered between two visible flanking lines. Imagined offsets should be as small as possible compared to the center of the two flanking lines.

The sensitivity for offsets of visible lines presented between the two flanking lines was increased by this mental training. The authors concluded that the neural processes underlying perceptual learning, which were usually assumed to be primarily dependent on presentations of stimuli, could be equally based on mentally generated signals. Similar results of mental imagery on perceptual performance were obtained investigating visual discrimination of motion directions [Tartaglia et al. (2012)]. The improvements in 2pd threshold performance observed in our study are inline with these findings. However, the intervention of r2-focussing is slightly different to mental imagery. In r2-focussing subjects were only asked to be aware of the spontaneously arising percepts in their right index finger where subjects in Tartaglia et al. (2009) and Tartaglia et al. (2012) were asked to imagine specific stimulus properties that directly related to the discrimination tasks. Our results indicate that in the somatosensory area merely being aware, without emphasis of mental imagery on a specific task, improves discrimination performance.

Recently, two important experiments were conducted showing an effect of internally generated brain activity on perceptual performance and neural representations [Shibata et al. (2011); Scharnowski et al. (2012)]. In both experiments, a group of subjects was trained to elicit specific brain activity in visual cortex by fMRI neurofeedback. By this, subjects induced specific brain activity in visual areas resulting in enhanced sensitivity for visual tasks. The authors of both studies concluded that merely the induction of activity patterns without stimulus presentation induces neural plasticity in early visual areas. It would be interesting to know how the activity patterns produced by neurofeedback relate to activity patterns produced by the intervention of sensory focussing used in our study.

The results obtained in our study are inline with those findings sharing the statement that internally generated brain activity via mental imagery [Tartaglia et al. (2009, 2012)], neurofeedback [Shibata et al. (2011); Scharnowski et al. (2012)], or somatosensory focussing induce changes in perceptual measures and brain organization.

5.5.5 Conclusion

Typically, neuroplasticity describes how external training shapes brain organization. Our findings support the view that this framework has to be extended to incorporate the observation that intrinsic brain activity created without external events can similarly alter perception and brain organization.

6 Main Discussion

In the studies presented in this doctoral thesis, several aspects of information integration and learning in neural systems were investigated at the levels of single neurons, networks, and perception.

6.1 Multiplicative Interactions in Single Neurons

In the first study we asked the question of how contextual, multiplicative interactions can be mediated by the physiological mechanisms available in the brain (chapter 3). Multiplicative interactions are omnipresent in the nervous system. Prominent examples are source-position estimations in the barn owl auditory system [Pena and Konishi (2001); Fisher et al. (2007)], looming stimulus detection [Gabbiani et al. (2002)], binocular interaction [Freeman (2004)], motion detection in the visual system [Hassenstein and Reichardt (1956); Reichardt (1961)], gaze direction gain fields and coordinate transforms in the visual system [Andersen and Mountcastle (1983); Andersen et al. (1985); Brotchie et al. (1995); Ono et al. (2010)], and modulation of neurons output firing rates by attentional context [Treue and Martinez-Trujillo (1999); McAdams and Maunsell (2000); Womelsdorf et al. (2006)]. Although a wealth of possible mechanisms of how multiplication is realized in the nervous system were proposed over the last decades, the origin of multiplicative interactions in the brain remains an open question [Koch (1999); Nezis and van Rossum (2011)]. A mechanism hardly studied in association with multiplicative interactions in the brain is permissive gating [Katz (2003); Gisiger and Boukadoum (2011)]. Here, the presence of the gating-input A opens a gate for input B and thus allows input B to pass and contribute to the membrane potential of the neuron. By this, input B can only contribute to the membrane potential of the neuron, if input A is present. This permissive form of gating can be thought of as being a basis for gain-modulation and multiplicative interactions as it implements a sort of an AND gate. We proposed a model neuron that incorporates a permissive gating mechanism and investigated the model analytically and numerically due to its abilities to realize multiplication between two input streams. Here,

a *feeding* input stream was associated with primary sensory input and a *gating* input stream was associated with contextual input. It turned out that the gating mechanism was capable of realizing multiplicative interactions on a wide range of parameters. The gating mechanism implemented in the model neuron turned out to be very robust in realizing multiplicative interaction in the tested parameter ranges. We conclude that permissive gating can be regarded as a candidate mechanism for how multiplication between two input streams can be realized in the brain.

6.2 Unsupervised Learning of Gaze-Invariance

In the second study we asked the question of how gaze-invariant neural representations in visual cortex that require a nonlinear interaction between sensory retinal and contextual gaze direction inputs can develop in a self-organizing network (chapter 4). The nonlinear interaction between retinal and gaze direction inputs was modeled via the multiplicative gating mechanism presented in the first study (chapter 3). We proposed a model network that learns gaze-invariant representations of visual space in an unsupervised way. Contextual information about the direction of gaze was integrated into the self-organizing network presented by Michler et al. (2009). The self-organizing network proposed by Michler et al. (2009) learns representations of a spatio-temporal input stream that are selective for the slowly varying features in the input stream and invariant to its fast changing features. The input stream reflected natural viewing statistics in which gaze direction changes on a fast time scale while gaze-invariant object positions change slowly corresponding to the exploration of a visual scene by saccadic eye movements. By self-organization of the mutual weights of the retinal input stream and the gaze direction input stream, the network developed a representation that showed gaze-invariant response properties.

The development of gaze-invariant representations was formerly modeled by learning mechanisms that apply some kind of teaching signals that represents knowledge about the gaze-invariant object positions [Zipser and Andersen (1988); Mazzoni et al. (1991); Salinas and Abbott (1997); Pouget and Snyder

(2000); White and Snyder (2004)]. The ability of a biologically plausible self-organizing network to learn gaze-invariant representations was previously unknown. To our knowledge we showed for the first time that gaze-invariant representations of visual space can be learned in an unsupervised way by exploiting the spatio-temporal statistics of natural viewing conditions, only. The strong influence of viewing statistics on the obtained representations of visual space argues for a strong involvement of environmental factors on the development of neural representations which is inline with previous studies [Barlow (1989); Simoncelli and Olshausen (2001); Einhäuser et al. (2002); Fahle and Poggio (2002); Dinse et al. (2003); Wachtler et al. (2007); Michler et al. (2009)].

Other mechanisms have been proposed for learning representations of spatio-temporal input streams [Földiák (1991); Wiskott and Sejnowski (2002); Einhäuser et al. (2002)]. All these mechanisms share the main principle to develop representations of input streams that are selective for the slowly varying features in the input stream and invariant for its fast varying features. Training these mechanisms with an input stream similar to the one used here, with multiplicatively interacting retinal and gaze direction inputs and statistics that mimic natural viewing statistics [Einhäuser et al. (2007)], should in principal lead to similar results as obtained in the study presented here.

In the first study of this doctoral thesis, the applicability of a permissive gating mechanism for realizing multiplicative interactions in an integrate-and-fire model neuron was investigated. This model neuron was included in the self-organizing network presented in the second study. The model neurons learned gain modulation of a visual input stream by gaze direction inputs for coordinate transformations (figure 11) and thus proved to be feasible for learning gain fields in a self-organizing network that incorporates Hebbian-like plasticity [Siegelbaum and Kandel (1991); Dan and Poo (2004)], short term synaptic plasticity [Siegelbaum and Kandel (1991); Dan and Poo (2004)], and adaptational effects [Miller and Mackay (1994)]. The model neuron presented in chapter 3 realizes nearly multiplicative interactions on a wide range of parameter values and is well suited to be used in networks that incorporate plasticity mechanisms. This robustness and applicability in self-organizing

networks makes permissive gating a feasible candidate mechanism as a mediator of gain field phenomena observed in biological neurons [Andersen and Mountcastle (1983); Salinas and Sejnowski (2001)].

6.3 Improvement of Tactile Perception by Meditation

In the third study we asked the question of how attention, without involvement of primary sensory training, influences the processing of sensory stimuli (chapter 5). Psychophysical experiments have shown that focussing attention on a training task increases the effectiveness of perceptual training in the auditory, visual, and somatosensory domain [Seitz and Dinse (2007)]. We asked the question of how effective perceptual learning is if only the focus of sustained attention onto a sensory area without any involvement of external training or stimulation is considered. The results presented in chapter 5 indicate that focussing sustained attention on a particular body part, here the right index finger, significantly affects tactile acuity indicating that merely being aware without external stimulation or training can improve tactile abilities.

From neurophysiological experiments it is known that attention modulates the response properties of sensory neurons in a nearly multiplicative way similar to the multiplicative modulation by gaze direction in parietal cortex [Spitzer et al. (1988); Mountcastle et al. (1987); Richmond and Sato (1987); Treue (2001)]. In this view, attention can be regarded as a contextual cue similar to the cue of gaze direction. In the second study presented in this doctoral thesis, we showed that the multiplicative contextual information about gaze direction has a strong effect on the development of neural representations in a self-organizing network. Viewing sensory layers in cortex as such self-organizing systems [Singer (1986)], it is rational to assume that the multiplicative contextual cue of the focus of attention has similar effects on the development of sensory neural representations. At the same time, organization and reorganization, development and plasticity of mature neural representations depend strongly on the spatio-temporal characteristics of the sensory environment. Our nervous system seems to adapt its skills and

representations to the actual sensory environments it is exposed to. Significant changes in sensory environments alter brain organization and perceptual abilities even in adult organisms [Fahle and Poggio (2002)]. For example, if I extensively practice playing the violin, which significantly changes the statistics of the sensory stimulation of the fingers of my left hand, the representation of my left hand changes as my sensory cortex adapts to the changed statistics of the environment [Elbert et al. (1995)]. If the environment changes, our brains change [Barlow (1961); Simoncelli and Olshausen (2001); Fahle and Poggio (2002)].

But what if not the statistics of the environment change but if the statistics of the attentional focus change. In which way does such an attentional asymmetry influence the neural representations involved? In the third study we investigated this question by having subjects focus sustained attention on their right index finger without any involvement of sensory training. The results were clear: the introduction of an asymmetry in the statistics of the attentional focus drastically improves perceptual abilities in the sensory entity where attention was focussed on - without any involvement of external sensory training. This argues for a strong involvement of internally generated neural signals on brain organization and perceptual abilities, as previously suggested by other authors [Kerr et al. (2008); Tartaglia et al. (2009); Shibata et al. (2011); Tartaglia et al. (2012); Scharnowski et al. (2012)].

To understand what happens in the brain when attention is focussed on the right index finger without the involvement of sensory stimulation and to understand which changes in brain organization underlie the observed alterations in perceptual abilities, we currently repeat this study under double-blind conditions and combine it with functional magnetic resonance imaging and computer models of neural fields which were previously applied to somatosensory learning phenomena [Wilimzig et al. (2012)]. In the last decades fMRI has been used extensively to study effects of training paradigms on brain organization and functionality in humans [Logothetis (2008)]. We think that the combination of this technique with computational models of neural fields will allow us to find the plasticity mechanisms involved in the alterations of perceptual measures produced by sustained sensory focussing. Furthermore,

we are conducting experiments with stroke patients in order to investigate how the results obtained with sensory focussing could be effectively combined with therapeutical methods [Johansson (2012)] or with new approaches [Kattenstroth et al. (2012)] for sensorimotor rehabilitation in stroke patients.

6.4 Neural Plasticity and Mental States

Before the studies of Jenkins et al. (1990) primary sensory representations and cortical maps were thought to be fixed after a critical period in development [Hubel and Wiesel (1965)]. However, this view on the nervous system turned out to be wrong. Jenkins et al. (1990) showed for the first time that mature neural representations in early sensory areas are still capable of adapting to significant changes in the environment. This study determined a breaking point in neuroscience concerning the plasticity of the nervous system and on the view of how the environment shapes neural representations even in adult organisms. The field of neural plasticity emerged and since then the nervous system is viewed as being in a steady state of use dependent self-organization that serves to constantly match perceptual and acting abilities to the actual environment the organism is confronted with [Dinse and Merzenich (2002)]. Today, we are at a similar breaking point: not only the environment, but merely the inner state of a subject seems to be sufficient to alter neural representations [Kerr et al. (2008); Tartaglia et al. (2009); Shibata et al. (2011); Tartaglia et al. (2012); Scharnowski et al. (2012)].

The revolutionary aspect of the investigation of the effects of subjects inner states on neural representations is that the inner state of a subject enters the natural sciences. In western culture we live in a society that is still strongly characterized by a picture of man in which body and mind are segregated. Since Descartes' postulate of *res extensa* (the material world) and *res cogitans* (the spiritual, mental world) as being segregated entities [Descartes (1641)] our scientific culture divided into two paths: first, a physical path governed by the natural sciences and, second, a humane, mental, spiritual path. Subtle, mental phenomena were generally excluded from neuroscientific research or from the natural sciences in general [Bauer (2008)].

Early psychological research at the beginning of the last century focussed mostly on the easily observable parameters of a subject such as behaviour [Watson (1913)] or task performance [Ashcraft (2005)], and not on supposedly unobservable phenomena that take place in the *minds* of subjects. Later in the last century, psychological research began to investigate the effects of attention on perceptual phenomena [Cherry (1953); Cherry and Taylor (1954); Broadbent (1956); Deutsch and Deutsch (1963); Treisman and Gelade (1980)]. Today it is known that attention has strong effects on stimulus processing that go all the way back to the very primary sensory cortices [Treue (2001)]. Furthermore, attention is known to be important for the learning of simple tasks in perceptual learning [Ahissar and Hochstein (1993, 2002)] and the attentional focus is known to increase the effectiveness of external perceptual training in the auditory, visual, and somatosensory domain [Seitz and Dinse (2007)]. Here, attention is viewed as being important for perceptual learning but external training or stimulation is still viewed as being the main driving force for changes in stimulus processing or cortical organization structures. In contrast, when conducting psychophysical experiments as the one presented in chapter 5 or the ones done by Tartaglia et al. (2009, 2012), when pre and post measures of sensory abilities are conducted, when environmentally nothing is changed in between these two measurements by training or external stimulation, when only changes in the inner state of the subject are instructed, and when then differences in the sensory abilities before and after the intervention of changing the inner state of the subject are found, then the effects of the mere inner state of a subject on stimulus processing are observed. In these studies, the inner attentional or awareness state of a subject is identified as being not only important, but actually sufficient to induce the observed changes in stimulus processing. Moreover, such changes in stimulus processing are most likely to be accompanied by changes in early cortical stages of sensory processing [Godde et al. (1996); Pleger et al. (2001); Lissek et al. (2009); Shibata et al. (2011); Scharnowski et al. (2012)]. The effects of *mental* inner states without the involvement of external training or stimulation on stimulus processing and - most likely - on *material* cortical representations reflect the interaction and interconnectedness between the

two supposedly segregated categories of *res extensa* and *res cogitans*. In terms of cognitive psychology, the changes in the inner state of a subject we focussed on can be captured by the term *controlled attention*. Controlled attention [Ashcraft (2005)] denotes the act of voluntarily directing attention to phenomena that are of interest for an organism without the necessary condition of significant changes in the environment¹⁶. In this way, controlled attention can be interpreted as a reflection of the *interest* of a subject. A voluntarily induced bias of our attentional focus to certain phenomena, which can be interpreted as a change in our interest, is likely to change our perception and cortical organization without an involvement of significant changes in the environment [chapter 5, Tartaglia et al. (2009, 2012); Kerr et al. (2008); Shibata et al. (2011)]. We seem to be able to change *ourselves* not just by experiencing the environment but merely by experiencing what goes on inside of us. A change in *our interests* changes *ourselves*.

6.5 Activity-Dependent Plasticity, the Inside, and the Outside

All these lines of thought are not surprising when we combine the theories of activity-dependent plasticity with recent results obtained by la Fougère et al. (2009). In our daily perception there is a strict segregation between the external world composed of supposed physical objects and the internal world of thoughts, ideas, imaginations, and emotions. However, la Fougère et al. (2009) showed that the difference between measured [(18)F]-FDG-PET signals after *real* locomotion in an environment and measured fMRI signals during *imagined* locomotion is only marginal: mostly the same areas in cortex were active during real locomotion in an environment and imagined locomotion. There is no reason why these results should not transfer to other sensory areas.

In the framework of activity-dependent plasticity the effectiveness of a synapse that connects neuron A and B is altered when pre- and postsynaptic spikes

¹⁶In contrast to the voluntarily process of controlled attention, input attention denotes a mostly input-driven, reactive, involuntary process.

are elicited at the same time. Therefore, activity in the brain inevitably changes brain organization by changing synaptic weights. If imagined and real phenomena share similar activity patterns in the brain, it is not surprising that mental, imagined phenomena can alter brain organization in the same way that *real* phenomena do.

The effect that altered statistics in the environment have on perception and brain organization [Fahle and Poggio (2002)] are - in a precise manner - effects of altered statistics in our neural activity that *originate* in changes in the statistics of the environment. Those altered statistics in neural activity change brain organization via activity-dependent synaptic plasticity. The *origin* of these altered statistics may only play a minor role in this view of the brain. Whether the *origin* for changes in the statistics of neural activity is in the environment or in the nervous system does not seem to have to matter in the view of neural plasticity I outlined in this thesis.

7 Acknowledgements

I would like to thank:

- PD Dr. Thomas Wachtler (LMU München) as the main supervisor of my thesis work,
- Prof. Dr. Andreas Herz (LMU München) and Prof. Dr. Tim Gollisch (Göttingen) for being very supportive and motivating parts of my thesis advisory committee,
- PD Dr. Hubert Dinse (RU Bochum) for supervision of the study presented in chapter 5,
- the members of the *Computational Neuroscience* at the LMU München for hosting, for great scientific support, and for a great time in München,
- Prof. Dr. Stefan Schmidt (Klinikum Freiburg) and his team for fruitful discussions on this thesis,
- Frank Michler for supporting me with simulations in chapter 4,
- Dr. Tobias Kalisch and Dr. Jan Christoph Kattenstroh (RU Bochum) for supporting me with statistical evaluations in chapter 5,
- John Wilson (Freiburg) and Armin Bahl (MPI Munich) for error checking and correction of this thesis,
- Gisela Drescher (*Zen-Linie Leere Wolke*) without who the study presented in chapter 5 would have never been possible,
- the whole team of the *Benediktushof* for hosting me during the measurements of the study presented in chapter 5,
- the *Graduate School of Systemic Neurosciences Munich* for education, financial support and excellent administrative, structural, and organizational support during my PhD time (special thanx to Dr. Alexandra Stein and Lena Bittl),
- my friends and family for always being there.

8 Supplementary Material

8.1 Multiplication in Neurons via Permissive Gating

A wealth of possible mechanisms has been proposed over the last decades in order to answer the question of how multiplication could in principle be realized by the physiological mechanisms available in the brain. Those models can be categorized in (1) models that explain multiplication as an emergent property of networks of ordinary single neurons that themselves are not capable of multiplying inputs and (2) models that explain multiplication on the level of single neurons.

8.1.1 Models of Multiplicative Interactions - Network Level

Multiplication in a recurrent network. Salinas and Abbott showed in 1996 that a recurrently connected network model of firing rate units can produce nearly multiplicative gain fields if recurrent connections are strong enough [Salinas and Abbott (1996)]. The single firing rate units themselves were not intrinsically capable of multiplying inputs. Firing rate units were recurrently connected in a way that neurons with overlapping receptive fields excite each other and neurons with separated receptive fields inhibit each other [Stemmler et al. (1995)]. Each neuron also received sensory retinal and gaze direction inputs that were summed linearly. Retinal receptive fields were tuned as a Gaussian function of retinal location where gaze direction inputs varied linearly as a function of gaze direction. Although retinal and gaze direction inputs were summed linearly, simulations showed that when recurrent connectivity was present, the gaze direction signal acted as a gain factor multiplying the retinal response.

Multiplication in a feedforward circuit. A recent study shows that a feedforward circuit of ordinary noisy integrate-and-fire model neurons is also capable of realizing multiplicative interactions [Nezis and van Rossum (2011)]. Here, the central idea is that a product of two firing rates can be well approximated by a smoothed minimum function. A minimum function of two input streams can be easily implemented in a small feedforward network of four ordinary noisy integrate-and-fire model neurons [van Rossum et al. (2002)] that are connected in an excitatory and inhibitory pattern [Nezis and van Rossum (2011)]. Such a feedforward circuit realizes multiplicative interactions of two input streams. Multiplication is most accurate if the minimum function implemented in the network is smoothed by appropriate

amounts of synaptic noise.

Multiplication via correlations in a recurrent network. Salinas and Sejnowski proposed a model for multiplicative interactions mediated by changes in correlations of recurrent connectivity [Salinas and Sejnowski (2000)]. In a study that combines an analytic, stochastic description of a leaky integrate-and-fire neuron model neuron with computer simulations of an integrate-and-fire neuron [Troyer and Miller (1997)] with hundreds of recurrent excitatory and inhibitory inputs and one feedforward input synapse, Salinas and Sejnowski [2000] investigated the impact of correlations on the average output firing rate of the model neuron. Correlations have the largest impact on the output firing rate of the neuron when excitatory and inhibitory synaptic inputs are in balance (same net influence of excitatory and inhibitory inputs). In this balanced regime, correlations among excitatory recurrent connections have a multiplicative effect on the output firing rate of the model neuron.

8.1.2 Models of Multiplicative Interactions - Single Neuron Level

Multiplication via coincidence detection. Srinivasan and Bernard [1976] showed that an integrate-and-fire like model neuron can detect coincident spikes in two separated input streams that are summed linearly and produce an output firing rate that is proportional to the product of the two input firing rates. The central idea is that synaptic time constants, input weights and inter-spike intervals can be fine-tuned such that one of the two input streams alone can not elicit supra-threshold EPSPs and thus can not produce an output spike. Only the coincident arrival of spikes from the two input streams elicits supra-threshold EPSPs that lead to output spikes. This detection of coincident spikes leads to multiplicative interactions on the basis of an AND condition. Srinivasan and Bernard [1976] define a temporal difference, Δ , that two EPSP's must have for their coincidence detector neuron to exceed the threshold level γ . At time $t = 0$, a spike elicits the first EPSP and increases the membrane potential to the peak amplitude $A < \gamma$. Assuming an exponential waveform the membrane potential will have the value $A \cdot \exp(-\frac{\Delta}{\tau})$ after time Δ , with τ being the time constant of the EPSP. A second spike elicits an EPSP which again increases the membrane potential by A . When the sum of these values equals at least the threshold γ , a spike will be elicited. The following equations are obtained:

$$\gamma = A \cdot \exp(-\frac{\Delta}{\tau}) + A \quad \Leftrightarrow \quad \Delta = \tau \cdot \ln(\frac{1}{\gamma/A - 1}) \quad (8.1)$$

Srinivasan and Bernard conclude that under the condition $\gamma/2 < A < \gamma$ a spike is triggered in the neuron only by a pair of input spikes and not by a single spike. At the same time, the smallest interspike interval in each of the input spike trains has to be larger than Δ . This ensures that the neuron does not detect false coincidences by temporal summation of EPSP's from one input stream. This mechanism works only for very low input firing rates where EPSPs of each individual input stream do not overlap. At the same time, only very low output firing rates are produced in this model.

Multiplication via a logarithmic-exponential cascade. The relationship between external stimuli and neural responses is often roughly logarithmic [Ratliff (1965); Tal and Schwartz (1997)]. Furthermore, experiments indicate that neurons in locust have nearly exponentially shaped output tuning curves [Gabbiani et al. (2002); Herz et al. (2006)]. Based on these two findings one can hypothesize that multiplication of two signals x and y can be realized via summation of logarithmically transformed signals on dendrites and forwarding of this sum to an exponential nonlinearity [Koch and Poggio (1992); Hatsopoulos et al. (1995); Herz et al. (2006)]. Mathematically written this states as $x \cdot y = \exp(\ln(x \cdot y)) = \exp(\ln(x) + \ln(y))$. Tal and Schwartz [Tal and Schwartz (1997)] showed that the transfer function of a leaky integrate-and-fire neuron can provide a compressive nonlinearity sufficiently close to that of a logarithmic transformation. The authors conclude that multiplication can be realized by summation over leaky integrate-and-fire neurons outputs yielding the logarithm of the product.

Multiplication via background activity. Recent results from simulations with a Hodgkin-Huxley-type model neuron suggest that variation in the background activity of cortical circuits may allow for gain modulation [Brostek (2012)]. Based on the assumption that neurons might have two classes of inputs, driving inputs and modulatory inputs [Sherman and Guillery (1998)], the authors [Brostek (2012)] constructed a Hodgkin-Huxley-type model neuron that incorporates sensory driving inputs and inputs representing background activity elicited by spontaneous activity of recurrent networks. Both inputs were mediated by different synaptic mechanisms. The authors [Brostek (2012)] found that an increase of background synaptic activity can result in multiplicative modulatory gain modulation of driving inputs. Similar results - a divisive modulatory mechanism - were obtained in a neural network by varying the level of balanced background excitatory and inhibitory inputs [Chance et al. (2002)].

Multiplication via dendritic interactions. Dendritic trees contain many

types of voltage-dependent channels that can boost synaptic inputs [Mel (1999)]. Such voltage-dependent membrane mechanisms in dendritic trees could underlie multiplicative interactions. Synapses on a dendritic tree can interact nonlinearly because the dendritic tree contains those active voltage sensitive channels. This can lead to multiplicative interactions at the output level of a neuron [Mel (1992, 1999); Poirazi et al. (2003)]. Moreover, experiments indicate that basal and distal apical dendrites of pyramidal neurons may have different functions in neural computation [Schiller et al. (1997); Golding and Staff (1998); Mel (1999)]. The computational function of the distal dendrites is thought to be a gain modulatory influence on the output firing rate of the neuron [Koch and Poggio (1992); Kepecs et al. (2002); Larkum et al. (2004); Mel (1999)]. In an elegant study it was shown that weak input to a distal dendritic region modulates the influence of proximal inputs on a neurons output firing rate [Larkum et al. (2004)]. By combining electrophysiological measurements in primary somatosensory cortex of rats with simulations in a two-compartment model this effect could be explained by an interaction between the two spatially segregated regions [Larkum et al. (1999)]. This interaction between distal and proximal dendritic regions is thought to be mediated by dendritic back-propagating Na^{2+} action potentials and dendritic forward-propagating Ca^{2+} action potentials [Larkum et al. (2004)]. Here, forward-propagating Ca^{2+} action potentials are caused by distal inputs and back-propagating Na^{2+} action potentials are caused by proximal inputs. The interaction between both kinds of dendritic action potentials results in an action potential burst in the axonal spike initiation zone of the neuron which increases the output firing rate of the neuron. This is as backpropagation Na^{2+} action potentials can lower the threshold for the initiation of forward-propagating Ca^{2+} action potentials which in turn can initiate a burst of action potentials in the soma. By this, the association between distal and proximal inputs leads to an increase in the neurons gain.

Multiplication via NMDA-gated receptors. The current flow through a group of NMDA-gated receptors is not only dependent on the amount of neurotransmitters docking the receptors but also depends on the postsynaptic potential [Purves et al. (2004)]. NMDA-receptors are blocked by a Mg^{2+} ion at voltage values around the resting potential. This block is released at a more depolarized membrane potential. In principal, such a synapse acts as an AND gate: a depolarization that is sufficient to generate an action potential can only occur when presynaptic transmitter release AND postsynaptic pre-depolarization are present. This mechanism - in principle - could realize multiplicative interactions [Mel (1999); Schiller et al. (2000)].

8.2 Improvement of Tactile Perception by Meditation

8.2.1 Original Data - Sensory Focussing Group

| r2 focus group | s1 | s2 | s3 | s4 | s5 | s6 | s7 | s8 | s9 | s10 |
|-------------------------------------|------|------|------|------|------|------|------|------|------|------|
| age [years] | 41 | 54 | 46 | 50 | 58 | 48 | 48 | 56 | 54 | 52 |
| med. experience [years] | 8 | 20 | 10 | 4 | 10 | 16 | 29 | 15 | 10 | 25 |
| med. per week [hours] | 5 | 2 | 7 | 1.5 | 4 | 5 | 2.5 | 3 | 5 | 3 |
| 2PD thresholds [mm] | | | | | | | | | | |
| day 0, r2 | 2.45 | 2.46 | 2.34 | 1.49 | 2.69 | 2.29 | 1.92 | 1.9 | 1.68 | 1.84 |
| day 0, r3 | 1.63 | 2.46 | 2.9 | 1.78 | 3.9 | 3.14 | 1.76 | 1.86 | 2.91 | 1.78 |
| day 0, l2 | 2.34 | 2.38 | 3.16 | 1.36 | 2.71 | 2.24 | 1.31 | 2.51 | 3.38 | 4.81 |
| day 3, r2 | 2.07 | 2.17 | 2.47 | 1.14 | 1.78 | 2.13 | 1.55 | 1.92 | 1.27 | 1.15 |
| day 3, r3 | 1.9 | 2.04 | 1.87 | 1.3 | 3.74 | 2.82 | 1.98 | 1.39 | 2.6 | 1.36 |
| day 3, l2 | 1.94 | 2.52 | 2.74 | 1.43 | 2.63 | 2.36 | 1.33 | 2.2 | 2.8 | 3.76 |
| day 4, r2 | 1.71 | 2.65 | 1.99 | 1.3 | 2.31 | 2.19 | 0.53 | 1.6 | 1.31 | 1.04 |
| day 4, r3 | 1.48 | 2.7 | 2.46 | 0.79 | 3.69 | 2.74 | 1.4 | 1.99 | 2.22 | 1.43 |
| day 4, l2 | 1.88 | 2.59 | 2.34 | 1.44 | 2.72 | 2.51 | 1.19 | 2.43 | 2.82 | 4.65 |
| Localization performance [%] | | | | | | | | | | |
| day 0, r2 | 62.5 | 83.3 | 83.3 | 66.7 | 62.5 | 66.7 | 79.2 | 66.7 | 79.2 | 70.8 |
| day 0, r3 | 41.7 | 70.8 | 70.8 | 58.3 | 75 | 66.7 | 83.3 | 54.2 | 79.2 | 75 |
| day 0, l2 | 91.7 | 83.3 | 75 | 75 | 54.2 | 29.2 | 87.5 | 70.8 | 54.2 | 70.8 |
| day 3, r2 | 95.8 | 66.7 | 66.7 | 79.2 | 66.7 | 54.2 | 83.3 | 83.3 | 75 | 58.3 |
| day 3, r3 | 79.2 | 70.8 | 62.5 | 75 | 58.3 | 70.8 | 75 | 95.8 | 70.8 | 70.8 |
| day 3, l2 | 79.2 | 79.2 | 75 | 58.3 | 75 | 70.8 | 79.2 | 70.8 | 79.2 | 75 |
| day 4, r2 | 62.5 | 70.8 | 83.3 | 83.3 | 66.7 | 62.5 | 70.8 | 87.5 | 87.5 | 83.3 |
| day 4, r3 | 70.8 | 66.7 | 70.8 | 70.8 | 66.7 | 50 | 83.3 | 66.7 | 79.2 | 58.3 |
| day 4, l2 | 79.2 | 75 | 66.7 | 70.8 | 54.2 | 62.5 | 87.5 | 79.2 | 66.7 | 50 |

Supplementary table 1: **Original data - sensory focussing group.** The table shows tactile performance measures of individual subjects in the sensory focussing group (s1-s10) as well as age, estimated meditation experience and estimated meditation hours per week in everyday life. 2pd thresholds and localization performance are shown for each finger (r2, r3, and l2) on each day (0, 3, and 4).

8.2.2 Original Data - Control Group

| control group | c1 | c2 | c3 | c4 | c5 | c6 | c7 | c8 | c9 | c10 |
|-------------------------------------|------|------|------|------|------|------|------|------|------|------|
| age [years] | 57 | 47 | 51 | 53 | 49 | 56 | 48 | 46 | 58 | 51 |
| med. experience [years] | 8 | 3 | 6 | 15 | 2 | 13 | 22 | 2 | 20 | 4 |
| med. per week [hours] | 4 | 4 | 2 | 5 | 3.5 | 7 | 4 | 2.5 | 3 | 4 |
| 2PD thresholds [mm] | | | | | | | | | | |
| day 0, r2 | 2.5 | 2.34 | 3.07 | 2.06 | 1.81 | 1.92 | 2.68 | 2.68 | 2.39 | 2.64 |
| day 0, r3 | 2.55 | 2.68 | 3.05 | 2.31 | 2.24 | 2.27 | 2.05 | 2.94 | 2.46 | 2.81 |
| day 0, l2 | 2.47 | 1.89 | 2.34 | 2.11 | 1.72 | 2.61 | 2.48 | 3.02 | 2.84 | 2.7 |
| day 3, r2 | 2.57 | 2.27 | 2.24 | 2.34 | 1.73 | 1.82 | 2.65 | 2.61 | 2.31 | 2.65 |
| day 3, r3 | 2.66 | 2.42 | 2.59 | 2.53 | 2.39 | 2.59 | 2.15 | 2.66 | 2.13 | 2.67 |
| day 3, l2 | 3.13 | 2.47 | 2.49 | 2.83 | 1.93 | 2.35 | 2.4 | 2.6 | 1.81 | 2.06 |
| day 4, r2 | 2.74 | 2.3 | 3.14 | 2.58 | 1.84 | 1.79 | 2.26 | 2.66 | 2.37 | 2.63 |
| day 4, r3 | 2.85 | 1.89 | 2.81 | 2.4 | 1.9 | 2.11 | 2.42 | 2.99 | 2.42 | 2.9 |
| day 4, l2 | 2.67 | 1.93 | 2.42 | 2.54 | 1.7 | 2.13 | 2.64 | 2.6 | 1.9 | 2.24 |
| Localization performance [%] | | | | | | | | | | |
| day 0, r2 | 41.7 | 66.7 | 83.3 | 83.3 | 83.3 | 62.5 | 79.2 | 66.7 | 70.8 | 37.5 |
| day 0, r3 | 45.8 | 62.5 | 79.2 | 83.3 | 66.7 | 62.5 | 58.3 | 83.3 | 62.5 | 87.5 |
| day 0, l2 | 37.5 | 45.8 | 87.5 | 95.8 | 66.7 | 66.7 | 62.5 | 62.5 | 83.3 | 41.7 |
| day 3, r2 | 54.2 | 66.7 | 87.5 | 66.7 | 83.3 | 75 | 66.7 | 87.5 | 66.7 | 75 |
| day 3, r3 | 70.8 | 66.7 | 75 | 83.3 | 83.3 | 66.7 | 58.3 | 79.2 | 83.3 | 62.5 |
| day 3, l2 | 70.8 | 62.5 | 87.5 | 95.8 | 62.5 | 91.7 | 54.2 | 70.8 | 83.3 | 70.8 |
| day 4, r2 | 41.7 | 83.3 | 87.5 | 87.5 | 75 | 66.7 | 58.3 | 75 | 75 | 50 |
| day 4, r3 | 45.8 | 70.8 | 87.5 | 79.2 | 54.2 | 70.8 | 75 | 87.5 | 66.7 | 62.5 |
| day 4, l2 | 62.5 | 50 | 79.2 | 87.5 | 75 | 79.2 | 33.3 | 83.3 | 87.5 | 75 |

Supplementary table 2: **Original data - control group.** The table shows tactile performance measures of individual subjects in the control group (c1-c10) as well as age, estimated meditation experience and estimated meditation hours per week in everyday life. 2pd thresholds and localization performance are shown for each finger on each day.

8.2.3 Evaluated Two Point Discrimination Thresholds - Right Index Finger (r2)

| r2 2PD thresholds | sensory focussing group | control group |
|--|-------------------------|-----------------|
| day 0: mean and std [mm] | 2.11 ± 0.37 | 2.41 ± 0.37 |
| day 0: median [mm] | 2.11 | 2.45 |
| day 3: mean and std [mm] | 1.77 ± 0.44 | 2.32 ± 0.31 |
| day3: median [mm] | 1.85 | 2.33 |
| day 4: mean and std [mm] | 1.66 ± 0.61 | 2.43 ± 0.39 |
| day 4: median [mm] | 1.66 | 2.48 |
| Wilcoxon p day 0 - day 3 | 0.013 | 0.12 |
| Wilcoxon p day 0 - day 4 | 0.014 | 0.92 |
| Wilcoxon p day 3 - day 4 | 0.65 | 0.14 |
| improvement $day0 - day3$ (mean and std) | $17 \pm 13\%$ | $(3 \pm 10\%)$ |
| improvement $day0 - day4$ (mean and std) | $22 \pm 21\%$ | $(-1 \pm 10\%)$ |

Supplementary table 3: **Evaluated data - 2pd thresholds - right index finger.** The table shows evaluated 2pd thresholds in the right index finger of subjects in both the sensory focussing and the control group. The table shows average 2pd thresholds on each day (0, 3, and 4), as well as median 2pd thresholds, standard deviations, significance values obtained by Wilcoxon's statistical test and improvements. Evaluation methods are described in detail in the main text (chapter 5).

8.2.4 Evaluated Two Point Discrimination Thresholds - Right Middle Finger (r3)

| r3 2PD thresholds | sensory focussing group | control group |
|--|-------------------------|-----------------|
| day 0: mean and std [mm] | 2.42 ± 0.73 | 2.54 ± 0.31 |
| day 0: median [mm] | 2.16 | 2.5 |
| day 3: mean and std [mm] | 2.1 ± 0.73 | 2.48 ± 0.19 |
| day 3: median [mm] | 1.94 | 2.56 |
| day4: mean and std [mm] | 2.09 ± 0.81 | 2.47 ± 0.39 |
| day4: median [mm] | 2.11 | 2.42 |
| Wilcoxon p day 0 - day 3 | 0.025 | 0.45 |
| Wilcoxon p day 0 - day 4 | 0.022 | 0.67 |
| Wilcoxon p day 3 - day 4 | 0.88 | 0.96 |
| improvement $day0 - day3$ (mean and std) | $12 \pm 16\%$ | $(1 \pm 10\%)$ |
| improvement $day0 - day4$ (mean and std) | $15 \pm 17\%$ | $(2 \pm 13\%)$ |

Supplementary table 4: **Evaluated data - 2pd thresholds - right middle finger.** The table shows evaluated 2pd thresholds in the right middle finger of subjects in both the sensory focussing and the control group.

8.2.5 Evaluated Two Point Discrimination Thresholds - Left Index Finger (l2)

| l2 2PD thresholds | sensory focussing group | control group |
|--|-------------------------|------------------|
| day0: mean and std [mm] | 2.62 ± 0.96 | 2.32 ± 0.4 |
| day 0: median [mm] | 2.44 | 2.41 |
| day 3: mean and std [mm] | 2.37 ± 0.67 | 2.41 ± 0.38 |
| day 3: median [mm] | 2.44 | 2.44 |
| day4: mean and std [mm] | 2.46 ± 0.9 | 2.28 ± 0.33 |
| day4: median [mm] | 2.47 | 2.33 |
| Wilcoxon p day 0 - day 3 | 0.086 | 0.58 |
| Wilcoxon p day 0 - day 4 | 0.26 | 0.96 |
| Wilcoxon p day 3 - day 4 | 0.33 | 0.17 |
| improvement <i>day0</i> – <i>day3</i> (mean and std) | $(7 \pm 10\%)$ | $(-6 \pm 19\%)$ |
| improvement <i>day0</i> – <i>day4</i> (mean and std) | $(5 \pm 12\%)$ | $(0.7 \pm 11\%)$ |

Supplementary table 5: **Evaluated data - 2pd thresholds - left index finger.** The table shows evaluated 2pd thresholds in the left index finger of subjects in both the sensory focussing and the control group.

8.2.6 Evaluated Localization Performance - Right Index Finger (r2)

| r2 localization performance | sens. foc. gr. | control group |
|--|--------------------|------------------|
| day 0: mean and std [%] | 72.1 ± 7.9 | 67.5 ± 15.8 |
| day 0: median [%] | 68.75 | 68.75 |
| day 3: mean and std [%] | 72.9 ± 12.1 | 72.9 ± 10.2 |
| day 3: median [%] | 70.8 | 70.8 |
| day 4: mean and std [%] | 75.8 ± 9.6 | 70 ± 14.9 |
| day 4: median [%] | 77 | 75 |
| Wilcoxon p day 0 - day 3 | 0.92 | 0.33 |
| Wilcoxon p day 0 - day 4 | 0.33 | 0.34 |
| Wilcoxon p day 3 - day 4 | 0.32 | 0.51 |
| improvement <i>day0</i> – <i>day3</i> mean and std | $(0.8 \pm 15.6\%)$ | $(5.5 \pm 15\%)$ |
| improvement <i>day0</i> – <i>day4</i> mean and std | $(3.6 \pm 10\%)$ | $(2.5 \pm 10\%)$ |

Supplementary table 6: **Evaluated data - localization performance - right index finger.** The table shows evaluated localization performance in the right index finger of subjects in both the sensory focussing and the control group.

8.2.7 Evaluated Localization Performance - Right Middle Finger (r3)

| r3 localization performance | sens. foc. gr | control group |
|--|--------------------|--------------------|
| day 0: mean and std [%] | 67.5 ± 12 | 69.2 ± 12.8 |
| day 0: median [%] | 70.8 | 64.6 |
| day 3: mean and std [%] | 72.9 ± 9.5 | 72.9 ± 8.8 |
| day 3: median [%] | 70.8 | 72.9 |
| day 4: mean and std [%] | 68.3 ± 9.5 | 70 ± 13.4 |
| day 4: median [%] | 68.8 | 70.8 |
| Wilcoxon p day 0 - day 3 | 0.81 | 0.36 |
| Wilcoxon p day 0 - day 4 | 1.0 | 0.51 |
| Wilcoxon p day 3 - day 4 | 0.39 | 0.77 |
| improvement <i>day0</i> – <i>day3</i> mean and std | $(5.5 \pm 19\%)$ | $(3.8 \pm 13.6\%)$ |
| improvement <i>day0</i> – <i>day4</i> mean and std | $(0.9 \pm 13.5\%)$ | $(1 \pm 11.6\%)$ |

Supplementary table 7: **Evaluated data - localization performance - right middle finger.** The table shows evaluated localization performance in the right middle finger of subjects in both the sensory focussing and the control group.

8.2.8 Evaluated Localization Performance - Left Index Finger (l2)

| l2 localization performance | sens. foc. gr | control group |
|--|-----------------|-----------------|
| day 0: mean and std [%] | 69.2 ± 18.7 | 65 ± 19.6 |
| day 0: median [%] | 72.9 | 64.6 |
| day 3: mean and std [%] | 74.2 ± 6.5 | 75 ± 13.9 |
| day 3: median [%] | 75 | 70.8 |
| day 4: mean and std [%] | 69.2 ± 11.7 | 71.3 ± 17.6 |
| day 4: median [%] | 68.8 | 77.1 |
| Wilcoxon t day 0 - day 3 | 0.57 | 0.13 |
| Wilcoxon t day 0 - day 4 | 0.94 | 0.28 |
| Wilcoxon t day 3 - day 4 | 0.37 | 0.33 |
| improvement <i>day0</i> – <i>day3</i> mean and std [%] | 4 ± 16.8 | 11.7 ± 12.9 |
| improvement <i>day0</i> – <i>day4</i> mean and std [%] | 0.3 ± 15.1 | 6.2 ± 17.3 |

Supplementary table 8: **Evaluated data - localization performance - left index finger.** The table shows evaluated localization performance in the left index finger of subjects in both the sensory focussing and the control group.

References

- Abrams, R. and Christ, S. (2003). Motion onset captures attention. *Psychological Science*, 14:427–432.
- Adrian, E. (1914). The all-or-none principle in nerve. *Journal of Physiology London XLVII*, 6:460–474.
- Ahissar, M. and Hochstein, S. (1993). Attentional control of early perceptual learning. *Proceedings of the National Academy of Sciences of the USA*, 90:5718–5722.
- Ahissar, M. and Hochstein, S. (2002). The role of attention in learning simple visual tasks. In: *Perceptual Learning* edited by Manfred Fahle and Thomaso Poggio. *MIT Press*, pages 254–272.
- Andersen, R., Essick, G., and Siegel, R. (1985). Encoding of spatial location by posterior parietal neurons. *Science*, 230(4724):456–458.
- Andersen, R. and Mountcastle, V. (1983). The influence of the angle of gaze upon the excitability of light-sensitive neurons of the posterior parietal cortex. *Journal of Neuroscience*, 3:532–548.
- Ashcraft, M. (2005). Cognition. *Pearson Education (US)*, volume 4.
- Bain, A. (1855). The senses and the intellect. *London: J.W. Parker*, page p. 91.
- Barlow, H. (1961). Possible principles underlying the transformation of sensory messages. *Sensory Communication*, ed. WA Rosenblith, 217-234. *Cambridge, MA: MIT Press*.
- Barlow, H. (1989). Unsupervised learning. *Neural Computation*, 1:295–311.
- Bauer, R. (2008). Gehirn oder Geist - Wer und was sind wir? *Logos Berlin*.
- Bell, C., Han, V., Sugawara, Y., and Grant, K. (1997). Synaptic plasticity in a cerebellum-like structure depends on temporal order. *Nature*, 387:278–281.
- Bell-Krotoski, J., Fess, E., Figarola, J., and Hiltz, D. (1995). Threshold detection and Semmes-Weinstein monofilaments. *Journal of Hand Therapy*, 8:155–162.
- Berkes, B. and Wiskott, L. (2005). Slow feature analysis yields a rich repertoire of complex cell properties. *Journal of Vision*, 5:579–602.
- Bi, G. and Poo, M. (1998). Activity-induced synaptic modification in hippocampal culture: dependence on spike timing, synaptic strength and cell type. *Journal of Neuroscience*, 18:10464–10472.

- Bienenstock, E., Cooper, L., and Munro, P. (1982). Theory for the development of neuron selectivity: orientation specificity and binocular interaction in visual cortex. *Journal of Neuroscience*, 2:32–48.
- Blakemore, C. and Cooper, G. (1972). Development of the brain depends on the visual environment. *Nature*, 228:477–478.
- Bliss, T. and Lomo, T. (1973). Long-lasting potentiation of synaptic transmission in the dentate area of the anaesthetized rabbit following stimulation of the perforant path. *Journal of Physiology*, 232(2):331–56.
- Borst, A. (2011). Fly vision: moving into the motion detection circuit. *Current Biology*, 21(24):990–992.
- Bosking, W., Zhang, Y., Schofield, B., and Fitzpatrick, D. (1997). Orientation selectivity and the arrangement of horizontal connections in tree shrew striate cortex. *The Journal of Neuroscience*, 17(6):2112–2127.
- Boussaoud, D. and Bremmer, F. (1999). Gaze effects in the cerebral cortex: reference frames for space coding and action. *Experimental Brain Research*, 128(1-2):170–180.
- Bradley, D., Maxwell, M., Andersen, R., Banks, M., and Shenoy, K. (1996). Mechanisms of heading perception in primate visual cortex. *Science*, 273:1544–1547.
- Brefczynski, J. and De Yoe, E. (1999). A physiological correlate of the spotlight of attention. *Nature Neuroscience*, 2:370–374.
- Bremmer, F. and Krekelberg, B. (2003). Seeing and acting at the same time: challenges for brain (and) research. *Neuron*, 38(3):367–370.
- Bremmer, F., Kubischik, M., Pekel, M., Hoffmann, K., and Lappe, M. (2010). Visual selectivity for heading in monkey area MST. *Experimental Brain Research*, 200:51–60.
- Broadbent, D. (1956). Successive responses to simultaneous stimuli. *Quarterly Journal of Experimental Psychology*, 8:145–152.
- Brostek, L. (2012). Eye velocity gain fields for visuo-motor coordinate transformations: A multi-level analysis of neuronal activity in cortical area MSTd. *Dissertation an der Graduate School of Systemic Neurosciences der Ludwig-Maximilians-Universität München*.
- Brotchie, P., Andersen, R., Snyder, L., and Goodman, S. (1995). Head position signals used by parietal neurons to encode locations of visual stimuli. *Nature*, 375:232–235.

- Brown, A., Yates, P., Burrola, P., Ortuno, D., Vaidya, A., Jessel, T., Pfaff, S., O'Leary, D., and Lemke, G. (2000). Topographic mapping from the retina to the midbrain is controlled by relative but not absolute levels of epha receptor signaling. *Cell*, 102:77–88.
- Brunel, N. and van Rossum, M. (2007). Lapicque's 1907 paper: from frogs to integrate-and-fire. *Biological Cybernetics*, 97(5):337–339.
- Büschges, A. and El Manira, A. (1998). Sensory pathways and their modulation in the control of locomotion. *Current Opinions in Neurobiology*, 8:733–739.
- Byrne, J. and Kandel, E. (1996). Persynaptic facilitation revisited: state and time dependence. *Journal of Neuroscience*, 16:425–435.
- Chance, F., Abbott, L., and Rezes, A. (2002). Gain modulation from balanced synaptic input. *Neuron*, 35:773–782.
- Cherry, E. (1953). Some experiments on the recognition of speech with one and with two ears. *Journal of the Acoustical Society of America*, 25:975–979.
- Cherry, E. and Taylor, W. (1954). Some further experiments on the recognition of speech with one and two ears. *Journal of the Acoustical Society of America*, 26:554–559.
- Chklovskii, D. and Koulakov, A. (2004). Maps in the brain: what can we learn from them? *Annual Review of Neuroscience*, 27:369–392.
- Choe, Y. and Mikkilainen, R. (1998). Self-organization and segmentation in a laterally connected orientation map of spiking neurons. *Neurocomputing*, 21(1):139–157.
- Cooper, S. (2005). Donald o. Hebb's synapses and learning rule: a history and commentary. *Neuroscience and Biobehavioral Reviews*, 28:851–874.
- Corbetta, M., Miezin, F., Dobmeyer, S., Shulman, G., and Petersen, S. (1990). Attentional modulation of neural processing of shape, color, and velocity in humans. *Science*, 248(4962):1556–1559.
- Cowan, J. and Sharp, D. (1988). Neural nets. *Quarterly Reviews of Biophysics*, 21(3):365–427.
- Cowan, N. (1995). Attention and memory: an integrated framework. *New York: Oxford University Press*.
- Crair, M. and Malenka, R. (1995). A critical period for long-term potentiation at thalamocortical synapses. *Nature*, 375(6529):325–328.

- Damasio, A. (1990). Synchronous activity in multiple cortical regions: a mechanism for recall. *Seminars in the Neurosciences*, 2:287–296.
- Dan, Y. and Poo, M. (2004). Spike timing dependent plasticity of neural circuits. *Neuron*, 44:23–30.
- Davison, A. and Fregnac, Y. (2006). Learning cross-modal spatial transformations through spike timing-dependent plasticity. *The Journal of Neuroscience*, 26:5604–5615.
- Dayan, P. and Abbott, L. (2002). Theoretical neuroscience. *The MIT Press*.
- Descartes, R. (1641). Meditationen über die Erste Philosophie / Meditationes de Prima Philosophia - Zweite Meditation. *Reclam 2008*.
- Desrosiers, J., Hebert, R., Bravo, G., and Dutil, E. (1996). Hand sensibility of healthy older people. *Journal of the American Geriatrics Society*, 44:974–978.
- Deutsch, J. and Deutsch, D. (1963). Attention: some theoretical considerations. *Psychological Review*, 70:80–90.
- Diamond, M., Armstrong-James, M., and Ebner, F. (1993). Experience-dependent plasticity in adult rat barrel cortex. *The Proceedings of the National Academy of Sciences USA*, 90:2082–2086.
- Dinse, H., Godde, B., Reuter, G., Cords, S., and Hilger, T. (2003). Auditory cortical plasticity under operation: reorganization of auditory cortex induced by electric cochlear stimulation reveals adaptation to altered sensory input statistics. *Speech Communication*, 41:201–219.
- Dinse, H., Kalisch, T., Ragert, P., Pleger, B., Schwenkreis, P., and Tegethoff, M. (2005). Improving human haptic performance in normal and impaired human populations through unattended activation-based learning. *ACM Transactions on Applied Perception*, pages 71–88.
- Dinse, H. and Merzenich, M. (2002). Adaptation of inputs in the somatosensory system. In: *Perceptual Learning* edited by Manfred Fahle and Thomaso Poggio. *MIT Press*, pages 19–42.
- Duhamel, J.-R., Bremmer, F., BenHamed, S., and Graf, W. (1997). Spatial invariance of visual receptive fields in parietal cortex neurons. *Nature*.
- Dupuis-Roy, N. and Gosselin, F. (2007). Perceptual learning without signal. *Vision Research*, 47(3):349–352.
- Eccles, J. (1964). The physiology of the synapses. *Berlin: Springer Verlag*.

- Eckhorn, R., Bauer, R., Jordan, W., Brosch, M., Kruse, W., Munk, M., and Reitboeck, H. (1988). Coherent oscillations: a mechanism for feature linking in the visual cortex? Multiple electrode and correlation analysis in the cat. *Biological Cybernetics*, 60:121–130.
- Eckhorn, R., Reitboeck, H., Arndt, M., and Dicke, P. (1990). Feature linking among distributed assemblies: simulation of results from cat visual cortex. *Neural Computation*, 2:293–306.
- Einhäuser, W., Hipp, J., Eggert, J., Körner, E., and König, P. (2005). Learning viewpoint invariant object representation using a temporal coherence principle. *Biological Cybernetics*, 93:79–90.
- Einhäuser, W., Kayser, C., König, P., and Körding, K. (2002). Learning the invariance properties of complex cells from their responses to natural stimuli. *European Journal of Neuroscience*, 15:475–486.
- Einhäuser, W., Schumann, F., Bardins, S., Bartl, K., Böning, E., and König, P. (2007). Human eye-head co-ordination in natural exploration. *Network: Computation in Neuroscience*, 18(3):267–297.
- Elbert, T., Pantev, C., Wienbruch, C., Rockstroh, B., and Taub, E. (1995). Increased cortical representation of the fingers of the left hand sting players. *Science*, 270:305–307.
- Engel, A., König, P., Kreiter, A., Schillen, T., and Singer, W. (1992). Temporal coding in the visual cortex: new vistas on integration in the nervous system. *Trends in Neuroscience*, 15(6):218–226.
- Evans, C., Jing, J., Rosen, S., and Cropper, E. (2003). Regulation of spike initiation and propagation in an aplysia sensory neuron: gating-in via central depolarization. *Journal of Neuroscience*, 23:2920–2931.
- Fahle, M. (1997). Specificity of learning curvature, orientation, and vernier discriminations. *Vision Research*, 1885-1895:37(14).
- Fahle, M. and Morgan, M. (1996). No transfer of perceptual learning between similar stimuli in the same retinal position. *Current Biology*, 6:292–297.
- Fahle, M. and Poggio, T. (2002). Perceptual learning. *MIT Press*.
- Fahle, M. and Skrandies, W. (1994). An electrophysiological correlate of learning in motion perception. *German Journal of Ophthalmology*, 3:427–432.
- Feller, M. (2009). Retinal waves are likely to instruct the formation of eye-specific retinogeniculate projections. *Neural Development*, 4:24:1–5.

- Fiorentini, A. and Berardi, N. (1980). Perceptual learning specific for orientation and spatial frequency. *Nature*, 287:43–44.
- Firth, S., Wang, C.-T., and Feller, M. (2004). Retinal waves: mechanisms and function in visual system development. *Cell Calcium*, 37:425–432.
- Fisher, B., Pena, J.-L., and Konishi, M. (2007). Emergence of multiplicative auditory response in the midbrain of the barn owl. *Journal of Neurophysiology*, 98:1181–1193.
- Földiák, P. (1991). Learning invariances from transformation sequences. *Neural Computation*, 3(2):194–200.
- Franzius, M., Sprekeler, H., and Wiskott, L. (2007). Slowness and sparseness lead to place, head-direction, and spatial-view cells. *PLOS Computational Biology*, 3(8):1605–1622.
- Freeman, R. (2004). Binocular interaction in the visual cortex. *The Visual Neurosciences*. Editors: L Chalupa and J Werner, MIT Press.
- Gabbiani, F., Krapp, H., Koch, C., and Laurent, G. (2002). Multiplicative computation in a visual neuron sensitive to looming. *Nature*, 420:320–324.
- Gandhi, S., Heeger, D., and Boynton, G. (1999). Spatial attention affects brain activity in human primary visual cortex. *The Proceedings of the National Academy of Sciences USA*, 96(6):3314–3319.
- Georgoulous, A., Schwartz, P., and Kettner, R. (1986). Neuronal population coding of movement direction. *Science*, 233:1416–1419.
- Gerstner, W., Kempter, R., Van Hemmen, J., and Wagner, H. (1996). A neuronal learning rule for submillisecond temporal learning. *Nature*, 383(6595):76–81.
- Gilbert, C., Ito, M., Kapardia, M., and Westheimer, G. (2000). Interactions between attention, context and learning in primary visual cortex. *Vision Research*, 40(10-12):1217–1226.
- Gilbert, C. and Wiesel, T. (1992). Receptive field dynamics in adult primary visual cortex. *Nature*, 356:150–152.
- Gisiger, T. and Boukadoum, M. (2011). Mechanisms gating the flow of information in the cortex: what they might look like and what their use may be. *Frontiers in Computational Neuroscience*, 5:1–15.
- Godde, B., Spengler, F., and Dinse, H. (1996). Associative pairing of tactile stimulation induces somatosensory cortical reorganisation in rats and humans. *Neuroreport*, 8:281–285.

- Godde, B., Stauffenberg, B., Spengler, F., and Dinse, H. (2000). Tactile coactivation-induced changes in spatial discrimination performance. *Journal of Neuroscience*, 20(4):1597–1604.
- Golding, N. and Staff, N. (1998). Dendritic sodium spikes are viable triggers of axonal action potentials in hippocampal CA1 pyramidal neurons. *Neuron*, 21(5):1189–1200.
- Gollisch, T. (2008). Throwing a glance at the neural code: rapid information transmission in the visual system. *HFSP Journal*, 3(1):36–46.
- Gross, C., Desimo, R., Albright, T., and Schwartz, E. (1985). Infero temporal cortex and pattern recognition. *Experimental Brain Research Suppl.*, 11:179–201.
- Hassenstein, B. and Reichardt, W. (1956). Systemtheoretische Analyse der Zeit-, Reihenfolgen-, und Vorzeichenbewertung bei der Bewegungspertzeption des Rüsselkäfers *Clorophanus*. *Zeitschrift für Naturforschung*, 11:513–524.
- Hatsopoulos, N., Gabbiani, F., and Laurent, G. (1995). Elementary computation of object approach by a wide field visual neuron. *Science*, 270:1000–1003.
- Hebb, D. (1949). The organization of behaviour. *New York: Wiley*.
- Herberholz, J., Antonsen, B., and Edwards, D. (2002). A lateral excitatory network in the escape circuit of crayfish. *Journal of Neuroscience*, 22:9078–9085.
- Herz, A., Gollisch, T., Machens, C., and Jaeger, D. (2006). Modeling single-neuron dynamics and computations: a balance of detail and abstraction. *Science*, 314:80–85.
- Hirsch, H. and Spinelli, D. (1971). Modification of the distribution of receptive field orientation in cats by selective visual exposure during development. *Experimental Brain Research*, 12(5):509–527.
- Hirsch, J. and Gilbert, C. (1991). Synaptic physiology of horizontal connections in the cat's visual cortex. *The Journal of Neuroscience*, 11(6):1800–1809.
- Hodgkin, A. (1951). The ionic basis of electrical activity in nerve and muscle. *Biological Reviews*, 26:339–409.
- Hodgkin, A. and Huxley, A. (1952). A quantitative description of membrane current and its application to conduction and excitation in nerve. *Journal of Physiology*, 116:507–544.
- Hubel, D. and Wiesel, T. (1962). Receptive fields, binocular interaction and functional architecture in the cats visual cortex. *Journal of Physiology*, 160(1):106–154.

- Hubel, D. and Wiesel, T. (1965). Binocular interaction in striate cortex of kittens reared with artificial squint. *Journal of Neurophysiology*, 28:1041–1059.
- Hubel, D. and Wiesel, T. (1968). Receptive fields and functional architecture of monkey striate cortex. *Journal of Physiology*, 195(1):215–243.
- Hubel, D. and Wiesel, T. (1974). Sequence regularity and geometry of orientation columns in the monkey striate cortex. *Journal of Comparative Neurology*, 158(3):267–293.
- Hubel, D. and Wiesel, T. (2005). Brain and visual perception. The story of a 25-year collaboration. Chapter 27. Nobel lecture David H. Hubel. Nobel lecture torsten N. Wiesel. *Oxford University Press*, pages 657–704.
- Ito, M. and Gilbert, C. (1999). Attention modulates contextual influences in the primary visual cortex of alert monkeys. *Neuron*, 22:593–604.
- Ito, M., Tamura, H., Fujita, I., and Tanaka, K. (1995). Size and position invariance of neuronal responses in monkey inferotemporal cortex. *Journal of Neurophysiology*, 19(73):218–226.
- Ivanov, A. and Calabrese, R. (2003). Modulation of spike-mediated synaptic transmission by presynaptic background Ca²⁺ in leech heart interneurons. *Journal of Neuroscience*, 23:1206–1218.
- Izhikevich, E. (2007). Dynamical systems in neuroscience: the geometry of excitability and bursting. *The MIT Press*.
- James, W. (1890). The principles of psychology. *New York: Dover*.
- Jenkins, W., Merzenich, M., Ochs, M., Allard, T., and Guic-Robles, E. (1990). Functional reorganization of primary somatosensory cortex in adult owl monkeys after behaviorally controlled tactile stimulation. *Journal of Neurophysiology*, 63(1):82–102.
- Johansson, B. (2012). Multisensory stimulation in stroke rehabilitation. *Frontiers in Human Neuroscience*, 6:60:doi: 10.3389/fnhum.2012.00060. Epub.
- Jürgens, M. and Dinse, H. (1997). Use-dependent plasticity of SI cortical hindpaw neurons induced by modification of walking in adult rats: a model for age related alterations. *Society for Neuroscience Abstract*, 23:1800.
- Kaas, J. (1997). Topographic maps are fundamental to sensory processing. *Brain Research Bulletin*, 44:107–112.
- Kapleau, P. (2000). The three pillars of Zen. *Anchor, Rev Exp edition New York: Anchor Books*.

- Karni, A. and Sagi, D. (1995). A memory system in the adult visual cortex. *Maturational windows and Adult cortical plasticity. SFI studies in the sciences of Complexity*. Editors: B. Julesz and I. Kovacs., 24.
- Kastner, S., Pinsk, M., De Weerd, P., Desimone, R., and Ungerleider, L. (1999). Increased activity in human visual cortex during directed attention in the absence of visual stimulation. *Neuron*, 22(4):751–761.
- Kattenstroth, J., Kalisch, T., Peters, S., Tegenthoff, M., and Dinse, H. (2012). Long-term sensory stimulation therapy improves hand function and restores cortical responsiveness in patients with chronic cerebral lesions. Three single case studies. *Frontiers in Human Neuroscience*, 6:244:doi: 10.3389/fnhum.2012.00244. Epub.
- Katz, P. (2003). Synaptic gating: the potential to open closed doors. *Current Biology*, 13:554–556.
- Katz, P. and Frost, N. (1996). Intrinsic neuromodulation: altering neuronal circuits from within. *Trends in Neuroscience*, 19:54–61.
- Keil, W. and Wolf, F. (2011). Coverage, continuity, and visual cortical architecture. *Neural Systems & Circuits*, 1(17):doi: 10.1186/2042–1001–1–17.
- Kepecs, A. and Raghavachari, S. (2007). Gating information by two-state membrane potential fluctuations. *Journal of Neurophysiology*, 97:3015–3023.
- Kepecs, A., Wang, X., and Lisman, J. (2002). Bursting neurons signal input slope. *Journal of Neuroscience*, 22(20):9053–9062.
- Kerr, C., Shaw, J., Wasserman, R., Chen, V., Kanojia, A., Bayer, T., and Kelley, J. (2008). Tactile acuity in experienced Tai Chi practitioners: evidence for use dependent plasticity as an effect of sensory-attentional training. *Experimental Brain Research*, 188(2):317–322.
- Kirkwood, A. and Bear, M. (1994). Homosynaptic long-term depression in the visual cortex. *Journal of Neuroscience*, 14:3404–3412.
- Koch, C. (1999). Biophysics of Computation. *Oxford University Press*, 477.
- Koch, C. and Poggio, T. (1992). Multiplying with synapses and neurons. *Single Neuron Computation*. Editors: T McKenna, J Davis and S F Zornetzer (San Diego, CA: Academic), pages 315–345.
- Kohonen, T. (1982). Self-organized formation of topologically correct feature maps. *Biological Cybernetics*, 43:59–69.

- Kohonen, T. (1984). Self-organization and associative memory. *Springer Series in Information Science*.
- Koulakov, A. and Chklovskii, D. (2001). Orientation preference patterns in mammalian visual cortex: a wire length minimization approach. *Neuron*, 29:519–527.
- Kuffler, W., Nicholls, J., and Martin, A. (1984). From neuron to brain. *Sinauer Associated*, 2:577–582.
- la Fougère, C., Zwergal, A., Rominger, A., Förster, S., Fesl, G., Dieterich, M., Brandt, T., Strupp, M., Bartenstein, P., and Jahn, K. (2009). Real versus imagined locomotion: a [18F]-FDG PET-fMRI comparison. *NeuroImage*, 50:1589–1598.
- Lapicque, L. (1907). Recherches quantitatives sur l’excitation électrique des nerfs traitée comme une polarisation. *J Physiol Pathol Gen*, 9:620–635.
- Larkum, M., Senn, W., and Lüscher, H.-R. (2004). Top-down dendritic input increases the gain of layer 5 pyramidal neurons. *Cerebral Cortex*, 14:1059–1070.
- Larkum, M., Zhu, J., and Sakmann, B. (1999). A new cellular mechanism for coupling inputs arriving at different cortical layers. *Nature*, 398(6725):338–341.
- Lee, D., Itti, L., Koch, C., and Braun, J. (1999). Attention activates winner-take-all competition among visual filters. *Nature*, 2(4):375–381.
- Lissek, S., Wilimzig, C., Stude, P., Pleger, B., Kalisch, T., Maier, C., Peters, S., Nicolas, V., Tegenthoff, M., and Dinse, H. (2009). Immobilization impairs tactile perception and shrinks somatosensory cortical maps. *Current Biology*, 19:837–842.
- Livingstone, M. and Hubel, D. (1981). Effects of sleep and arousal on the processing of visual information in the cat. *Nature*, 291(5816):554–561.
- Logothetis, N. (2008). What we can do and what we cannot do with fMRI. *Nature*, 453:869–878.
- MacDermott, A., Role, L., and Siegelbaum, S. (1999). Presynaptic ionotropic receptors and the control of transmitter release. *Annual Reviews in Neuroscience*, 22:443–485.
- MacLean, J., Watson, B., Aaron, G., and Yuste, R. (2005). Internal dynamics determine the cortical response to thalamic stimulation. *Neuron*, 48:811–823.
- Magee, J. and Johnston, D. (1997). A synaptically controlled associative signal for Hebbian plasticity in hippocampal neurons. *Science*, 275:209–213.

- Markram, H., Lubke, J., Frotscher, M., and Sakman, B. (1997). Regulation of synaptic efficacy by coincidence of postsynaptic APs and EPSPs. *Science*, 275:213–215.
- Martinez, A., Anllo-Vento, L., Sereno, M., Frank, L., Buxton, R., Dubowitz, D., Wong, E., Hinrichs, H., Heinze, H., and Hillyard, S. (1999). Involvement of striate and extrastriate visual cortical areas in spatial attention. *Nature Neuroscience*, 2:364–369.
- Mazzoni, P., Andersen, R., and Jordan, M. (1991). A more biologically plausible learning rule than backpropagation applied to a network model of cortical area 7a. *Cerebral Cortex*, 1:293–307.
- McAdams, C. and Maunsell, J. (1998). Attention-regulated activity in human primary visual cortex. *Journal of Neurophysiology*, 19:431–441.
- McAdams, C. and Maunsell, J. (1999). Effects of attention on orientation-tuning functions of single neurons in macaque cortical areas. *Journal of Neuroscience*, 19:431–441.
- McAdams, C. and Maunsell, J. (2000). Attention in both space and feature modulates neuronal responses in macaque area V4. *Journal of Neurophysiology*, 83:1751–1755.
- McLaughlin, T. and O’Leary, D. (2005). Molecular gradients and development of retinotopic maps. *Annual Review of Neuroscience*, 28:327–355.
- Meinhardt, H. and Gierer, A. (2000). Pattern formation by local self-activation and lateral inhibition. *BioEssays*, 22:753–760.
- Mel, B. (1992). NMDA-based pattern discrimination in a modeled cortical neuron. *Neural Computation*, 4:502–517.
- Mel, B. (1999). Why have dendrites? A computational perspective. *Oxford University Press in Stuart G. et al.: Dendrites*, pages p.271–289.
- Merzenich, M. and Jenkins, W. (1991). Reorganization of cortical representations of the hand following alterations of skin inputs induced by nerve injury, skin island transfers, and experience. *J Hand Therap*, 6(2):89–104.
- Michler, F., Eckhorn, R., and Wachtler, T. (2009). Using spatio-temporal correlations to learn topographic maps for invariant object recognition. *Journal of Neurophysiology*, 102:953–964.
- Miller, K. and Mackay, D. (1994). The role of constraints in Hebbian learning. *Neural Computation*, 6:100–126.

- Mountcastle, V., Motter, B., Steinmetz, M., and Sestokas, A. (1987). Common and differential effects of attentive fixation on the excitability of parietal and prestriate (V4) cortical visual neurons in the macaque monkey. *Journal of Neuroscience*, 7(7):2239–2255.
- Murkey, R. and Malenka, R. (1992). Mechanisms underlying induction of homosynaptic long-term depression in area ca1 of the hippocampus. *Neuron*, 9:967–975.
- Naeser, M. and Lilly, J. (1971). The repeating word effect: phonetic analysis of reported alternates. *Journal of Speech and Hearing Research*.
- Newsome, W., Wurtz, R., and Komatsu, H. (1988). Relation of cortical areas MT and MST to pursuit eye movements. II. Differentiation of retinal from extraretinal inputs. *Journal of Neurophysiology*, 60:604–620.
- Nezis, P. and van Rossum, M. (2011). Accurate multiplication with noisy spiking neurons. *Journal of Neural Engineering*, 8:1–5.
- Obermayer, K. and Blasden, G. (1993). Geometry of orientation and ocular dominance columns in monkey striate cortex. *Journal of Neuroscience*, 13(10):4114–4129.
- O’Donnell, R. and Grace, A. (1995). Synaptic interactions among excitatory afferents to nucleus accumbens neurons: hippocampal gating of prefrontal cortical input. *Journal of Neuroscience*, 15:3622–3639.
- O’Keefe, J. (1976). Place units in hippocampus of the freely moving rat. *Experimental Neurology*, 51(1):78–109.
- O’Leary, D., Yates, P., and McLaughlin, T. (1999). Molecular development of sensory maps: representing sight and smell in the brain. *Cell*, 96:255–269.
- Ono, S., Brostek, L., Nuding, U., Glasauer, S., Büttner, U., and Mustari, M. (2010). The response of MSTd neurons to perturbations in target motion during ongoing smooth-pursuit eye movements. *Journal of Neurophysiology*, 103:519–530.
- Pauly, M. L. (2000). Ein aufmerksamkeitsgestütztes, biologienahes Objekt-Erkennungs- und Verfolgungssystem mit impulscodierenden Neuronen. *Dissertation zur Erlangung des Doktorgrades der Naturwissenschaften, Marburg/Lahn*.
- Pena, J.-L. and Konishi, M. (2001). Auditory spatial receptive fields created by multiplication. *Science*, 292:249–252.
- Pettigrew, J., Olson, C., and Hirsch, H. (1973). Cortical effect of selective visual experience: degeneration or reorganization? *Brain Research*, 51:345–351.

- Philipp, S. (2009). Model simulations of learning mechanisms for coordinate transforms in a network of spiking neurons. *Philipps Universität Marburg, AG Neurophysik. Diplomarbeit.*
- Pleger, B., Dinse, H., Ragert, P., Schwenkreis, P., Malin, J., and Tegenthoff, M. (2001). Shifts in cortical representations predict human discrimination performance. *The Proceedings of the Natural Academy of Sciences USA*, 98:12255–12260.
- Poirazi, P., Brannon, T., and Mel, B. (2003). Pyramidal neuron as 2-layer neural network. *Neuron*, 37:989–999.
- Pouget, A., Deneve, S., and Duhamel, J.-R. (2002). A computational perspective on the neural basis of multisensory spatial integration. *Nature Reviews Neuroscience*, 3:741–747.
- Pouget, A. and Sejnowski, T. (1997). Spatial transformations in the parietal cortex using basis functions. *Journal of Cognitive Neuroscience*, 9:222–237.
- Pouget, A. and Snyder, L. (2000). Computational approaches to sensorimotor transformations. *Nature Neuroscience*, 3:1192–1198.
- Purves, D., Augustine, G., Fitzpatrick, D., Hall, W., LaMantia, A.-S., McNamara, J., and Williams, S. (2004). Neuroscience. *Sinauer Associates, Inc.*, 3.
- Ragert, P., Schmidt, A., Altenmüller, E., and Dinse, H. (2004). Superior tactile performance and learning in professional pianists: evidence for meta-plasticity in musicians. *European Journal of Neuroscience*, 19:473–478.
- Ramon y Cajal, S. (1911). Histologie du système nerveux de l’homme et des vertébrés. *Paris, Maloine.*
- Ramon y Cajal, S. (1984). The neuron and the glia cell. (*Translated by J. de la Torre and W.C. Gibson*) Springfield, IL: Charles C. Thomas.
- Ratliff, F. (1965). Mach bands: quantitative studies on neural networks in the retina. *Holden-Day, New York*, page 129.
- Recanzone, G., Schreiner, C., and Merzenich, M. (1993). Plasticity in the frequency representation of primary auditory cortex following discrimination training in adult owl monkeys. *Journal of Neuroscience*, 13:87–103.
- Reichardt, W. (1961). Autocorrelation, a principle for the evaluation of sensory information by the central nervous system. *Sensory Communication. Editor: W A Rosenblith, MIT Press*, pages 303–317.

- Richmond, B. and Sato, T. (1987). Enhancement of inferior temporal neurons during visual discrimination. *Journal of Neurophysiology*, 58(6):1292–1306.
- Rieke, F., Bialek, W., and Warland, D. (1999). Spikes: exploring the neural code. *MIT Press*.
- Roelfsema, P., Lamme, V., and Spekreijse, H. (1998). Object-based attention in the primary visual cortex of the macaque monkey. *Nature*, 395(6700):376–381.
- Rolls, E. and Baylis, G. (1986). Size and contrast have only small effects on the response to faces of neurons in the cortex of the superior temporal sulcus of the monkey. *Experimental Brain Research*, 65:38–48.
- Rolls, E., Baylis, G., and Hasselmo, M. (1987). The responses of neurons in the cortex in the superior temporal sulcus of the monkey to band-pass spatial frequency filtered faces. *Vision Research*, 27:311–326.
- Rolls, E., Baylis, G., and Leonard, C. (1985). Role of low and high spatial frequencies in the face-selective response of neurons in the cortex in the superior temporal sulcus. *Vision Research*, 25:1021–1035.
- Rosenthal, R. and Rubin, D. (1978). Interpersonal expectancy effects: the first 345 studies. *Behavioral and Brain Sciences*, 1:377–386.
- Royer, S. and Pare, D. (2003). Conservation of total synaptic weight through balanced synaptic depression and potentiation. *Nature*, 422(6931):518–522.
- Rudomin, P. (1999). Presynaptic selection of afferent inflow in the spinal cord. *Journal of Physiology*, 93:329–347.
- Saam, M. and Eckhorn, R. (2000). Lateral spike conduction velocity in the visual cortex affects spatial range of synchronization and receptive field size without visual experience: a learning model with spiking neurons. *Biological Cybernetics*, 83:L1–L9.
- Salinas, E. and Abbott, L. (1995). Transfer of coded information from sensory to motor networks. *The Journal of Neuroscience*, 15:6461–6474.
- Salinas, E. and Abbott, L. (1996). A model of multiplicative neural responses in parietal cortex. *The Proceedings of the National Academy of Sciences USA*, 93:11956–61.
- Salinas, E. and Abbott, L. (1997). Invariant visual response from attentional gain fields. *Journal of Neurophysiology*, 77:3267–3272.
- Salinas, E. and Sejnowski, T. (2000). Impact of correlated synaptic input on output firing rate and variability in simple neuronal models. *Journal of Neuroscience*, 20:6193–209.

- Salinas, E. and Sejnowski, T. (2001). Gain modulation in the central nervous system: where behavior, neurophysiology, and computation meet. *The Neuroscientist*, 5:430–440.
- Scharnowski, F., Hutton, C., Josephs, O., Weiskopf, N., and Rees, G. (2012). Improving visual perception through neurofeedback. *Journal of Neuroscience*, 32:17830–17841.
- Schiller, J., Major, G., Koester, H., and Schiller, Y. (2000). NMDA spikes in basal dendrites of cortical pyramidal neurons. *Nature*, 404(6775):285–289.
- Schiller, J., Schiller, Y., Stuart, G., and Sakmann, B. (1997). Calcium action potentials restricted to distal apical dendrites of rat neocortical pyramidal neurons. *Journal of Physiology*, 3:605–616.
- Seitz, A. and Dinse, H. (2007). A common framework for perceptual learning. *Current Opinion in Neurobiology*, 17(2):148–153.
- Sheldrake, R. (1998). Experimenter effects in scientific research: How widely are they neglected? *Journal of Scientific Exploration*, 12(1):73–78.
- Sherman, S. and Guillery, R. (1998). On the actions that one nerve cell can have on another: distinguishing drivers from modulators. *PNAS*, 95:7121–7126.
- Sherrington, C. (1909). Observations on the scratch-reflex in the spinal dog. *Journal of Physiology*, 13;34(1-2):1–50.
- Shibata, K., Watanabe, T., Sasaki, Y., and Kawato, M. (2011). Perceptual learning incepted by decoded fMRI neurofeedback without stimulus presentation. *Science*, 334:1413–1415.
- Siegel, R., Raffi, M., Phinney, R., J.A., T., and Jandó, G. (2003). Functional architecture of eye position gain fields in visual association cortex of behaving monkey. *Journal of Neurophysiology*, 90:1279–1294.
- Siegelbaum, S. and Kandel, E. (1991). Learning-related synaptic plasticity: LTP and LTD. *Current Opinion in Neurobiology*, 1(1):113–120.
- Simoncelli, E. and Olshausen, B. (2001). Natural image statistics and neural representation. *Annual Reviews in Neuroscience*, 24:1193–1216.
- Singer, W. (1986). The brain as a self-organizing system. *European Archives of Psychiatry and Neurological Sciences*, 236:4–9.
- Somers, D., Dale, A., Seiffert, A., and Tootell, R. (1999). Functional MRI reveals spatially specific attentional modulation in human primary visual cortex. *The Proceedings of the Natural Academy of Sciences USA*, 96(4):1663–1668.

- Song, S., Miller, K., and Abbott, L. (2000). Competitive learning through spike-timing-dependent synaptic plasticity. *Nature Neuroscience*, 3:919–936.
- Spence, C. and Read, L. (2003). Speech shadowing while driving: on the difficulty of splitting attention between eye and ear. *Psychological Science*, 14:251–256.
- Spitzer, H., Desimone, R., and Moran, J. (1988). Increased attention enhances both behaviour and neuronal performance. *Science*, 240(4850):388–340.
- Srinivasan, M. and Bernard, G. (1976). A proposed mechanism for multiplication of neural signals. *Biological Cybernetics*, 21:227–236.
- Stemmler, M., Usher, M., and Niebur, E. (1995). Lateral interactions in primary visual cortex: a model bridging physiology and psychophysics. *Science*, 269(5232):1877–1880.
- Sterr, A., Mueller, M., Elbert, T., Rockstroh, B., Pantev, C., and Taub, E. (1998). Perceptual correlates of changes in cortical representation of fingers in blind multifinger braille readers. *Journal of Neuroscience*, 18:4417–4423.
- Stevens, J. (1989). Temperature and two-point discrimination. *Somatosensory and Motor Research*, 6:275–284.
- Stevens, J., Alvarez-Reeves, M., Dipietro, L., Mack, G., and Green, B. (2003). Decline of tactile acuity in aging: a study of body site, blood flow, and lifetime habits of smoking and physical activity. *Somatosensory and Motor Research*, 20(3-4):271–279.
- Stone, M. (1948). The generalized Weierstrass approximation theorem. *Mathematics Magazine*, 21:167–183,237–254.
- Strayer, D. and Johnston, W. (2001). Driven to distraction: Dual-task studies of simulated driving and conversing on a cellular phone. *Psychological Science*, 12:462–466.
- Stringer, S., Perry, G., Rolls, E., and Proske, J. (2006). Learning invariant object recognition in the visual system with continuous transformations. *Biological Cybernetics*, 94(2):128–142.
- Swindale, N. (2000). How many maps are there in visual cortex? *Cerebral Cortex*, pages 633–643.
- Tal, D. and Schwartz, E. (1997). Computing with the leaky integrate-and-fire neuron: logarithmic computation and multiplication. *Neural Computation*, 9(2):305–318.

- Tanaka, K. (1996). Inferotemporal cortex and object vision. *Annual Review of Neuroscience*, 19:109–139.
- Tanaka, K. (2003). Columns for complex visual object features in the inferotemporal cortex: clustering of cells with similar but slightly different stimulus selectivities. *Cerebral Cortex*, 13:90–99.
- Tartaglia, E., Bamert, L., Herzog, M., and Mast, F. (2012). Perceptual learning of motion discrimination by mental imagery. *Journal of Vision*, 12(6):doi:10.1167/12.6.14.
- Tartaglia, E., Bamert, L., Mast, F., and Herzog, M. (2009). Human perceptual learning by mental imagery. *Current Biology*, 19(24):2081–2085.
- Theunissen, F. and Miller, J. (1995). Temporal encoding in the nervous system: a rigorous definition. *Journal of Computational Neuroscience*, 2:149–162.
- Thivierge, J.-P. and Marcus, G. (2007). The topographic brain: from neural connectivity to cognition. *TRENDS in Neuroscience*, 30(6):251–259.
- Tovee, M., Rolls, E., and Azzopardi, P. (1994). Translation invariance in the response to faces of single neurons in the temporal visual cortical areas of the alert macaque. *Journal of Neurophysiology*, pages 1049–1060.
- Treisman, A. and Gelade, G. (1980). A feature integration theory of attention. *Cognitive Psychology*, 12:97–136.
- Treue, S. (2001). Neural correlates of attention in primary visual cortex. *Trends in Neuroscience*, 24(5):295–300.
- Treue, S. and Martinez-Trujillo, J. (1999). Feature-based attention influences motion processing gain in macaque visual cortex. *Nature*, 399:575–579.
- Troyer, T. and Miller, K. (1997). Physiological gain leads to high ISI variability in a simple model of a cortical regular spiking cell. *Neural Computation*, 9:971–983.
- Tsodyks, M., Pawelzik, K., and Markram, H. (1998). Neural networks with dynamic synapses. *Neural Computation*, 10(4):821–835.
- van Rossum, M., Turrigiano, G., and Nelson, S. (2002). Fast propagation of firing rates through layered networks of noisy neurons. *Journal of Neuroscience*, 22:1956–1966.
- Vanrullen, R., Guyonneau, R., and Thorpe, S. (2005). Spike times make sense. *Trends in Neuroscience*, 28:1–4.
- Vitten, H. and Isaacson, J. (2001). Synaptic transmission: exciting times for presynaptic receptors. *Current Biology*, 11:695–697.

- von der Malsburg, C. (1973). Self-organisation of orientation sensitive cells in the striate cortex. *Kybernetik*, 14:85–100.
- von Foerster, H. (1988). On constructing a reality. *Adolesc Psychiatry*, 15:77–95.
- Wachtler, T., Doi, E., Lee, T.-W., and Sejnowski, T. (2007). Cone selectivity derived from the responses of the retinal cone mosaic to natural scenes. *Journal of Vision*, 7(8),6:1–14.
- Walach, H. (2011). Placebo controls: historical, methodological and general aspects. *Philos Trans R Soc Lond Biol Sci*, 366(1572):1870–1878.
- Walach, H., Schmidt, S., and Jonas, W. (2011). Neuroscience, consciousness and spirituality (studies in neuroscience, consciousness and spirituality). *Springer*.
- Wallis, G. (1996). Using spatio-temporal correlations to learn invariant object recognition. *Neural Computation*, 9(9):1513–1519.
- Wallis, G., Backus, B., Langer, M., Huebner, G., and Bülthoff, H. (2009). Learning illumination- and orientation-invariant representations of objects through temporal associations. *Journal of Vision*, 9(7):6:1–8.
- Wallis, G. and Rolls, E. (1997). A model of invariant object recognition in the visual system. *Progress in Neurobiology*, 51:167–194.
- Wang, G., Tanaka, K., and Tanifuji, M. (1996). Optical imaging of functional organization in the monkey inferotemporal cortex. *Science*, 272(5268):1665–1668.
- Wang, X., Merzenich, M., Sameshima, K., and Jenkins, W. (1995). Remodeling of hand representation in adult cortex determined by timing of tactile stimulation. *Nature*, 378:71–75.
- Watson, J. (1913). Psychology as the behaviorist views it. *Psychological Review*, pages 158–177.
- Weisz, N., Wienbruch, C., Hoffmeister, S., and Elbert, T. (2004). Tonotopic organisation of the human auditory cortex probed with frequency-modulated tones. *Hearing Research*, 191:49–58.
- White, R. and Snyder, L. (2004). A neural network model of flexible spatial updating. *Journal of Neurophysiology*, 91:1608–1619.
- Wilimzig, C., Ragert, P., and Dinse, H. (2012). Cortical topography of intracortical inhibition influences the speed of decision making. *The Proceedings of the National Academy of Sciences USA*, 109(8):3107–3112.
- Wiskott, L. and Sejnowski, T. (2002). Slow feature analysis: Unsupervised learning of invariances. *Neural Computation*, pages 715–770.

- Womelsdorf, T., Anton-Erxleben, K., Pieper, F., and Treue, S. (2006). Dynamic shifts of visual receptive fields in cortical area MT by spatial attention. *Nature Neuroscience*, 9:1156–1160.
- Wyss, R., König, P., and Verschure, P. (2006). A model of the ventral visual system based on temporal stability and local memory. *Nature Neuroscience*, 4(5):836–843.
- Zhang, L., Tao, H., Holt, C., Harris, W., and Poo, M. (1998). A critical window for cooperation and competition among developing retinotectal synapses. *Nature*, 395:37–44.
- Zipser, D. and Andersen, R. (1988). A back-propagation programmed network that simulates response properties of a subset of posterior parietal neurons. *Nature*, 331:679–684.

9 List of Contributions

- Sebastian Philipp* conducted the studies presented in this thesis.
- The thesis was supervised by PD Dr. Thomas Wachtler*.
- PD Dr. Hubert Dinse[°] was involved in the conception and realization of the study presented in chapter 5.
- Frank Michler[∇] helped on software development in chapter 4.
- Dr. Tobias Kalisch[°] and Dr. Jan Christoph Kattenstroh[°] helped on statistical evaluations in chapter 5.

* Department Biologie II, Ludwig-Maximilians Universität München, Germany

[°] Institute for Neuroinformatics, Ruhr-Universität Bochum, Germany

[∇] Neurophysik, Philipps-Universität Marburg, Germany